Article

Optimization of Peptidomimetics as Selective Inhibitors for the #-Catenin/T-Cell Factor Protein-Protein Interaction

Zhen Wang, Min Zhang, Jin Wang, and Haitao Ji

J. Med. Chem., **Just Accepted Manuscript** • DOI: 10.1021/acs.jmedchem.9b00147 • Publication Date (Web): 11 Mar 2019

Optimization of Peptidomimetics as Selective Inhibitors for the β-Catenin/T-Cell Factor Protein−Protein Interaction

Zhen Wang, [†,#] *Min Zhang,* [†,#] *Jin Wang,* [†] *Haitao Ji*[†,‡,]*

[†]Drug Discovery Department, H. Lee Moffitt Cancer Center and Research Institute, Tampa, Florida 33612–9497, United States

[‡]Departments of Oncologic Sciences and Chemistry, University of South Florida, Tampa, Florida 33620–9497, United States

ABSTRACT: The β-catenin/T-cell factor (Tcf) protein−protein interaction (PPI) plays a critical role in the β-catenin signaling pathway which is hyperactivated in many cancers and fibroses. Based on compound **1**, which was designed to target the Tcf4 $G^{13}ANDE^{17}$ binding site of β-catenin, extensive structure-activity relationship (SAR) studies have been conducted. As a result, compounds **53** and **57** were found to disrupt the β-catenin/Tcf PPI with the K_i of 0.64 and 0.44 μM, respectively, and exhibit good selectivity for β-catenin/Tcf over β-catenin/E-cadherin and β-catenin/adenomatous polyposis coli (APC) PPIs. The MTS tetrazolium cell viability assays revealed that **56**, the ethyl ester of **53**, was more potent than **53** in inhibiting viability of most of the Wnt/β-catenin hyperactive cancer cells. Further cell-based studies indicated that **56** disrupted the β-catenin/Tcf PPI without affecting the β-catenin/E-cadherin and β-catenin/APC PPIs, suppressed transactivation of Wnt/β-catenin signaling in dose-dependent manners, and inhibited migration and invasiveness of Wnt/β-catenin dependent cancer cells.

INTRODUCTION

The Wnt/β-catenin signaling pathway plays a critical role in regulation of cell proliferation, differentiation, and survival.[1-3] The aberrant activation of Wnt/β-catenin signaling has been implicated in initiation and progression of many cancers[4-9] and fibroses[10-11]. For instance, loss of adenomatous polyposis coli (APC) function can lead to the inappropriate stabilization of β-catenin and promote the formation of the constitutive complex between β-catenin and the T-cell factor (Tcf)/lymphoid enhancer-binding factor (Lef) family of transcriptional factors, which transcribes specific Wnt target genes that produce crypt progenitor-like cells in the surface intestinal epithelium, eventually causing sporadic colorectal cancer.[4-5] The autocrine activation of Wnt ligands can stabilize β-catenin into the dephosphorylated state and result in an increased level of nuclear β-catenin to interact with Tcf/Lef to induce overexpression of Wnt target genes and cause initiation and progression of triple negative breast cancers (TNBCs).[8-9] Hyperactivation of β-catenin signaling was detected in cancer stem cells, which control tumor growth, seed metastases, and result in cancer recurrence after remission.[12-14] In addition, activation of β-catenin signaling was demonstrated to exclude $CD8^+$ T cells from the tumor microenvironment and promote intratumoral regulator T cell (Treg) survival and infiltration, thus impairing antitumor immunity.[15-18] Therefore, the suppression of this signaling pathway holds great promise for designing new targeted cancer therapy. Further biological studies indicated that the formation of β-catenin/Tcf complex in the cell nucleus is the penultimate step of the Wnt/β-catenin signaling pathway and the activation of Wnt/β-catenin target genes is dependent on the formation of this complex.[19-21] Therefore, the β-catenin/Tcf PPI has emerged as an appealing therapeutic target to suppress hyperactive β-catenin signaling.

Extensive efforts have been made to identify several small-molecule inhibitors for this PPI.[22-

[29] However, the binding mode of these compounds remains unknown, making it difficult for further optimization.[30] The large peptides or peptide-based macrocycles have also been designed as β-catenin/Tcf inhibitors.[31-34] Hydrocarbon-stapled peptide, aStAx-35, designed based on the Axin sequence and the phage display result, was reported to bind with the Axin-binding site of β-catenin and inhibit the β-catenin/Tcf PPI.[31] Further design offered a more cell-permeable derivative, NLS-StAx-h, by substituting all six arginine residues with homoarginine and introducing the nuclear localization sequence (NLS) to the *N*-terminus.[33] Recently, Logan, Kirshenbaum, and coworkers disclosed the design of peptoid-peptide macrocycles as β-catenin/Tcf inhibitors, which showed promising efficacy in prostate cancer models.[34] In the previous studies, our group reported small-molecule inhibitors for the β-catenin/Tcf PPI using different strategies.[35-37] By targeting the Tcf4 G[13]ANDE[17] binding site, selective small-molecule inhibitors for β-catenin/Tcf PPI have been synthesized.[36] The best compound **1** (UU-T02) disrupted β-catenin/Tcf PPI with a K_i of 1.36 μM in the fluorescence polarization (FP) competitive inhibition assay and displayed 175- and 64-fold selectivity over β-catenin/E-cadherin and β-catenin/APC, respectively. However, this compound was almost inactive in cell-based assays unless converted into the ester form, including MTS tetrazolium cell viability assays and TOPFlash/FOPFlash luciferase reporter assays. Herein, we report our further medicinal chemistry efforts on optimization, synthesis, and biological characterization of new derivatives.

RESULTS

Structure-activity relationship (SAR) studies. The indole scaffold represents as one of the important privileged structures for the discovery of new drug candidates.[38] However, its electron-rich nature renders the indole ring susceptible to metabolism, often by oxidation at the C-3 position of indole, which has the highest electron density.[39] Most of the reported indole-related drugs and

probes contain substituents at indole 3-postion to block this metabolically labile site.[38-40] Therefore, to minimize the potential issue with indole in **1**, three different strategies were employed at the initial stage of our inhibitor optimization. As a direct approach, compounds **2** and **3** with indole C-3 position substitution were designed and synthesized. Both compounds showed a great loss of potency (Table 1). Alternatively, various electron-deficient heterocycles were introduced to replace the indole ring (**4**–**8**). While most compounds (**4**–**7**) in this series turned out to be inactive, compound **8** showed a K_i of 22 μM for the β-catenin/Tcf PPI. In addition, we designed **9** with the indole ring directly attaching to the amide group. This design is expected to reduce the electron density of the indole ring, thus increasing compound metabolic stability. Literature search revealed that this 1*H*-indole-2-carboxamido motif had been widely adopted in various medicinal chemistry programs.[41-44] The FP competitive inhibition assay [45] showed **9** inhibited the β-catenin/Tcf PPI with a promising K_i of 11 μM. Based on these results, we envisioned compound **9** would represent a new starting point for further modification, and extensive SAR studies on this new scaffold were conducted.

Preliminary SAR studies on **9** suggested both a Cl substituent at indole C-5 position is optimal among all mono-substitution analogues (Table 1, **9**–**17**). Switching the Cl substituent from C-5 position to C-4 (**10**) or C-6 (**11**) led to decreased activity. Meanwhile, the derivatives in which the Cl atom at the C-5 position was replaced by the other groups, including both electron withdrawing (F (**12**), Br (**13**), CF_3 (**16**), NO_2 (**17**)) and donating (Me (**14**), OMe (**15**)) groups, were also made. The results revealed that the electron withdrawing groups were more tolerated than the electron donating groups, while all of them were less potent than **9**. Two compounds with di-Cl substitutions (**18** and **19**) were synthesized, and both showed improved potency, especially **19**, which inhibited the β-catenin/Tcf PPI with a K_i of 4.3 μM, ~3-fold potency improvement over **9**.

Table 1. FP Competitive Inhibition Assay Results of Inhibitors **1**–**19**.[a]

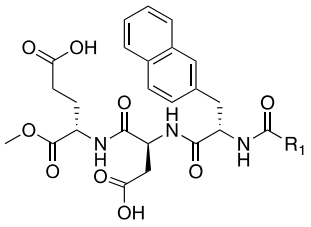

No.	R_1	IC_{50} ± SD (μM)	K_i ± SD (μM)	No.	R_1	IC_{50} ± SD (μM)	K_i ± SD (μM)
1	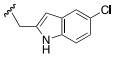	15 ± 5.9	3.8 ± 1.5	**11**	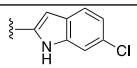	60 ± 2.2	15 ± 0.56
2		>400	> 100	**12**	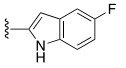	349 ± 34	89 ± 8.6
3	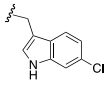	>400	> 100	**13**	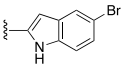	62 ± 6.6	16 ± 1.7
4	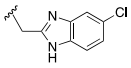	>400	>100	**14**	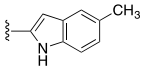	>400	>100
5	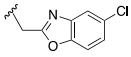	>400	>100	**15**	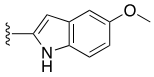	>400	>100
6	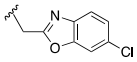	>400	>100	**16**	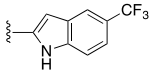	47 ± 4.1	12 ± 1.0
7	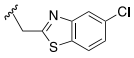	>400	>100	**17**	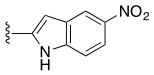	67 ± 6.0	17 ± 1.5
8	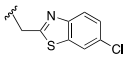	88 ± 12	22 ± 3.0	**18**	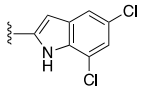	38 ± 4.1	9.7 ± 1.0
9	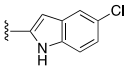	45 ± 3.6	11 ± 0.92	**19**	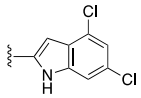	17 ± 1.4	4.3 ± 0.34
10	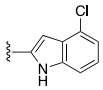	60 ± 5.1	15 ± 1.3				

[a] Each set of data was expressed as mean ± standard deviation (n = 3). The K_i value for the parent peptide $G^{13}ANDE^{17}$ was determined to be 290 ± 1.3 μM. [36]

Next, to increase the stability of the *C*-terminal ester group that tends to be hydrolyzed under relatively weak basic condition (as shown in Supplementary Note 1), a collection of derivatives with amides, instead of the methyl ester, was designed and synthesized. As shown in Table 2, Introduction of isobutyl (**20**) and phenyl (**21**) amides in replacement of the methyl ester resulted in the compounds with increased activities. For instance, compound **21** inhibited the β-catenin/Tcf PPI with a K_i of 3.3 μM, which is 3.4-fold more potent than **9**. Moreover, these more stable amides overcame the instability problem of the methyl ester in **1** (Supplementary Note 1). Further substitution of the phenyl group in **21** with benzyl and phenylethyl groups as in **22** and **23**, respectively, showed decreased activities. Next, compounds **24**–**29** were designed and synthesized to explore the optimal substitution type on the phenyl group. As a result, compounds **24**–**26** with F substitution showed the similar activities, while **27** and **28** were 3- to 4-fold more potent than **29**, indicating the *para*- and *meta*-substitutions on the phenyl ring are preferable to the *ortho* derivatives. Therefore, more substituents were explored for these two positions. Compounds **33**–**38** were synthesized, and the results were summarized in Table 2. It was shown that most of these compounds displayed slight improvement of the inhibitory potency, when compared with **21**. Specifically, compounds **30** and **34**, featuring *para*-CF_3 and *para*-OCF_3 on the phenyl ring, respectively, were slightly more potent than the other compounds (the FP competitive inhibition assay curves of **30** and **34** are shown in Supplementary Figure S3). Compounds with double substitutions (**36**–**38**) were also explored at these two positions, but they did not show potency improvement.

Table 2. FP Competitive Inhibition Assay Results of Inhibitors **20**–**38**. [a]

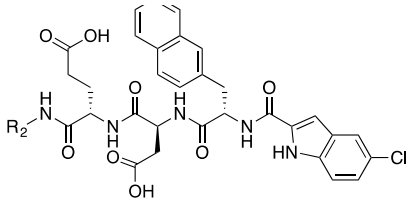

No.	R_2	IC_{50} ± SD (μM)	K_i ± SD (μM)	No.	R_2	IC_{50} ± SD (μM)	K_i ± SD (μM)
20		33 ± 3.8	8.5 ± 0.98	**30**	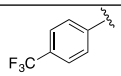	7.3 ± 0.78	1.9 ± 0.20
21		13 ± 2.5	3.3 ± 0.64	**31**	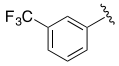	8.9 ± 0.68	2.3 ± 0.17
22		30 ± 3.7	7.6 ± 0.94	**32**	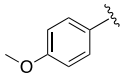	10 ± 1.4	2.6 ± 0.37
23		35 ± 3.6	8.9 ± 0.91	**33**	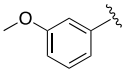	9.3 ± 1.2	2.4 ± 0.31
24		17 ± 3.4	4.5 ± 0.88	**34**	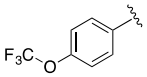	7.5 ± 0.51	1.9 ± 0.13
25	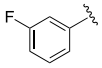	13 ± 1.5	3.3 ± 0.37	**35**	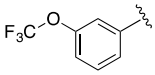	8.5 ± 0.60	2.2 ± 0.15
26		14 ± 2.9	3.6 ± 0.74	**36**	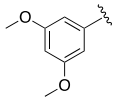	13 ± 1.1	3.3 ± 0.26
27	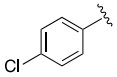	11 ± 2.0	2.7 ± 0.50	**37**	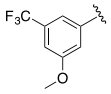	10 ± 0.81	2.6 ± 0.20
28	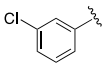	12 ± 2.0	3.1 ± 0.51	**38**	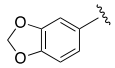	9.8 ± 3.3	2.5 ± 0.83
29		38 ± 8.4	9.6 ± 2.1				

[a] Each set of data was expressed as mean ± standard deviation (n = 3). The K_i value for the parent peptide $G^{13}ANDE^{17}$ was determined to be 290 ± 1.3 μM. [36]

Further SAR studies on the naphthyl group were undertaken (Table 3). It was shown that most

of the synthesized compounds were less potent than **21**. Only compounds **40** and **46** exhibited comparable activity, indicating that the large hydrophobic moieties are critical for maintaining the activity at this site.

Table 3. FP Competitive Inhibition Assay Results of Inhibitors **39–46**.[a]

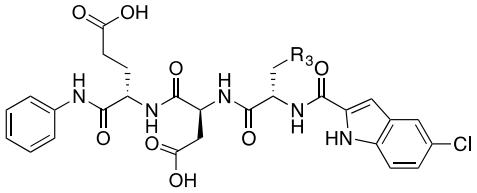

No.	R_3	IC_{50} ± SD (μM)	K_i ± SD (μM)	No.	R_3	IC_{50} ± SD (μM)	K_i ± SD (μM)
39		273 ± 37	70 ± 9.5	**43**	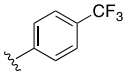	37 ± 4.5	9.3 ± 1.2
40	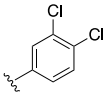	14 ± 2.3	3.7 ± 0.58	**44**	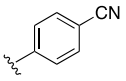	79 ± 6.8	20± 1.7
41	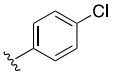	44 ± 3.9	11± 1.0	**45**	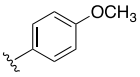	99 ± 7.5	25± 1.9
42		55 ± 3.5	14± 0.89	**46**	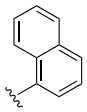	11 ± 1.8	2.9 ± 0.45

[a] Each set of data is expressed as mean ± standard deviation (n = 3). The K_i value for the parent peptide $G^{13}ANDE^{17}$ was determined to be 290 ± 1.3 μM. [36]

Our extensive SAR studies revealed that the primary configuration (*S*, *S*, *S*) was optimal for this series, since individually reversing the configuration of each amino acid resulted in decreased activity (Table 4). Base on the inhibitory activity data, we can also conclude that the sensitivity of these three chiral amino acids to the configurational change was decreased following the order of glutamic acid (**47**), naphthyl substituted amino acid (**49**), and aspartic acid (**48**), with glutamic acid

being the most sensitive residue, when compared with those in **33**.

Table 4. FP Competitive Inhibition Assay Results of Inhibitors **47-49**. [a]

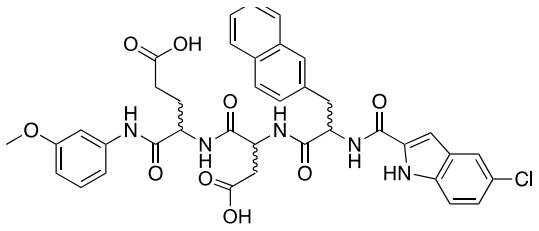

No.	*R,S*	IC_{50} ± SD (μM)	K_i ± SD (μM)
47	*R, S, S*	39 ± 2.9	10 ± 0.73
48	*S, R, S*	26 ± 1.6	6.6 ± 0.42
49	*S, S, R*	31 ± 1.7	8.0 ± 0.42

[a] Each set of data is expressed as mean ± standard deviation (n = 3). The K_i value for the parent peptide $G^{13}ANDE^{17}$ was determined to be 290 ± 1.3 μM. [36]

Our next modification was focused on the two carboxylic acid groups, with the aim of improving both potency and cell permeability.[46] One common bioisostere of carboxylic acid, amide, was first used to replace the carboxylic acids in **34** individually. The resulting compounds **50** and **51** showed decreased activities. To our delight, introduction of tetrazole, another common bioisostere of carboxylic acid, resulted in the derivatives with the improved potency. For instance, compound **53**, for the first time, displayed the submicromolar K_i (0.64 μM) for this challenging PPI target. In an attempt to eliminate both carboxylic acids in **34**, the amide was further introduced into the tetrazole derivatives **52** and **53**. However, the resulting compounds **54** and **55** displayed 3- to 6-fold potency loss. The ester derivative (**56**) of compound **53** was also synthesized to improve compound's cell permeability. This compound inhibited the β-catenin/Tcf PPI with a K_i

of 5.2 μM. In addition, compound **57** was synthesized based on the previous SAR results. This compound inhibited the β-catenin/Tcf PPI with a K_i of 0.44 μM, which was the most potent inhibitor of this series. The competitive FP inhibition assay curves of **52**–**57** are shown in Supplementary Figure S3.

Table 5. FP Competitive Inhibition Assay Results of Inhibitors **50-57**. [a]

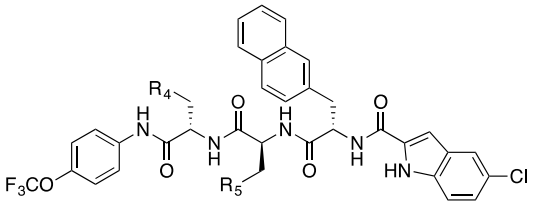

No.	R_4	R_5	IC_{50} ± SD (μM)	K_i ± SD (μM)
50	CH_2CONH_2	COOH	26 ± 2.3	6.7 ± 0.60
51	CH_2COOH	$CONH_2$	42 ± 3.4	10 ± 0.88
52	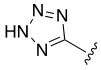	COOH	5.9 ± 0.27	1.5 ± 0.066
53	CH_2COOH	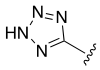	2.5 ± 0.48	0.64 ± 0.12
54	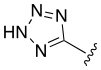	$CONH_2$	19 ± 2.3	4.9 ± 0.58
55	CH_2CONH_2	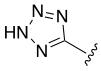	16 ± 0.62	3.9 ± 0.16
56	CH_2COOEt	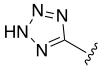	21 ± 0.28	5.2 ± 0.070
57	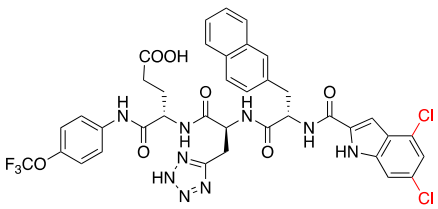		1.7 ± 0.39	0.44 ± 0.098

(Et)-15	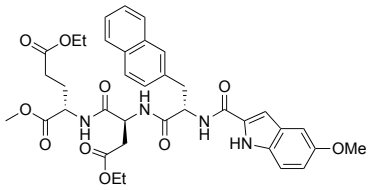	>400	>100

[a] Each set of data was expressed as mean ± standard deviation (n = 3). The K_i value for the parent peptide G[13]ANDE[17] was determined to be 290 ± 1.3 μM. [36]

Inhibitor selectivity between *β*-catenin/Tcf, *β*-catenin/E-cadherin, and *β*-catenin/APC PPIs. *β*-Catenin not only interacts with Tcf/Lef, BCL9/B9L, CBP/p300, etc. to culminate Wnt/*β*-catenin signaling, but also forms the complexes with E-cadherin and APC, respectively, to play specific roles *in cellulo*. The PPI between *β*-catenin and E-cadherin is essential for cell–cell adhesion, while the *β*-catenin/APC PPI is critical for *β*-catenin phosphorylation and degradation. The crystallographic analyses of *β*-catenin in complexes with Tcf, E-cadherin, and APC indicated that *β*-catenin uses the same armadillo repeats to bind Tcf/Lef[47-50], cadherin[51], and APC[52-54]. Biochemical analyses confirmed that the binding mode of Tcf, cadherin, and APC with *β*-catenin was identical and mutually exclusive.[55-58] The selectivities of **53** and **57** between *β*-catenin/Tcf4, *β*-catenin/E-cadherin, and *β*-catenin/APC-R3 interactions were quantified using the FP selectivity assay.[29] As shown in Table 6, the selectivities of **53** for *β*-catenin/Tcf4 over *β*-catenin/E-cadherin and *β*-catenin/APC-R3 interactions are 50- and 137-fold, respectively. The selectivities of **57** for *β*-catenin/Tcf4 over *β*-catenin/E-cadherin and *β*-catenin/APC-R3 interactions are 30- and 395-fold.

Table 6. The Selectivities of **53** and **57** for *β*-Catenin/Tcf over *β*-Catenin/E-Cadherin and *β*-Catenin/APC Interactions. [a]

	K_i ± SD (μM)	Selectivity

Compounds	β-catenin/Tcf	β-catenin/E-cadherin	β-catenin/APC	TCF/E-cadherin	TCF/APC
53	0.64 ± 0.12	32 ± 2.8	88 ± 7.3	50	137
57	0.44 ± 0.098	13 ± 0.60	173 ± 15	31	395

[a] Each set of data was expressed as mean ± standard deviation (n = 3).

Cell-based studies. MTS tetrazolium cell viability assays were performed to evaluate the effect of β-catenin/Tcf inhibitors on growth of different cancer cell lines with hyperactive Wnt signaling, including colorectal cancer cells (SW480 and HCT116) and TNBC cells (MDA-MB-231, MDA-MB-468, and BT-20), and one cancer cell line with normal Wnt signaling, A549. The half maximal inhibitory concentrations (IC_{50}) of three representative compounds (**53**, **55,** and **56**) were determined. An inactive analogue (**Et**)-**15** (K_i >100 μM, Table 5) was also assessed in parallel. As shown in Table 7 and Supplementary Figure S4, compounds **53**, **55**, and **56** except (**Et**)-**15** inhibited viability of Wnt/β-catenin hyperactive cancer cells. Compound **56** is the most potent and selective inhibitor for most of the Wnt/β-catenin hyperactive cancer cells over Wnt/β-catenin normal cancer cells.

Table 7. The MTS Assay to Monitor the Inhibitory Activities of (**Et**)-**15**, **53**, **55,** and **56** on Viability of Cancer Cells. [a]

	MTs IC_{50} ± SD (μM)					
	Wnt/β-catenin hyperactive					Wnt/β-catenin normal
No.	SW480	HCT116	MDA-MB-231	MDA-MB-468	BT-20	A549
(Et)-**15**	>200	>200	>200	>200	>200	> 200
53	40.5 ± 1.78	45.8 ± 1.37	26.4 ± 0.74	20.6 ± 0.72	24.7 ± 1.00	71.7 ± 2.66

55	24.6 ± 1.01	57.8 ± 3.75	29.3 ± 2.15	26.9 ± 1.54	29.3 ± 2.20	47.5 ± 2.63
56	17.7 ± 0.54	60.6 ± 4.93	16.6 ± 1.16	10.6 ± 0.30	20.1 ± 0.52	67.9 ± 2.09

[a] Each set of data was expressed as mean ± standard deviation (n = 3).

The suppressing effect of the inhibitors on transactivation of β-catenin signaling was evaluated by TOPFlash/FOPFlash luciferase reporter assays. As shown in Figure 1, the inactive compound (**Et**)-**15** did not inhibit the TOPFlash (in which the luciferase reporter has three wild-type Tcf4 binding sites) luciferase activity at the concentration of up to 200 μM. Compounds **55** and **56** suppressed the TOPFlash luciferase activities in dose-dependent manners, while did not inhibit the FOPFlash (with three mutant Tcf4 binding sites) luciferase reporter activities. However, it was noted that **56** did not show the sigmoidal curve at high concentrations. The cause of this result warrants further studies.

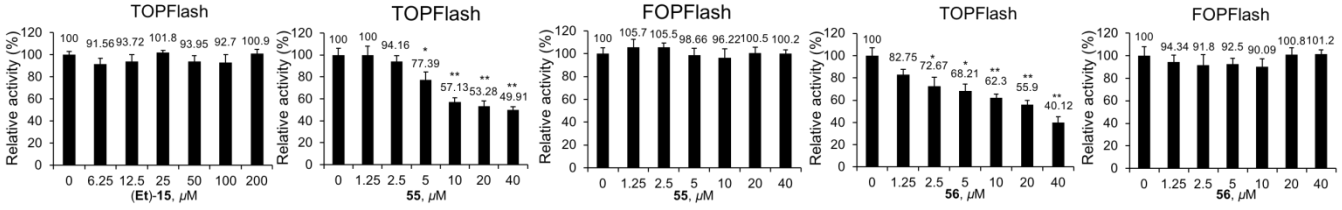

Figure 1. Wnt-responsive TOPFlash and FOPFlash luciferase reporter assay results of **(Et)-15 (negative control)** and inhibitors **55** and **56** in β-catenin activated HEK293 cells. *P< 0.05, ** P < 0.01, as determined by the unpaired, two-tailed Student *t* test.

Co-immunoprecipitation (co-IP) experiments were conducted to assess the effect of the inhibitors for disruption of the interaction between β-catenin and Tcf using SW480 cell lysates. The results were shown in Figure 2 and Supplementary Figure S5. Compound **53** can disrupt the

interaction between full-length β-catenin and full-length Tcf in a dose-dependent manner after 4-h incubation with SW480 cell lysates. The effect of **56** on disruption of the β-catenin/Tcf PPI and on the selectivity between three PPIs in the cellular context were also evaluated by co-IP experiments using HCT116 cells. As shown in Figure 2 and Supplementary Figure S5, compound **56** dose-dependently inhibited the β-catenin/Tcf PPI, but had no effect on the β-catenin/E-cadherin and β-catenin/APC PPIs at the concentrations that were sufficient to disrupt the β-catenin/Tcf PPI.

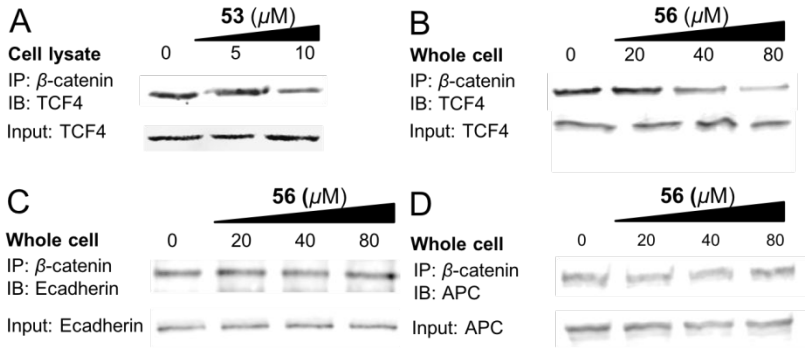

Figure 2. (A) Co-IP experiments to evaluate the disruption of the β-catenin/TCF PPI by **53** in SW480 cell lysate. (B–D) Co-IP experiments to evaluate the disruption of the β-catenin/Tcf PPI by **56** and the inhibitory selectivity of **56** between β-catenin/Tcf, β-catenin/E-cadherin, and β-catenin/APC PPIs using HCT116 cells. IP, immunoprecipitation; IB, immunoblotting; input, 10% of cell lysate. Each experiment was performed in duplicate.

β-Catenin signaling induces and maintains migration, invasion and metastasis of cancer cells, including TNBC cells.[59-70] Scratch wound healing and Matrigel invasion assays using TNBC MDA-MB-231 cells were conducted. As shown in Figure 3, compound **56** can effectively inhibit TNBC cell migration (Figure 3A) and invasion (Figure 3B) at 10 μM. The effects are comparable with that of β-catenin/CBP inhibitor ICG-001[71] at 5 μM.

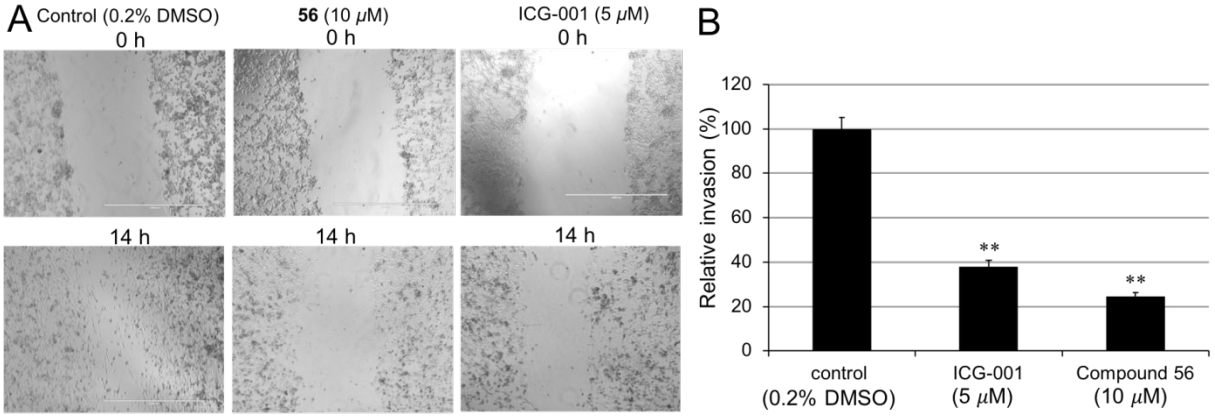

Figure 3. (A) Wound-healing assays showed that **56** (10 μM) inhibited migration of human TNBC MDA-MB-231 cells induced by serum (10% in media). Control, 0.2% DMSO in 10% FBS. The β-catenin/CBP inhibitor ICG-001 (5 μM) was assessed in parallel. In all experiments, mitomycin (10 μg/mL) was added to inhibit cell proliferation and allow examination of the effects on cell migration. **(B)** Matrigel invasion assays showed that **56** (10 μM) inhibited invasion of human TNBC MDA-MB-231 cells. Control, 0.2% DMSO in 10% FBS. ICG-001 (5 μM) was assessed in parallel. **P < 0.01, as determined by the unpaired, two-tailed Student t test. Each set of data is expressed as mean ± standard deviation (n = 3).

Chemistry. The synthetic routes for final products **20**–**21**, **30**–**38**, **53**, and **55**–**57** are shown in Schemes 1–3. The synthetic routes for the other final products and intermediates are shown in Supplementary Schemes S1–S14. The synthetic routes for **20**–**21** and **30**–**38** are shown in Scheme 1, in which CH_2Cl_2 was employed as the solvent for the amide coupling reactions. The amide bond coupling reaction between *N*-Cbz-L-glutamic acid 5-*tert*-butyl ester and various amines generated intermediate **62**, which underwent the hydrogenation reaction to remove the Cbz protecting group and then coupled with *N*-Cbz-L-aspartic acid to yield **63**. Hydrogenation of **63** and coupling with

N-Cbz-L-2-naphthylalanine produced **64**. Removal of the Cbz protecting group in **64** and then coupling with 5-chloroindole-2-carboxylic acid gave **65**, in which the *tert*-butyl ester protecting group was removed by TFA in CH_2Cl_2 solution to offer the final products.

Scheme 1. Synthesis of **20**–**21** and **30**–**38**.

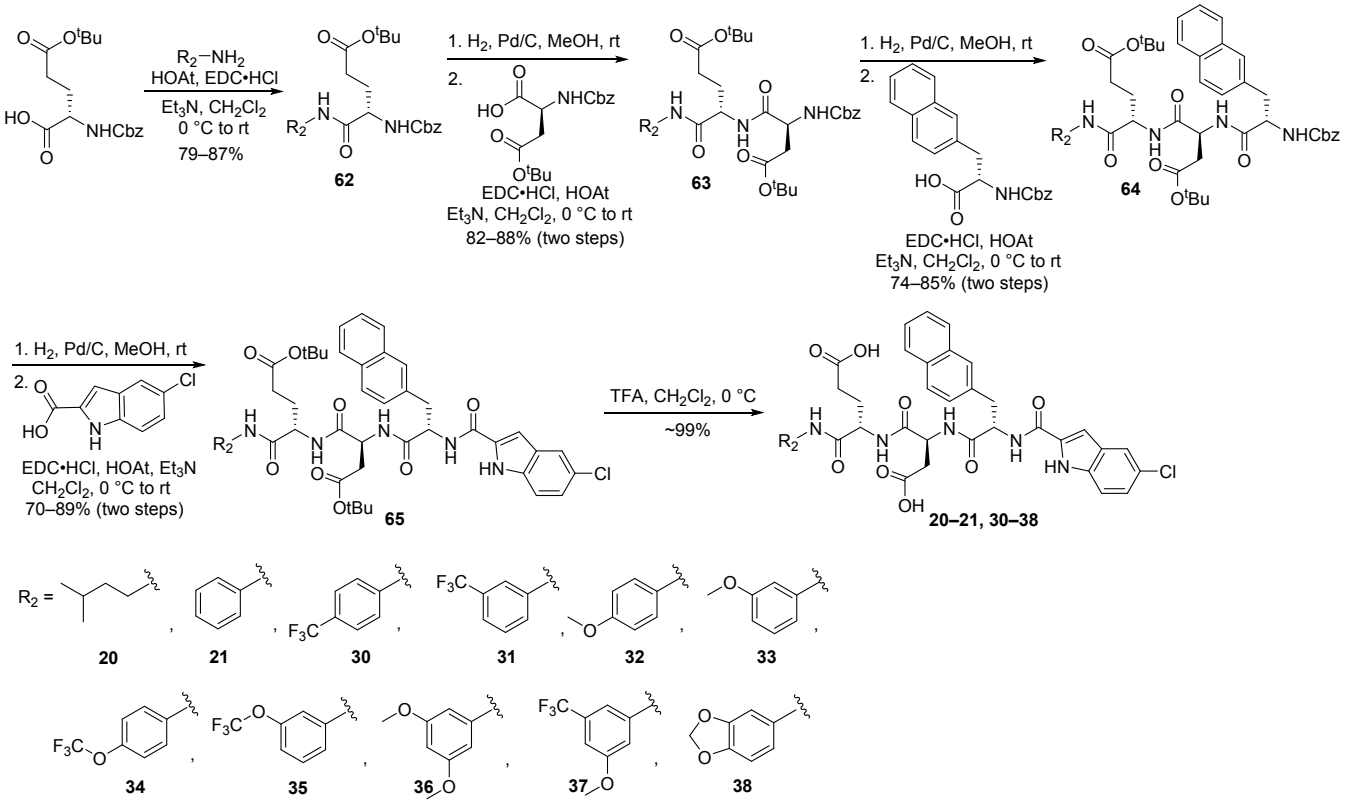

The synthetic routes for **53**, **56**, and **57** are shown in Scheme 2, in which DMF was used as the solvent for all the amide coupling reactions. The amide bond coupling reactions between *N*-Cbz-L-glutamic acid 5-*tert*-butyl ester or *N*-Cbz-L-glutamic acid 5-ethyl ester and various amines produced intermediate **62g** or **90**, which underwent the hydrogenation reaction to remove the Cbz protecting group and then the coupling reaction with (*S*)-2-((((9*H*-fluoren-9-yl)methoxy)carbonyl)amino)-3-(2*H*-tetrazol-5-yl)propanoic acid to yield **91a,b**. Removal of the

Fmoc protecting group under the basic condition and then coupling with **68a,h** gave **92**, in which the Boc (and *tert*-butyl) protecting group(s) was removed by TFA in CH_2Cl_2 solution to offer the final products.

Scheme 2. Synthesis of **53**, **56**, **and 57**.

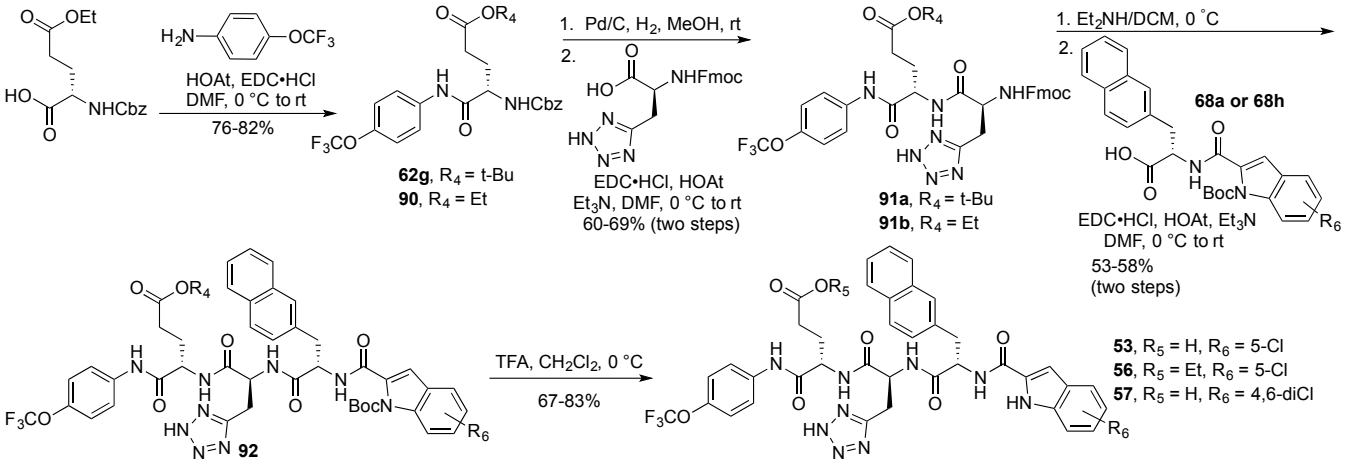

The synthetic route for **55** is shown in Scheme 3. The amide bond coupling reaction between *N*-Cbz-L-glutamine and 4-(trifluoromethoxy) aniline and then the deprotection of the Cbz protecting group produced **95**, which was coupled with (*S*)-2-((((9*H*-fluoren-9-yl)methoxy)carbonyl)amino)-3-(2*H*-tetrazol-5-yl)propanoic acid to afford **96**. Removal of the Fmoc group in **96** and coupling with intermediate **86a** gave **97**. The Boc deprotection yielded final product **55**.

Scheme 3. Synthesis of **55**.

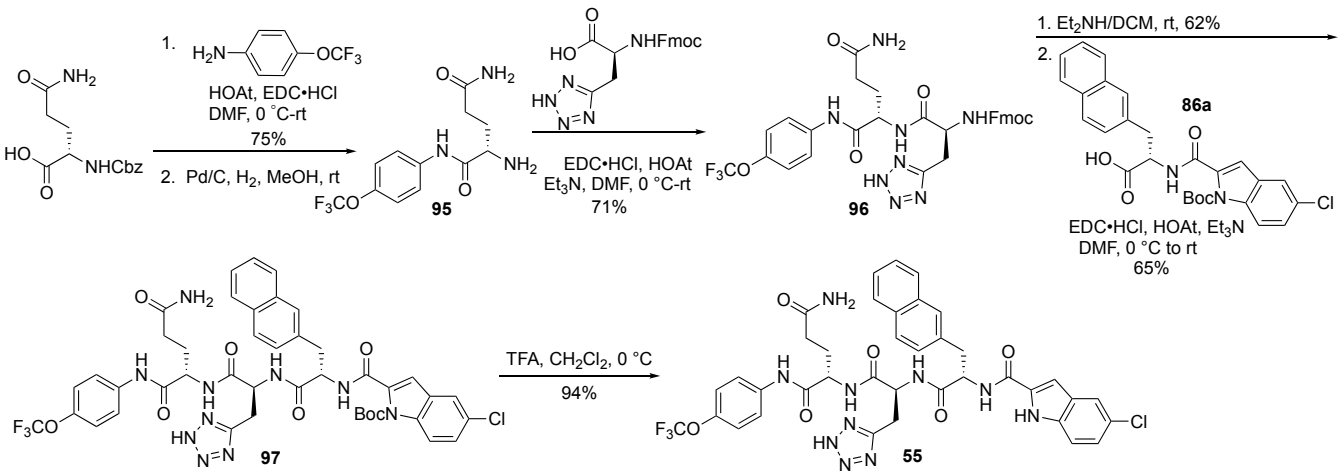

DISCUSSION AND CONCLUSIONS

The *β*-catenin signaling pathway is frequently overactivated in many cancers and fibroses. The *β*-catenin/Tcf PPI represents an appealing therapeutic target to suppress this signaling pathway, since the transcriptional overactivation of *β*-catenin signaling is dependent on the formation of the key downstream effector, the *β*-catenin/Tcf complex, in the cell nucleus. However, selective targeting of the *β*-catenin/Tcf PPI remains a great challenge. On one side, *β*-catenin and Tcf have a large contacting surface area and the tight binding affinity (K_d = 7−10 nM), which makes it challenging to achieve potent inhibition. One the other side, *β*-catenin uses the same armadillo repeats to bind Tcf, cadherin, and APC, and the crystallographic studies show their binding mode is identical, indicating the selectivity would be a major issue when designing *β*-catenin/Tcf inhibitors. In this work, the SAR studies on compound **1** has yielded inhibitors (compounds **53** and **57**) with improved activities for the *β*-catenin/Tcf PPI in this series. They also showed good selectivity for *β*-catenin/Tcf over *β*-catenin/E-cadherin and *β*-catenin/APC PPIs in the FP selectivity assay.

The structure–activity relationship (SAR) is to study the correlation between the chemical structures of a series of derivatives and their biological activities. The SAR study has been widely

used to facilitate step-by-step inhibitor optimization. Herein, extensive SAR studies on the structure of **1** were conducted. It not only yielded more potent inhibitors for the *β*-catenin/Tcf PPI, the SAR results obtained can also guide the future inhibitor optimization. This is quite important given that no co-crystal structure of a small-molecule inhibitor with *β*-catenin has been reported. For instance, the study revealed the naphthyl group of **1** can only be substituted by the large hydrophobic groups. This gives us two directions to further investigate this site. One is to introduce larger moieties to examine whether the compound can further improve potency and selectivity. The other is to adopt nitrogen-containing benzoheterocyclic rings, which are large and hydrophobic enough, and at the same time might capture potential polar interactions with the protein and balance the physiochemical property of the inhibitors. This study revealed that the indole moiety was crucial for inhibitor potency. The feasible method to further optimize this substructure is to extensively modify the indole ring and the adjacent methylene group that connects indole with the amide group. In addition, the SAR results confirmed the importance of the two carboxylic acid groups, but they can be replaced by tetrazole, one of its bioisosteres, to improve the potency. This prompts us to try the other bioisosteres of carboxylic acid in the future optimization.

The prodrug strategy was designed to address undesirable physicochemical properties of the drug and has been widely applied in contemporary drug design and development.[72] In this work, we were interested whether this strategy could be applied to compound **53** to improve its cellular uptake, since **53** has a carboxylic acid moiety, which could impair its cell permeability. Based on this hypothesis, compound **56** was synthesized. The preliminary cell-based studies indicated that **56** was indeed more potent and selective than **53** in inhibiting growth of most cancer cells with hyperactive Wnt/*β*-catenin signaling. Interestingly, the HPLC-MS based cell bioavailability

assay[73] revealed that compound **56** did not transform into **53** after 24-h incubation with SW480 cells in 5 mL of DMEM media with 10% FBS, suggesting **56** might not act as a prodrug of **53** (Supplementary Note 2 and Supplementary Figures S6–S8). Further analyses revealed compound **56** did achieve a higher cell-bound concentration than **53**. For instance, the cell-bound concentration of **56** at 37 °C was determined to be 1.4 nmol/million SW480 cells, which is 8-fold higher than 0.17 nmol/million SW480 cells determined for **53**, for the 3-h incubation in 5 mL of DMEM media with 10% FBS, when the input concentration was set to 25 μM. The increased cell-bound concentration might explain why **56** exhibited the better cellular activity than **53**, although it showed the higher K_i value in FP assays. Further cell-based co-IP experiments indicated that compound **56** disrupted the β-catenin/Tcf PPI while leaving the β-catenin/E-cadherin and β-catenin/APC PPIs unaffected, demonstrating the selectivity of new inhibitors on the cell-based level. This compound also dose-dependently inhibited TOPFlash luciferase reporter activity without affecting FOPFlash luciferase reporter activity. In contrast, the negative control **(Et)-15** did not suppress Wnt specific TOPFlash luciferase reporter activity and did not inhibit growth of the cancer cells with hyperactive Wnt/β-catenin signaling.

In summary, the β-catenin/Tcf PPI has emerged as an appealing therapeutic target to suppress the overactivated β-catenin signaling for targeted cancer therapy. Extensive SAR studies were conducted based on compound **1**, which was designed to target the Tcf4 $G^{13}ANDE^{17}$ binding site of β-catenin. Compounds **53** and **57** were found to disrupt the β-catenin/Tcf PPI with the K_i of 0.64 and 0.44 μM, respectively, and showed good selectivity for β-catenin/Tcf over β-catenin/E-cadherin and β-catenin/APC PPIs. Cell-based studies indicated that compound **56**, the ethyl ester derivative of **53**, disrupted the β-catenin/Tcf interaction without affecting the β-catenin/E-cadherin and β-catenin/APC interactions, dose-dependently suppressed transactivation of Wnt/β-catenin

signaling, and inhibited viability, migration and invasiveness of Wnt/β-catenin dependent cancer cells. The extensive SAR results offered the directions for future inhibitor optimization.

EXPERIMENTAL SECTION

Chemical Synthesis. *General Methods, Reagents, and Materials.* All reagents were purchased from commercial sources and used without further purification unless stated otherwise. ^{1}H NMR and ^{13}C NMR spectra were recorded on Bruker AVANCEIIIHD 500 (500 MHz) spectrometers (125.7 MHz for ^{13}C NMR spectra) in d_6-DMSO, d_6-acetone, d_4-methanol, and $CDCl_3$. Chemical shifts were reported as values in parts per million (ppm), and the reference resonance peaks were set at 7.26 ppm ($CHCl_3$), 3.31 ppm (CD_2HOD), 2.50 ppm [$(CD_2H)_2SO$], 2.05 ppm [$(CD_2H)_2CO$] for ^{1}H NMR spectra and 77.23 ppm ($CDCl_3$), 49.00 ppm (CD_3OD), 39.52 ppm (d_6-DMSO), and 29.84 ppm (d_6-acetone) for ^{13}C NMR spectra. Low-resolution mass spectra were determined on an Agilent 6120 single quadrupole mass spectrometer with 1220 infinity LC system (HPLC-MS) and an ESI source. High-resolution mass spectra were determined on Agilent G6230BA TOF LCMS Mass Spectrometer with a TOF mass detector. Thin-layer chromatography was carried out on E. Merck pre-coated silica gel 60 F254 plates with a UV–visible lamp. Column chromatography was performed with SilicaFlash@ F60 (230–400 mesh). The purity of final compounds **2**–**57** was determined by HPLC analyses with two different conditions (see the Supporting Information). The instrument was an Agilent 1260 Infinity II HPLC system with a quaternary pump, a vial sampler, and a DAD detector. A Kromasil 300–5–C18 column (4.6 × 250 mm) was used. The DAD detector was set to 220, 254, and 280 nm. The purity of all tested compounds was >95%.

General peptide coupling procedure. a. CH_2Cl_2 as the solvent: At 0 ˚C, to a suspension of carboxylic acid (1 equiv), amine (1 equiv), EDC•HCl (2 equiv), and HOAt (1.5 equiv) in

dichloromethane (CH_2Cl_2) was added triethylamine (3 equiv) dropwise. The reaction mixture was warmed to room temperature and stirred overnight. After completion of the reaction, more CH_2Cl_2 was added. The CH_2Cl_2 phase was washed by 1 M HCl, saturated $NaHCO_3$, and brine, and was dried over Na_2SO_4 and concentrated under reduced pressure. Column chromatography was used to purify the target compound. b. DMF as the solvent: At 0 ˚C, to a suspension of carboxylic acid (1 equiv), amine (1 equiv) in dimethylformamide (DMF) was added EDC•HCl (2 equiv) and HOAt (2 equiv). The reaction mixture was warmed to room temperature and stirred overnight. The mixture was poured into water and the solid was collected. The pure compounds were obtained by recrystallization using the hexane and ethyl acetate mixture or CH_2Cl_2.

General procedure for deprotection of the Cbz-protected amines. To the solution of the Cbz-protected amine in methanol was added 10% Pd/C under Ar. The mixture was stirred overnight at room temperature under H_2. The resulting product was collected by removal of the Pd/C catalyst and used directly in next step without further purification.

General procedure for deprotection of *tert*-butyl ester or Boc-protected indoles. At 0 ˚C, to a solution of *tert*-butyl ester or Boc-protected indole in CH_2Cl_2 (5 mL) was added 5 mL trifluoroacetic acid (TFA) dropwise. The reaction was kept at 0 ˚C for 4 h. Upon completion, the solvent was removed under reduced pressure. TFA was completely removed by adding CH_2Cl_2 three times to afford the desired product.

General procedure for deprotection of Fmoc-protected amines. At 0 ˚C, to a stirred solution of the Fmoc protected amine (1 mmol) in dichloromethane (10 mL), diethylamine (10 mL) was added dropwise. The reaction was kept at 0 ˚C for 6 h until TLC showed no starting material left. Upon completion, the mixture was evaporated under reduced pressure. The diethyl amine residue was removed by adding dichloromethane at least three times. The residue was purified by flash column,

except Asn and Gln-containing compounds, which were recrystallized in dichloromethane.

(*S*)-4-((*S*)-3-carboxy-2-((*S*)-2-(5-chloro-1*H*-indole-2-carboxamido)-3-(naphthalen-2-yl)propanamido)propanamido)-5-(isopentylamino)-5-oxopentanoic acid (20). ^{1}H NMR (500 MHz, DMSO-d_6) δ 12.27 (s, 2H), 11.63 (d, J = 2.2 Hz, 1H), 8.80 (d, J = 8.5 Hz, 1H), 8.66 (d, J = 7.6 Hz, 1H), 7.92 (d, J = 8.0 Hz, 1H), 7.85 (d, J = 1.6 Hz, 1H), 7.83 – 7.73 (m, 4H), 7.70 (d, J = 2.1 Hz, 1H), 7.56 (dd, J = 8.5, 1.7 Hz, 1H), 7.42 (pd, J = 6.8, 1.6 Hz, 2H), 7.36 (d, J = 8.7 Hz, 1H), 7.24 – 7.19 (m, 1H), 7.14 (dd, J = 8.7, 2.1 Hz, 1H), 4.99 – 4.78 (m, 1H), 4.62 (q, J = 7.2 Hz, 1H), 4.21 (td, J = 8.3, 5.0 Hz, 1H), 3.27 (d, J = 3.6 Hz, 1H), 3.20 – 2.96 (m, 3H), 2.78 (dd, J = 16.6, 6.1 Hz, 1H), 2.60 (dd, J = 16.7, 7.4 Hz, 1H), 2.24 (dd, J = 9.6, 7.0 Hz, 2H), 2.05 – 1.89 (m, 1H), 1.84 – 1.69 (m, 1H), 1.55 (dt, J = 13.4, 6.7 Hz, 1H), 1.29 (q, J = 7.2 Hz, 2H), 0.85 (d, J = 6.6 Hz, 6H). ^{13}C NMR (126 MHz, DMSO-d_6) δ 174.4, 172.4, 172.0, 170.9, 170.7, 161.0, 136.5, 135.2, 133.4, 133.1, 132.2, 128.5, 128.3, 127.91, 127.90, 127.84, 127.80, 126.4, 125.8, 124.6, 123.9, 121.1, 114.3, 103.3, 54.8, 52.5, 50.2, 38.4, 37.9, 37.3, 36.4, 30.5, 27.9, 25.5, 22.83, 22.80. HRMS (ESI) Calcd for $C_{36}H_{40}ClN_5O_8$ $(M - H)^-$ 704.2487, found 704.2492. HPLC purity 95.6%, t_R = 14.01 min (condition A2); 96.6%, t_R = 16.83 min (condition B2).

(*S*)-4-((*S*)-3-carboxy-2-((*S*)-2-(5-chloro-1*H*-indole-2-carboxamido)-3-(naphthalen-2-yl)propanamido)propanamido)-5-oxo-5-(phenylamino)pentanoic acid (21). ^{1}H NMR (500 MHz, DMSO-d_6) δ 12.30 (s, 2H), 11.63 (d, J = 2.3 Hz, 1H), 9.86 (s, 1H), 8.81 (d, J = 8.5 Hz, 1H), 8.67 (d, J = 7.6 Hz, 1H), 8.13 (d, J = 7.8 Hz, 1H), 7.85 (d, J = 1.6 Hz, 1H), 7.83 – 7.75 (m, 3H), 7.70 (d, J = 2.1 Hz, 1H), 7.62 (d, J = 1.4 Hz, 1H), 7.60 (d, J = 1.2 Hz, 1H), 7.56 (dd, J = 8.5, 1.7 Hz, 1H), 7.48 – 7.39 (m, 2H), 7.36 (d, J = 8.7 Hz, 1H), 7.33 – 7.27 (m, 2H), 7.21 (d, J = 2.0 Hz, 1H), 7.15 (dd, J = 8.7, 2.1 Hz, 1H), 7.10 – 7.03 (m, 1H), 5.12 – 4.82 (m, 1H), 4.67 (td, J = 7.5, 6.0 Hz, 1H), 4.43 (td, J = 8.2, 5.0 Hz, 1H), 3.31 (d, J = 8.8 Hz, 1H), 3.16 (dd, J = 13.9, 11.0 Hz, 1H),

2.81 (dd, *J* = 16.7, 6.0 Hz, 1H), 2.63 (dd, *J* = 16.6, 7.6 Hz, 1H), 2.32 (td, *J* = 10.2, 6.2 Hz, 2H), 2.05 (ddt, *J* = 15.0, 9.9, 5.7 Hz, 1H), 1.89 (ddt, *J* = 13.6, 8.7, 4.7 Hz, 1H). ^{13}C NMR (126 MHz, DMSO-d_6) δ 174.3, 172.4, 172.1, 171.1, 170.3, 161.1, 139.1, 136.5, 135.2, 133.4, 133.1, 132.2, 129.2, 128.5, 128.3, 127.9, 127.89, 127.85, 127.7, 126.4, 125.8, 124.6, 123.99, 123.92, 121.1, 119.9, 114.3, 103.3, 54.8, 53.3, 50.2, 38.0, 36.4, 30.6, 27.8. HRMS (ESI) Calcd for $C_{37}H_{34}ClN_5O_8$ $(M - H)^-$ 710.2018, found 710.2024. HPLC purity 97.9%, t_R = 13.98 min (condition A2); 98.8%, t_R = 16.59 min (condition B2).

(*S*)-4-((*S*)-3-carboxy-2-((*S*)-2-(5-chloro-1*H*-indole-2-carboxamido)-3-(naphthalen-2-yl)propanamido)propanamido)-5-oxo-5-((4-(trifluoromethyl)phenyl)amino)pentanoic acid (30). ^{1}H NMR (500 MHz, DMSO-d_6) δ 12.31 (s, 2H), 11.64 (s, 1H), 10.24 (s, 1H), 8.82 (d, *J* = 8.5 Hz, 1H), 8.67 (d, *J* = 7.6 Hz, 1H), 8.23 (d, *J* = 7.5 Hz, 1H), 7.98 – 7.74 (m, 6H), 7.74 – 7.59 (m, 3H), 7.56 (d, *J* = 8.4 Hz, 1H), 7.48 – 7.30 (m, 3H), 7.21 (s, 1H), 7.14 (d, *J* = 8.8 Hz, 1H), 4.90 (d, *J* = 8.1 Hz, 1H), 4.66 (q, *J* = 7.1 Hz, 1H), 4.42 (q, *J* = 7.1 Hz, 1H), 3.44 – 3.22 (m, 1H), 3.16 (t, *J* = 12.5 Hz, 1H), 2.80 (dd, *J* = 16.8, 5.9 Hz, 1H), 2.62 (dd, *J* = 16.6, 7.6 Hz, 1H), 2.33 (td, *J* = 10.2, 6.3 Hz, 2H), 2.11 – 2.03 (m, 1H), 1.95 – 1.80 (m, 1H). ^{13}C NMR (126 MHz, DMSO-d_6) δ 174.3, 172.4, 172.0, 171.2, 171.0, 161.1, 142.7, 136.5, 135.2, 133.4, 133.1, 132.2, 128.4, 128.3, 127.9, 127.7, 126.45, 126.40, 125.8, 124.6, 123.9, 121.1, 119.8, 114.3, 103.3, 54.8, 53.6, 50.2, 38.0, 36.5, 30.6, 27.5. HRMS (ESI) Calcd for $C_{38}H_{33}ClF_3N_5O_8$ $(M - H)^-$ 778.1892, found 778.1894. HPLC purity 95.1%, t_R = 14.58 min (condition A2); 97.5%, t_R = 17.13 min (condition B2).

(*S*)-4-((*S*)-3-carboxy-2-((*S*)-2-(5-chloro-1*H*-indole-2-carboxamido)-3-(naphthalen-2-yl)propanamido)propanamido)-5-oxo-5-((3-(trifluoromethyl)phenyl)amino)pentanoic acid (31). ^{1}H NMR (500 MHz, DMSO-d_6) δ 12.32 (s, 2H), 11.63 (s, 1H), 10.23 (s, 1H), 8.81 (d, *J* = 8.6 Hz, 1H), 8.66 (d, *J* = 7.6 Hz, 1H), 8.19 (d, *J* = 7.6 Hz, 1H), 8.12 (s, 1H), 7.93 – 7.73 (m, 5H), 7.70

(s, 1H), 7.55 (t, *J* = 7.7 Hz, 2H), 7.47 – 7.33 (m, 4H), 7.21 (s, 1H), 7.15 (d, *J* = 8.8 Hz, 1H), 4.97 – 4.86 (m, 1H), 4.75 – 4.59 (m, 1H), 4.42 (t, *J* = 7.0 Hz, 1H), 3.40-3.31 (m, 1H), 3.16 (t, *J* = 12.5 Hz, 1H), 2.80 (dd, *J* = 16.8, 5.8 Hz, 1H), 2.63 (dd, *J* = 16.7, 7.8 Hz, 1H), 2.34 (dt, *J* = 16.2, 7.7 Hz, 2H), 2.15 – 2.03 (m, 1H), 1.95 – 1.76 (m, 1H). ^{13}C NMR (126 MHz, DMSO-d_6) δ 174.3, 172.3, 172.1, 171.2, 170.9, 161.1, 139.9, 136.5, 135.2, 133.4, 133.1, 132.2, 130.4, 128.5, 128.3, 127.9, 127.8, 127.7, 126.4, 125.8, 124.6, 123.9, 123.5, 121.1, 120.3, 115.9, 114.3, 103.3, 54.8, 53.5, 50.2, 38.0, 36.5, 30.5, 27.5. HRMS (ESI) Calcd for $C_{38}H_{33}ClF_3N_5O_8$ $(M - H)^-$ 778.1892, found 778.1898. HPLC purity 96.5%, t_R = 14.56 min (condition A2); 96.5%, t_R = 17.11 min (condition B2).

(*S*)-4-((*S*)-3-carboxy-2-((*S*)-2-(5-chloro-1*H*-indole-2-carboxamido)-3-(naphthalen-2-yl)propanamido)propanamido)-5-((4-methoxyphenyl)amino)-5-oxopentanoic acid (32). ^{1}H NMR (500 MHz, DMSO-d_6) δ 12.31 (s, 2H), 11.63 (d, *J* = 2.2 Hz, 1H), 9.72 (s, 1H), 8.81 (d, *J* = 8.5 Hz, 1H), 8.69 (d, *J* = 7.5 Hz, 1H), 8.09 (d, *J* = 7.9 Hz, 1H), 7.93 – 7.73 (m, 4H), 7.70 (d, *J* = 2.1 Hz, 1H), 7.56 (dd, *J* = 8.5, 1.7 Hz, 1H), 7.54 – 7.48 (m, 2H), 7.47 – 7.39 (m, 2H), 7.36 (d, *J* = 8.7 Hz, 1H), 7.21 (d, *J* = 2.2 Hz, 1H), 7.15 (dd, *J* = 8.7, 2.1 Hz, 1H), 6.91 – 6.81 (m, 2H), 4.93 – 4.82 (m, 1H), 4.66 (q, *J* = 7.1 Hz, 1H), 4.40 (td, *J* = 8.3, 5.1 Hz, 1H), 3.71 (s, 3H), 3.30 (s, 1H), 3.16 (dd, *J* = 13.9, 11.0 Hz, 1H), 2.81 (dd, *J* = 16.6, 6.0 Hz, 1H), 2.63 (dd, *J* = 16.6, 7.6 Hz, 1H), 2.31 (dq, *J* = 16.6, 10.5 Hz, 2H), 2.11 – 1.99 (m, 1H), 1.87 (dq, *J* = 10.2, 5.3, 4.2 Hz, 1H). ^{13}C NMR (126 MHz, DMSO-d_6) δ 174.3, 172.4, 172.1, 171.0, 169.7, 161.1, 155.9, 136.5, 135.2, 133.4, 133.1, 132.23, 132.20, 128.5, 128.3, 127.9, 127.89, 127.85, 127.7, 126.4, 125.8, 124.6, 123.9, 121.5, 121.1, 114.3, 103.3, 55.6, 54.8, 53.2, 50.2, 38.0, 36.4, 30.5, 27.9. HRMS (ESI) Calcd for $C_{38}H_{36}ClN_5O_9$ $(M - H)^-$ 740.2123, found 740.2128. HPLC purity 96.1%, t_R = 13.87 min (condition A2); 95.8%, t_R = 16.47 min (condition B2).

(*S*)-4-((*S*)-3-carboxy-2-((*S*)-2-(5-chloro-1*H*-indole-2-carboxamido)-3-(naphthalen-2-yl)propanamido)propanamido)-5-((3-methoxyphenyl)amino)-5-oxopentanoic acid (33). ^{1}H NMR (500 MHz, DMSO-d_6) δ 12.31 (s, 2H), 11.63 (d, J = 2.2 Hz, 1H), 9.86 (s, 1H), 8.81 (d, J = 8.5 Hz, 1H), 8.68 (d, J = 7.5 Hz, 1H), 8.11 (d, J = 7.8 Hz, 1H), 7.94 – 7.73 (m, 4H), 7.70 (d, J = 2.1 Hz, 1H), 7.56 (dd, J = 8.4, 1.7 Hz, 1H), 7.42 (pd, J = 6.9, 1.6 Hz, 2H), 7.37 (d, J = 8.7 Hz, 1H), 7.31 (t, J = 2.2 Hz, 1H), 7.25 – 7.18 (m, 2H), 7.17 – 7.10 (m, 2H), 6.65 (dd, J = 8.2, 2.5 Hz, 1H), 4.91 (ddd, J = 11.8, 8.6, 3.7 Hz, 1H), 4.67 (q, J = 7.1 Hz, 1H), 4.41 (td, J = 8.3, 5.1 Hz, 1H), 3.71 (s, 3H), 3.32 (s, 1H), 3.17 (dd, J = 13.9, 11.0 Hz, 1H), 2.81 (dd, J = 16.7, 5.9 Hz, 1H), 2.63 (dd, J = 16.7, 7.7 Hz, 1H), 2.31 (dq, J = 16.6, 10.4 Hz, 2H), 2.14 – 1.91 (m, 1H), 1.88 (dq, J = 10.3, 5.3, 4.3 Hz, 1H). ^{13}C NMR (126 MHz, DMSO-d_6) δ 174.3, 172.3, 172.1, 171.1, 170.3, 161.1, 159.9, 140.3, 136.5, 135.2, 133.4, 133.1, 132.2, 130.0, 128.5, 128.3, 127.9, 127.8, 127.7, 126.4, 125.8, 124.6, 123.9, 121.1, 114.3, 112.2, 109.5, 105.7, 103.3, 55.4, 54.9, 53.4, 50.2, 38.0, 36.4, 30.5, 27.8. HRMS (ESI) Calcd for $C_{38}H_{36}ClN_5O_9$ $(M - H)^-$ 740.2123, found 740.2127. HPLC purity 95.3%, t_R = 14.00 min (condition A2); 97.0%, t_R = 16.60 min (condition B2).

(*S*)-4-((*S*)-3-carboxy-2-((*S*)-2-(5-chloro-1*H*-indole-2-carboxamido)-3-(naphthalen-2-yl)propanamido)propanamido)-5-oxo-5-((4-(trifluoromethoxy)phenyl)amino)pentanoic acid (34). ^{1}H NMR (500 MHz, DMSO-d_6) δ 12.30 (s, 2H), 11.64 (s, 1H), 10.07 (s, 1H), 8.82 (d, J = 8.5 Hz, 1H), 8.67 (d, J = 7.5 Hz, 1H), 8.19 (d, J = 7.7 Hz, 1H), 7.97 – 7.65 (m, 7H), 7.56 (d, J = 8.4 Hz, 1H), 7.50 – 7.26 (m, 5H), 7.23 – 7.01 (m, 2H), 4.91 (ddd, J = 11.9, 8.4, 3.7 Hz, 1H), 4.66 (q, J = 7.1 Hz, 1H), 4.40 (td, J = 8.1, 5.0 Hz, 1H), 3.31 (s, 1H), 3.16 (dd, J = 13.9, 10.9 Hz, 1H), 2.80 (dd, J = 16.7, 6.0 Hz, 1H), 2.62 (dd, J = 16.6, 7.5 Hz, 1H), 2.32 (pd, J = 10.1, 3.2 Hz, 2H), 2.05 (ddt, J = 15.0, 11.1, 5.8 Hz, 1H), 1.89 (dt, J = 14.5, 4.3 Hz, 1H). ^{13}C NMR (126 MHz, DMSO-d_6) δ 174.3, 172.4, 172.1, 171.2, 170.5, 161.1, 138.3, 136.5, 135.2, 133.4, 133.1, 132.2, 128.5,

128.3, 127.9, 127.88, 127.85, 127.7, 126.4, 125.8, 124.6, 123.9, 122.1, 121.3, 121.1, 114.3, 103.3, 54.8, 53.4, 50.2, 38.0, 36.5, 30.5, 27.6. HRMS (ESI) Calcd for $C_{38}H_{33}ClF_3N_5O_9$ $(M - H)^-$ 794.1841, found 794.1846. HPLC purity 100%, t_R = 10.24 min (condition A1); 100%, t_R = 12.59 min (condition B1).

(*S*)-4-((*S*)-3-carboxy-2-((*S*)-2-(5-chloro-1*H*-indole-2-carboxamido)-3-(naphthalen-2-yl)propanamido)propanamido)-5-oxo-5-((3-(trifluoromethoxy)phenyl)amino)pentanoic acid (35). ^{1}H NMR (500 MHz, DMSO-d_6) δ 12.30 (s, 2H), 11.62 (d, *J* = 2.2 Hz, 1H), 10.16 (s, 1H), 8.80 (d, *J* = 8.5 Hz, 1H), 8.66 (d, *J* = 7.5 Hz, 1H), 8.16 (d, *J* = 7.6 Hz, 1H), 7.97 – 7.76 (m, 5H), 7.70 (d, *J* = 2.1 Hz, 1H), 7.55 (ddd, *J* = 10.6, 8.3, 1.8 Hz, 2H), 7.48 – 7.34 (m, 4H), 7.21 (d, *J* = 2.2 Hz, 1H), 7.15 (dd, *J* = 8.7, 2.1 Hz, 1H), 7.05 (dd, *J* = 8.3, 2.3 Hz, 1H), 4.91 (ddd, *J* = 11.8, 8.6, 3.7 Hz, 1H), 4.67 (td, *J* = 7.6, 5.7 Hz, 1H), 4.41 (td, *J* = 8.3, 5.2 Hz, 1H), 3.46 – 3.27 (m, 1H), 3.16 (dd, *J* = 13.9, 10.9 Hz, 1H), 2.81 (dd, *J* = 16.7, 5.8 Hz, 1H), 2.63 (dd, *J* = 16.7, 7.8 Hz, 1H), 2.39 – 2.24 (m, 2H), 2.05 (td, *J* = 8.8, 4.5 Hz, 1H), 1.90 (ddt, *J* = 13.5, 8.7, 4.7 Hz, 1H). ^{13}C NMR (126 MHz, DMSO-d_6) δ 174.2, 172.3, 172.1, 171.2, 170.8, 161.1, 148.9, 140.7, 136.5, 135.2, 133.4, 133.1, 132.2, 130.9, 128.5, 128.3, 127.9, 127.87, 127.84, 127.7, 126.4, 125.8, 124.6, 123.9, 121.5, 121.1, 119.5, 118.5, 116.0, 114.3, 112.0, 103.3, 54.8, 53.5, 50.2, 38.0, 36.4, 30.5, 27.5. HRMS (ESI) Calcd for $C_{38}H_{33}ClF_3N_5O_9$ $(M - H)^-$ 794.1841, found 794.1854. HPLC purity 98.2%, t_R = 14.67 min (condition A2); 100%, t_R = 17.23 min (condition B2).

(*S*)-4-((*S*)-3-carboxy-2-((*S*)-2-(5-chloro-1*H*-indole-2-carboxamido)-3-(naphthalen-2-yl)propanamido)propanamido)-5-((3,5-dimethoxyphenyl)amino)-5-oxopentanoic acid (36). ^{1}H NMR (500 MHz, DMSO-d_6) δ 12.30 (s, 2H), 11.62 (d, *J* = 2.2 Hz, 1H), 9.84 (s, 1H), 8.81 (d, *J* = 8.5 Hz, 1H), 8.68 (d, *J* = 7.5 Hz, 1H), 8.08 (d, *J* = 7.8 Hz, 1H), 7.94 – 7.74 (m, 4H), 7.70 (d, *J* = 2.0 Hz, 1H), 7.56 (dd, *J* = 8.5, 1.7 Hz, 1H), 7.49 – 7.32 (m, 3H), 7.21 (dd, *J* = 2.1, 0.9 Hz, 1H),

7.15 (dd, *J* = 8.7, 2.1 Hz, 1H), 6.87 (d, *J* = 2.3 Hz, 2H), 6.23 (t, *J* = 2.3 Hz, 1H), 5.01 – 4.83 (m, 1H), 4.66 (td, *J* = 7.6, 5.8 Hz, 1H), 4.40 (td, *J* = 8.3, 5.1 Hz, 1H), 3.70 (s, 6H), 3.30 (d, *J* = 3.7 Hz, 1H), 3.17 (dd, *J* = 13.9, 11.0 Hz, 1H), 2.80 (dd, *J* = 16.7, 5.8 Hz, 1H), 2.63 (dd, *J* = 16.7, 7.8 Hz, 1H), 2.38 – 2.23 (m, 2H), 2.11 – 1.96 (m, 1H), 1.87 (ddt, *J* = 13.6, 8.7, 4.8 Hz, 1H). ^{13}C NMR (126 MHz, DMSO-d_6) δ 174.3, 172.3, 172.1, 171.0, 170.3, 161.1, 160.9, 140.7, 136.5, 135.2, 133.4, 133.0, 132.2, 128.5, 128.3, 127.9, 127.88, 127.85, 127.7, 126.4, 125.8, 124.6, 123.9, 121.1, 114.3, 103.4, 98.2, 96.0, 55.5, 54.9, 53.4, 50.2, 38.0, 36.4, 30.5, 27.8. HRMS (ESI) Calcd for $C_{39}H_{38}ClN_5O_{10}$ $(M - H)^-$ 770.2229, found 770.2237. HPLC purity 98.1%, t_R = 14.08 min (condition A2); 97.6%, t_R = 16.69 min (condition B2).

(*S*)-4-((*S*)-3-carboxy-2-((*S*)-2-(5-chloro-1*H*-indole-2-carboxamido)-3-(naphthalen-2-yl)propanamido)propanamido)-5-((3-methoxy-5-(trifluoromethyl)phenyl)amino)-5-oxopentanoic acid (37). ^{1}H NMR (500 MHz, DMSO-d_6) δ 12.30 (s, 2H), 11.62 (s, 1H), 10.19 (s, 1H), 8.80 (d, *J* = 8.5 Hz, 1H), 8.66 (d, *J* = 7.6 Hz, 1H), 8.16 (d, *J* = 7.6 Hz, 1H), 7.92 – 7.75 (m, 4H), 7.74 – 7.68 (m, 1H), 7.66 (s, 1H), 7.55 (s, 1H), 7.51 – 7.35 (m, 4H), 7.31 – 7.19 (m, 1H), 7.15 (dd, *J* = 8.7, 2.1 Hz, 1H), 6.95 (s, 1H), 4.99 – 4.82 (m, 1H), 4.67 (q, *J* = 7.1 Hz, 1H), 4.40 (q, *J* = 7.3 Hz, 1H), 3.80 (s, 3H), 3.42 – 3.28 (m, 1H), 3.25 – 3.05 (m, 1H), 2.81 (dd, *J* = 16.7, 5.7 Hz, 1H), 2.63 (dd, *J* = 16.6, 7.9 Hz, 1H), 2.33 (td, *J* = 9.9, 6.3 Hz, 2H), 2.06 (td, *J* = 11.2, 8.9, 5.3 Hz, 1H), 2.00 – 1.83 (m, 1H). ^{13}C NMR (126 MHz, DMSO-d_6) δ 174.2, 172.3, 172.1, 171.2, 170.9, 161.1, 160.4, 141.1, 136.5, 135.2, 133.4, 133.0, 132.2, 130.9 (d, *J* = 31.8 Hz), 128.5, 128.3, 127.9, 127.87, 127.86, 127.7, 126.4, 125.8, 125.4, 124.6, 123.9, 123.3, 121.1, 114.3, 108.9, 108.4, 105.9, 103.4, 56.1, 54.9, 53.6, 50.2, 37.9, 36.4, 30.5, 27.5. HRMS (ESI) Calcd for $C_{39}H_{35}ClF_3N_5O_9$ $(M - H)^-$ 808.1997, found 808.2004. HPLC purity 99.6%, t_R = 14.68 min (condition A2); 98.3%, t_R = 17.28 min (condition B2).

(*S*)-5-(benzo[*d*][1,3]dioxol-5-ylamino)-4-((*S*)-3-carboxy-2-((*S*)-2-(5-chloro-1*H*-indole-2-carboxamido)-3-(naphthalen-2-yl)propanamido)propanamido)-5-oxopentanoic acid (38). ^{1}H NMR (500 MHz, DMSO-d_6) δ 12.30 (s, 2H), 11.62 (s, 1H), 9.76 (s, 1H), 8.80 (d, J = 8.4 Hz, 1H), 8.67 (d, J = 7.5 Hz, 1H), 8.09 (d, J = 7.7 Hz, 1H), 7.93 – 7.74 (m, 4H), 7.70 (s, 1H), 7.56 (d, J = 8.4 Hz, 1H), 7.42 (p, J = 6.9 Hz, 2H), 7.37 (d, J = 8.7 Hz, 1H), 7.29 (s, 1H), 7.21 (s, 1H), 7.15 (d, J = 8.8 Hz, 1H), 7.00 (d, J = 8.4 Hz, 1H), 6.84 (d, J = 8.3 Hz, 1H), 5.98 (s, 2H), 5.00 – 4.79 (m, 1H), 4.66 (q, J = 7.1 Hz, 1H), 4.38 (q, J = 7.4 Hz, 1H), 3.31 (s, 1H), 3.16 (t, J = 12.5 Hz, 1H), 2.81 (dd, J = 16.8, 6.0 Hz, 1H), 2.63 (dd, J = 16.7, 7.5 Hz, 1H), 2.39 – 2.21 (m, 2H), 2.10 – 1.95 (m, 1H), 1.87 (dt, J = 15.3, 7.8 Hz, 1H). ^{13}C NMR (126 MHz, DMSO-d_6) δ 174.3, 172.4, 172.1, 171.0, 169.9, 161.1, 147.5, 143.6, 136.5, 135.2, 133.4, 133.3, 133.1, 132.2, 128.5, 128.3, 127.9, 127.88, 127.85, 127.7, 126.4, 125.8, 124.6, 123.9, 121.1, 114.3, 112.8, 108.5, 103.3, 102.1, 101.4, 54.8, 53.2, 50.2, 38.0, 36.4, 30.5, 27.8. HRMS (ESI) Calcd for $C_{38}H_{34}ClN_5O_{10}$ $(M-H)^-$ 754.1916, found 754.1924. HPLC purity 98.6%, t_R = 13.83 min (condition A2); 96.1%, t_R = 16.39 min (condition B2).

(*S*)-4-((*S*)-2-((*S*)-2-(5-Chloro-1*H*-indole-2-carboxamido)-3-(naphthalen-2-yl)propanamido)-3-(2*H*-tetrazol-5-yl)propanamido)-5-oxo-5-((4-(trifluoromethoxy)phenyl)amino)pentanoic acid (53). Yield, 82%. ^{1}H NMR (500 MHz, DMSO-d_6) δ 12.14 (s, 1H), 11.69 – 11.53 (m, 1H), 10.25 (s, 1H), 8.79 (d, J = 8.3 Hz, 1H), 8.69 (d, J = 7.5 Hz, 1H), 8.31 (d, J = 7.4 Hz, 1H), 7.90 – 7.64 (m, 8H), 7.53 (d, J = 8.4 Hz, 1H), 7.49 – 7.26 (m, 5H), 7.25 – 7.09 (m, 2H), 4.94 – 4.73 (m, 2H), 4.40 (td, J = 8.0, 5.1 Hz, 1H), 3.56 – 3.41 (m, 2H), 3.14 (dd, J = 13.9, 10.8 Hz, 2H), 2.39 – 2.22 (m, 2H), 2.04 (ddt, J = 15.1, 10.6, 5.7 Hz, 1H), 1.89 (dtd, J = 14.5, 9.0, 5.8 Hz, 1H). ^{13}C NMR (126 MHz, DMSO-d_6) δ 174.2, 172.1, 170.5, 170.4, 161.2, 144.3, 138.2, 136.3, 135.3, 133.4, 133.0, 132.2, 128.4, 128.2, 127.9, 127.8, 126.4, 125.8, 124.7, 124.0, 122.0, 121.5, 121.1, 114.3,

103.4, 55.0, 53.6, 51.7, 37.8, 30.5, 27.6. HRMS (ESI) Calcd for $C_{38}H_{33}ClF_3N_9O_7$ $(M - H)^-$ 818.2065, found 818.2065. HPLC purity 98.5%, t_R = 10.44 min (condition A1); 100%, t_R = 12.85 min (condition B1).

(*S*)-2-((*S*)-2-((*S*)-2-(5-Chloro-1*H*-indole-2-carboxamido)-3-(naphthalen-2-yl)propanamido)-3-(2*H*-tetrazol-5-yl)propanamido)-*N*^{1}-(4-(trifluoromethoxy)phenyl)pentanediamide (55). Yield, 75%. ^{1}H NMR (500 MHz, DMSO-d_6) δ 11.65 (s, 1H), 10.27 (s, 1H), 8.81 (d, *J* = 8.1 Hz, 1H), 8.65 (d, *J* = 7.5 Hz, 1H), 8.29 (d, *J* = 7.1 Hz, 1H), 7.97 – 7.66 (m, 7H), 7.52 (d, *J* = 8.4 Hz, 1H), 7.49 – 7.26 (m, 6H), 7.21 – 7.07 (m, 2H), 6.85 (s, 1H), 4.83 (ddd, *J* = 21.3, 12.4, 5.4 Hz, 2H), 4.35 (q, *J* = 7.0 Hz, 1H), 3.44 (dd, *J* = 15.3, 6.0 Hz, 1H), 3.39 – 3.22 (m, 2H), 3.15 (dd, *J* = 13.9, 10.7 Hz, 1H), 2.18 (t, *J* = 8.0 Hz, 2H), 2.01 (p, *J* = 7.6 Hz, 1H), 1.92 (dq, *J* = 15.2, 8.0 Hz, 1H). ^{13}C NMR (126 MHz, DMSO-d_6) δ 174.1, 172.1, 170.7, 170.3, 161.3, 144.2, 138.3, 136.4, 135.3, 133.4, 132.9, 132.2, 128.4, 128.2, 127.9, 127.8, 127.7, 126.4, 125.9, 124.7, 124.0, 122.0, 121.4, 121.1, 120.6 (d, *J* = 255.0 Hz), 114.3, 103.4, 55.2, 54.0, 51.8, 37.7, 31.7, 28.1, 26.2. HRMS (ESI) Calcd for $C_{38}H_{34}ClF_3N_{10}O_6$ $(M - H)^-$ 817.2225, found 817.2226. HPLC purity 98.3%, t_R = 14.29 min (condition A2); 100%, t_R = 12.78 min (condition B1).

Ethyl (*S*)-4-((*S*)-2-((*S*)-2-(5-chloro-1*H*-indole-2-carboxamido)-3-(naphthalen-2-yl)propanamido)-3-(2*H*-tetrazol-5-yl)propanamido)-5-oxo-5-((4-(trifluoromethoxy)phenyl)amino)pentanoate (56). Yield, 67%. ^{1}H NMR (500 MHz, DMSO-d_6) δ 11.76 – 11.50 (m, 1H), 10.26 -10.22 (m, 1H), 8.91 – 8.63 (m, 2H), 8.37-8.33 (m, 1H), 8.01 – 7.61 (m, 7H), 7.55 – 7.25 (m, 6H), 7.23 – 7.05 (m, 2H), 4.85 (ddt, *J* = 29.7, 14.3, 5.9 Hz, 2H), 4.41 (tt, *J* = 8.7, 4.5 Hz, 1H), 4.13 – 3.86 (m, 2H), 3.62 – 2.91 (m, 4H), 2.38 (qd, *J* = 9.9, 9.3, 4.4 Hz, 2H), 2.07 (td, *J* = 8.7, 4.8 Hz, 1H), 1.91 (dtd, *J* = 14.3, 8.9, 5.8 Hz, 1H), 1.08 (t, *J* = 7.0 Hz, 3H). ^{13}C NMR (126 MHz, DMSO-d_6) δ 172.6, 172.1, 170.4, 161.2, 144.3, 138.2, 136.3, 135.3, 133.4,

133.0, 132.2, 128.4, 128.2, 127.9, 127.7, 126.4, 125.9, 124.7, 124.0, 122.0, 121.5, 121.4, 121.1, 119.6, 114.3, 103.4, 60.4, 55.0, 53.4, 51.7, 37.8, 30.4, 27.5, 14.4. HRMS (ESI) Calcd for $C_{40}H_{37}ClF_3N_9O_7$ $(M - H)^-$ 846.2378, found 846.2375. HPLC purity 98.8%, t_R = 11.13 min (condition A1); 98.7%, t_R = 13.32 min (condition B1).

(*S*)-4-((*S*)-2-((*S*)-2-(4,6-Dichloro-1*H*-indole-2-carboxamido)-3-(naphthalen-2-yl)propanamido)-3-(2*H*-tetrazol-5-yl)propanamido)-5-oxo-5-((4-(trifluoromethoxy)phenyl)amino)pentanoic acid (57). Yield, 83%. ^{1}H NMR (500 MHz, DMSO-d_6) δ 11.90 (d, *J* = 36.1 Hz, 1H), 10.23 (d, *J* = 28.1 Hz, 1H), 8.95 (t, *J* = 7.8 Hz, 1H), 8.73 (dd, *J* = 28.2, 7.8 Hz, 1H), 8.35 (dd, *J* = 42.8, 7.3 Hz, 1H), 7.92 – 7.64 (m, 6H), 7.59 – 7.16 (m, 8H), 5.00 – 4.76 (m, 2H), 4.40 (p, *J* = 7.0 Hz, 1H), 3.31 – 2.97 (m, 4H), 2.33 (ttd, *J* = 16.5, 12.7, 9.8, 6.1 Hz, 2H), 2.06 (dt, *J* = 13.7, 6.2 Hz, 1H), 2.00 – 1.81 (m, 1H). ^{13}C NMR (126 MHz, DMSO-d_6) δ 174.25, 174.22, 172.0, 171.8, 170.5, 170.4, 170.3, 160.7, 144.3, 138.2, 137.24, 137.20, 136.37, 136.34, 133.4, 133.2, 132.2, 128.25, 128.21, 127.9, 127.8, 127.7, 126.8, 126.4, 125.9, 125.1, 122.0, 121.9, 121.6, 121.5, 121.4, 119.9, 119.6, 111.5, 102.0, 55.0, 54.9, 53.7, 53.6, 51.7, 51.6, 37.8, 30.6, 30.5, 27.6, 27.5, 26.2. HRMS (ESI) Calcd for $C_{38}H_{32}Cl_2F_3N_9O_7$ $(M-H)^-$ 852.1676, found 852.1686. HPLC purity 99.0%, t_R = 10.93 min (condition A1); 100%, t_R = 13.60 min (condition B1).

***tert*-Butyl (*S*)-4-(((benzyloxy)carbonyl)amino)-5-(isopentylamino)-5-oxopentanoate (62a).** Yield, 87%. ^{1}H NMR (500 MHz, Chloroform-*d*) δ 7.41 – 7.27 (m, 5H), 6.35 (t, *J* = 5.8 Hz, 1H), 5.76 (d, *J* = 7.9 Hz, 1H), 5.08 (s, 2H), 4.17 (q, *J* = 7.4 Hz, 1H), 3.30 – 3.16 (m, 2H), 2.40 (dt, *J* = 16.5, 7.1 Hz, 1H), 2.28 (dt, *J* = 16.6, 7.0 Hz, 1H), 2.05 (dtd, *J* = 14.3, 7.2, 5.5 Hz, 1H), 1.91 (dt, *J* = 14.4, 7.3 Hz, 1H), 1.66 – 1.51 (m, 1H), 1.43 (s, 11H), 0.89 (d, *J* = 6.6 Hz, 6H). ^{13}C NMR (126 MHz, Chloroform-*d*) δ 172.8, 171.0, 156.2, 136.2, 128.5, 128.2, 128.0, 81.0, 67.0, 54.4, 38.3, 37.9,

31.7, 28.2, 28.1, 25.8, 22.4 (d, J = 2.8 Hz). MS (ESI) m/z = 407.3 $[M + H]^+$, MS (ESI) m/z = 429.2 $[M + Na]^+$.

***tert*-Butyl (*S*)-4-(((benzyloxy)carbonyl)amino)-5-oxo-5-(phenylamino)pentanoate (62b).** Yield, 82%. ^{1}H NMR (500 MHz, Chloroform-*d*) δ 8.60 (s, 1H), 7.42 (d, J = 8.0 Hz, 2H), 7.30 – 7.13 (m, 7H), 7.08 – 6.86 (m, 1H), 5.88 (d, J = 7.8 Hz, 1H), 5.11 – 4.94 (m, 2H), 4.32 (d, J = 6.9 Hz, 1H), 2.41 (dd, J = 16.5, 7.2 Hz, 1H), 2.29 (dt, J = 16.7, 6.9 Hz, 1H), 2.17 – 2.01 (m, 1H), 2.01 – 1.86 (m, 1H), 1.36 (s, 9H). ^{13}C NMR (126 MHz, Chloroform-*d*) δ 173.1, 169.7, 156.6, 137.6, 136.1, 128.9, 128.5, 128.2, 128.0, 124.5, 120.0, 81.3, 67.2, 55.0, 53.5, 31.9, 28.1. MS (ESI) m/z = 435.2 $[M + Na]^+$.

***tert*-Butyl (*S*)-4-(((benzyloxy)carbonyl)amino)-5-oxo-5-((4-(trifluoromethyl)phenyl)amino)pentanoate (62c).** Yield, 79%. ^{1}H NMR (500 MHz, Chloroform-*d*) δ 9.01 (s, 1H), 7.48 (d, J = 8.4 Hz, 2H), 7.39 (d, J = 8.4 Hz, 2H), 7.23 (q, J = 4.1 Hz, 5H), 5.93 (d, J = 7.7 Hz, 1H), 5.14 – 4.94 (m, 2H), 4.32 (d, J = 7.0 Hz, 1H), 2.44 (dt, J = 16.5, 7.0 Hz, 1H), 2.32 – 2.24 (m, 1H), 2.08 (ddt, J = 13.8, 7.8, 6.0 Hz, 1H), 1.96 – 1.82 (m, 1H), 1.36 (s, 9H). ^{13}C NMR (126 MHz, Chloroform-*d*) δ 173.1, 170.2, 156.8, 140.7, 136.0, 128.6, 128.3, 128.0, 126.1 (d, J = 3.7 Hz), 125.9, 124.0 (d, J = 271.5 Hz), 119.4, 81.5, 67.4, 55.2, 31.9, 28.0, 27.8. MS (ESI) m/z = 503.2 $[M + Na]^+$.

***tert*-Butyl (*S*)-4-(((benzyloxy)carbonyl)amino)-5-oxo-5-((3-(trifluoromethyl)phenyl)amino)pentanoate (62d).** Yield, 80%. ^{1}H NMR (500 MHz, Chloroform-*d*) δ 9.23 (s, 1H), 7.87 (s, 1H), 7.58 (s, 1H), 7.30 (t, J = 6.2 Hz, 7H), 6.23 (d, J = 12.1 Hz, 1H), 5.10 (q, J = 12.4 Hz, 2H), 4.48 (d, J = 9.3 Hz, 1H), 2.51 – 2.30 (m, 2H), 2.17 (p, J = 7.4 Hz, 1H), 2.09 – 1.94 (m, 1H), 1.43 (s, 9H). ^{13}C NMR (126 MHz, Chloroform-*d*) δ 172.8, 170.4, 156.9, 138.3 (d, J = 2.5 Hz), 136.0, 131.2 (q, J = 32.1 Hz), 129.4, 128.5, 128.2, 127.9, 123.8 (q, J

= 271.2 Hz), 122.8, 120.8, 116.5 (d, J = 4.1 Hz), 81.3, 67.3, 55.1, 31.7, 28.0, 27.8. MS (ESI) m/z = 503.2 $[M + Na]^+$.

***tert*-Butyl (*S*)-4-(((benzyloxy)carbonyl)amino)-5-((4-methoxyphenyl)amino)-5-oxopentanoate (62e).** Yield, 85%. ^{1}H NMR (500 MHz, Chloroform-*d*) δ 8.48 (s, 1H), 7.39 (d, J = 8.5 Hz, 2H), 7.35 – 7.28 (m, 5H), 6.90 – 6.73 (m, 2H), 5.92 (d, J = 7.8 Hz, 1H), 5.29 – 4.96 (m, 2H), 4.49 – 4.25 (m, 1H), 3.77 (s, 3H), 2.58 – 2.42 (m, 1H), 2.36 (dt, J = 16.6, 6.9 Hz, 1H), 2.15 (dq, J = 13.4, 6.3 Hz, 1H), 2.06 – 1.93 (m, 1H), 1.45 (s, 9H). ^{13}C NMR (126 MHz, Chloroform-*d*) δ 173.1, 169.4, 156.5, 136.1, 130.7, 128.5, 128.2, 128.0, 121.7, 114.1, 81.2, 67.2, 55.5, 54.9, 31.9, 28.2, 28.1. MS (ESI) m/z = 443.1 $[M + H]^+$, MS (ESI) m/z = 465.2 $[M + Na]^+$.

***tert*-Butyl (*S*)-4-(((benzyloxy)carbonyl)amino)-5-((3-methoxyphenyl)amino)-5-oxopentanoate (62f).** Yield, 87%. ^{1}H NMR (500 MHz, Chloroform-*d*) δ 8.75 (s, 1H), 7.28 – 7.14 (m, 6H), 7.05 (t, J = 8.1 Hz, 1H), 6.96 – 6.74 (m, 1H), 6.54 (dd, J = 8.3, 2.5 Hz, 1H), 5.98 (d, J = 8.2 Hz, 1H), 5.05 – 4.89 (m, 2H), 4.33 (d, J = 8.4 Hz, 1H), 3.64 (s, 3H), 2.44 – 2.33 (m, 1H), 2.28 (dt, J = 16.8, 7.0 Hz, 1H), 2.10 – 2.04 (m, 1H), 1.96 – 1.83 (m, 1H), 1.34 (s, 9H). ^{13}C NMR (126 MHz, Chloroform-*d*) δ 172.9, 169.9, 160.1, 156.6, 138.9, 136.1, 129.6, 128.5, 128.2, 128.0, 112.1, 110.5, 105.5, 81.1, 67.2, 55.2, 55.1, 38.6, 31.8, 28.1. MS (ESI) m/z = 465.2 $[M + Na]^+$, MS (ESI) m/z = 907.4 $[2M + Na]^+$.

***tert*-Butyl (*S*)-4-(((benzyloxy)carbonyl)amino)-5-oxo-5-((4-(trifluoromethoxy)phenyl)amino)pentanoate (62g).** Yield, 82%. ^{1}H NMR (500 MHz, Chloroform-*d*) δ 8.97 (s, 1H), 7.75 – 7.40 (m, 2H), 7.31 (d, J = 4.1 Hz, 5H), 7.09 (d, J = 8.6 Hz, 2H), 6.03 (d, J = 7.8 Hz, 1H), 5.10 (d, J = 5.2 Hz, 2H), 4.39 (t, J = 7.2 Hz, 1H), 2.50 (dt, J = 16.6, 7.1 Hz, 1H), 2.38 (dt, J = 16.8, 6.8 Hz, 1H), 2.15 (ddt, J = 13.9, 7.4, 5.9 Hz, 1H), 2.02 (dt, J = 14.4, 7.2 Hz, 1H), 1.44 (s, 9H). ^{13}C NMR (126 MHz, Chloroform-*d*) δ 173.1, 169.9, 156.7, 145.3, 136.3,

136.0, 128.6, 128.3, 128.0, 121.6, 121.0, 120.5 (q, J = 190 Hz), 81.4, 67.3, 55.1, 31.8, 28.0, 27.9. MS (ESI) m/z = 519.2 $[M + Na]^+$

***tert*-Butyl (*S*)-4-(((benzyloxy)carbonyl)amino)-5-oxo-5-((3-(trifluoromethoxy)phenyl)amino)pentanoate (62h).** Yield, 80%. ^{1}H NMR (500 MHz, Chloroform-*d*) δ 9.10 (s, 1H), 7.50 (s, 1H), 7.24 – 7.13 (m, 6H), 7.09 (t, J = 8.2 Hz, 1H), 6.80 (d, J = 8.2 Hz, 1H), 6.10 (d, J = 7.9 Hz, 1H), 4.98 (q, J = 12.3 Hz, 2H), 4.34 (t, J = 7.3 Hz, 1H), 2.36 (dt, J = 16.7, 7.3 Hz, 1H), 2.28 (dt, J = 16.8, 6.9 Hz, 1H), 2.06 (dtd, J = 14.5, 7.2, 5.5 Hz, 1H), 1.97 – 1.85 (m, 1H), 1.33 (s, 9H). ^{13}C NMR (126 MHz, Chloroform-*d*) δ 172.9, 170.3, 156.8, 149.4 (d, J = 1.9 Hz), 139.2, 136.0, 129.8, 128.5, 128.2, 127.9, 120.4 (d, J = 257.2 Hz), 117.9, 116.3, 112.6, 81.3, 67.3, 55.1, 31.7, 28.0, 27.8. MS (ESI) m/z = 519.2 $[M + Na]^+$, MS (ESI) m/z = 495.3 $[M - H]^-$.

***tert*-Butyl (*S*)-4-(((benzyloxy)carbonyl)amino)-5-((3,5-dimethoxyphenyl)amino)-5-oxopentanoate (62i).** Yield, 85%. ^{1}H NMR (500 MHz, Chloroform-*d*) δ 8.62 (s, 1H), 7.33 (d, J = 4.0 Hz, 5H), 6.77 (d, J = 2.3 Hz, 2H), 6.23 (t, J = 2.2 Hz, 1H), 5.88 (d, J = 7.7 Hz, 1H), 5.27 – 4.84 (m, 2H), 4.55 – 4.22 (m, 1H), 3.75 (s, 6H), 2.51 (dt, J = 14.7, 6.8 Hz, 1H), 2.42 – 2.31 (m, 1H), 2.15 (ddt, J = 13.8, 7.5, 6.0 Hz, 1H), 2.01 (dt, J = 14.4, 7.2 Hz, 1H), 1.45 (s, 9H). ^{13}C NMR (126 MHz, Chloroform-*d*) δ 173.1, 169.7, 161.0, 156.6, 139.3, 136.0, 128.5, 128.2, 128.0, 98.1, 97.0, 81.3, 67.2, 55.4, 55.1, 31.9, 28.1. MS (ESI) m/z = 473.3 $[M + H]^+$, MS (ESI) m/z = 495.3 $[M + Na]^+$, MS (ESI) m/z = 967.4 $[2M + Na]^+$

***tert*-Butyl (*S*)-4-(((benzyloxy)carbonyl)amino)-5-((3-methoxy-5-(trifluoromethyl)phenyl)amino)-5-oxopentanoate (62j).** Yield, 81%. ^{1}H NMR (500 MHz, Chloroform-*d*) δ 9.06 (s, 1H), 7.39 – 7.11 (m, 7H), 6.72 (s, 1H), 6.02 (d, J = 7.8 Hz, 1H), 5.01 (q, J = 12.2 Hz, 2H), 4.34 (d, J = 7.1 Hz, 1H), 3.65 (s, 3H), 2.49 – 2.34 (m, 1H), 2.29 (dt, J = 16.7,

6.9 Hz, 1H), 2.11 – 2.00 (m, 1H), 2.02 – 1.88 (m, 1H), 1.34 (s, 9H). ^{13}C NMR (126 MHz, Chloroform-*d*) δ 172.9, 170.3, 160.2, 156.8, 139.5, 135.9, 131.9 (q, *J* = 32.6 Hz), 128.5, 128.3, 128.0, 123.7 (q, *J* = 272.5 Hz), 108.7, 108.3, 106.9 (d, *J* = 4.0 Hz), 81.3, 67.4, 55.5, 55.2, 31.7, 28.0, 27.8. MS (ESI) m/z = 533.2 $[M + Na]^+$, MS (ESI) m/z = 509.2 $[M - H]^-$.

***tert*-Butyl (*S*)-5-(benzo[*d*][1,3]dioxol-5-ylamino)-4-(((benzyloxy)carbonyl)amino)-5-oxopentanoate (62k).** Yield, 85%. ^{1}H NMR (500 MHz, Chloroform-*d*) δ 8.75 (s, 1H), 7.27 – 7.13 (m, 5H), 7.07 (d, *J* = 2.2 Hz, 1H), 6.65 (dd, *J* = 8.4, 2.1 Hz, 1H), 6.52 (d, *J* = 8.3 Hz, 1H), 6.13 (d, *J* = 8.0 Hz, 1H), 5.77 (s, 2H), 5.10 – 4.78 (m, 2H), 4.32 (d, *J* = 7.3 Hz, 1H), 2.30 (qt, *J* = 16.6, 7.3 Hz, 2H), 2.11 – 1.99 (m, 1H), 1.92 (dt, *J* = 14.4, 7.4 Hz, 1H), 1.33 (s, 9H). ^{13}C NMR (126 MHz, Chloroform-*d*) δ 172.7, 169.8, 156.7, 147.6, 144.2, 136.1, 131.9, 128.5, 128.1, 127.9, 113.3, 107.9, 102.8, 101.2, 81.0, 67.1, 55.0, 31.8, 28.1. MS (ESI) m/z = 457.3 $[M + H]^+$, MS (ESI) m/z = 479.2 $[M + Na]^+$, MS (ESI) m/z = 935.4 $[2M + Na]^+$.

***tert*-Butyl (*S*)-4-((*S*)-2-(((benzyloxy)carbonyl)amino)-4-(*tert*-butoxy)-4-oxobutanamido)-5-(isopentylamino)-5-oxopentanoate (63a).** Yield, 86%. ^{1}H NMR (500 MHz, Chloroform-*d*) δ 7.46 – 7.28 (m, 6H), 6.57 (d, *J* = 5.9 Hz, 1H), 5.86 (d, *J* = 8.3 Hz, 1H), 5.12 (q, *J* = 12.2 Hz, 2H), 4.46 (dt, *J* = 8.5, 5.4 Hz, 1H), 4.35 (td, *J* = 8.1, 4.7 Hz, 1H), 3.31 – 3.15 (m, 2H), 2.89 (dd, *J* = 16.9, 4.7 Hz, 1H), 2.70 (dd, *J* = 16.9, 6.1 Hz, 1H), 2.43 – 2.34 (m, 1H), 2.33 – 2.23 (m, 1H), 2.17 – 2.05 (m, 1H), 1.95 (dq, *J* = 14.5, 7.1 Hz, 1H), 1.58 (td, *J* = 13.3, 6.6 Hz, 1H), 1.42 (d, *J* = 5.0 Hz, 20H), 0.89 (dd, *J* = 6.6, 0.9 Hz, 6H). ^{13}C NMR (126 MHz, Chloroform-*d*) δ 173.6, 170.9, 170.7, 170.4, 156.1, 136.0, 128.6, 128.3, 128.1, 81.9, 81.0, 67.3, 53.3, 51.67, 38.3, 37.9, 37.3, 31.7, 28.05, 28.03, 27.1, 25.8, 22.4. MS (ESI) m/z = 600.3 $[M + Na]^+$.

***tert*-Butyl (*S*)-4-((*S*)-2-(((benzyloxy)carbonyl)amino)-4-(*tert*-butoxy)-4-oxobutanamido)-5-oxo-5-(phenylamino)pentanoate (63b).** Yield, 83%. ^{1}H NMR (500 MHz, Chloroform-*d*) δ 8.69

(s, 1H), 7.60 (t, *J* = 8.9 Hz, 3H), 7.46 – 7.22 (m, 7H), 7.15 – 6.99 (m, 1H), 5.91 (d, *J* = 8.2 Hz, 1H), 5.24 – 5.02 (m, 2H), 4.53 (tt, *J* = 10.3, 5.3 Hz, 2H), 2.92 (dd, *J* = 16.9, 4.8 Hz, 1H), 2.73 (dd, *J* = 16.9, 6.1 Hz, 1H), 2.51 (ddd, *J* = 17.1, 8.2, 5.6 Hz, 1H), 2.36 (ddd, *J* = 17.1, 7.3, 5.6 Hz, 1H), 2.25 – 2.16 (m, 1H), 2.05 (dt, *J* = 14.5, 7.4 Hz, 1H), 1.44 (s, 9H), 1.41 (s, 9H). ^{13}C NMR (126 MHz, Chloroform-*d*) δ 173.8, 171.1, 170.9, 168.9, 156.2, 137.8, 136.0, 128.8, 128.6, 128.3, 128.2, 124.3, 120.1, 82.1, 81.3, 67.4, 53.9, 51.8, 37.3, 31.8, 28.1, 28.0, 26.9. MS (ESI) m/z = 606.3 $[M + Na]^+$.

***tert*-Butyl (*S*)-4-((*S*)-2-(((benzyloxy)carbonyl)amino)-4-(*tert*-butoxy)-4-oxobutanamido)-5-oxo-5-((4-(trifluoromethyl)phenyl)amino)pentanoate (63c).** Yield, 82%. ^{1}H NMR (500 MHz, Acetone-d_6) δ 9.50 (s, 1H), 7.94 (d, *J* = 8.4 Hz, 2H), 7.84 (d, *J* = 8.0 Hz, 1H), 7.65 (d, *J* = 8.5 Hz, 2H), 7.44 – 7.17 (m, 5H), 6.91 (d, *J* = 7.6 Hz, 1H), 5.23 – 4.97 (m, 2H), 4.77 – 4.37 (m, 2H), 2.95 – 2.83 (m, 1H), 2.76 (dd, *J* = 16.5, 6.8 Hz, 1H), 2.38 (ddd, *J* = 11.3, 9.1, 6.3 Hz, 2H), 2.28 – 2.18 (m, 1H), 2.00 – 1.83 (m, 1H), 1.41 (s, 9H), 1.41 (s, 9H). ^{13}C NMR (126 MHz, Acetone-d_6) δ 171.8, 171.0, 170.2, 170.0, 156.5, 142.3, 136.9, 128.4, 127.9, 127.8, 125.9 (q, *J* = 3.8 Hz), 124.7 (d, *J* = 32.5 Hz), 124.5 (d, *J* = 268.7 Hz), 119.5, 119.4, 80.7, 79.7, 66.3, 53.5, 52.2, 37.0, 31.2, 27.4, 27.3, 26.8. MS (ESI) m/z = 674.3 $[M + Na]^+$.

***tert*-Butyl (*S*)-4-((*S*)-2-(((benzyloxy)carbonyl)amino)-4-(*tert*-butoxy)-4-oxobutanamido)-5-oxo-5-((3-(trifluoromethyl)phenyl)amino)pentanoate (63d).** Yield, 83%. ^{1}H NMR (500 MHz, Chloroform-*d*) δ 9.06 (s, 1H), 7.84 (s, 1H), 7.78 – 7.59 (m, 2H), 7.41 – 6.94 (m, 7H), 6.04 (d, *J* = 9.7 Hz, 1H), 5.23 – 4.85 (m, 2H), 4.60 – 4.33 (m, 2H), 2.85 – 2.66 (m, 2H), 2.42 – 2.21 (m, 2H), 2.18 – 2.06 (m, 1H), 1.99 – 1.88 (m, 1H), 1.40 – 1.32 (m, 9H), 1.30 (d, *J* = 2.3 Hz, 9H). ^{13}C NMR (126 MHz, Chloroform-*d*) δ 173.4, 171.4, 170.8, 169.6, 156.3, 138.5, 136.0, 131.0 (q, *J* = 32.5 Hz), 129.3, 128.5, 128.2, 128.0, 123.9 (q, *J* = 271.2 Hz), 123.2, 120.7 (d, *J* = 4.0 Hz), 116.8 (d, *J*

= 4.3 Hz), 82.1, 81.2, 67.3, 53.9, 51.9, 37.3, 31.7, 28.0, 27.9, 26.7. MS (ESI) m/z = 674.2 [M + Na]$^+$.

***tert*-Butyl (*S*)-4-((*S*)-2-(((benzyloxy)carbonyl)amino)-4-(*tert*-butoxy)-4-oxobutanamido)-5-((4-methoxyphenyl)amino)-5-oxopentanoate (63e).** Yield, 82%. ^{1}H NMR (500 MHz, Chloroform-*d*) δ 8.56 (s, 1H), 7.59 (d, *J* = 7.4 Hz, 1H), 7.48 (d, *J* = 8.6 Hz, 2H), 7.37 – 7.27 (m, 5H), 6.90 – 6.65 (m, 2H), 5.92 (d, *J* = 8.1 Hz, 1H), 5.13 (q, *J* = 12.2 Hz, 2H), 4.52 (tt, *J* = 10.3, 5.3 Hz, 2H), 3.77 (s, 3H), 2.90 (dd, *J* = 16.9, 4.9 Hz, 1H), 2.73 (dd, *J* = 16.8, 6.1 Hz, 1H), 2.48 (ddd, *J* = 17.0, 8.0, 5.9 Hz, 1H), 2.40 – 2.29 (m, 1H), 2.23 – 2.12 (m, 1H), 2.04 (d, *J* = 2.7 Hz, 1H), 1.43 (s, 9H), 1.40 (s, 9H). ^{13}C NMR (126 MHz, Chloroform-*d*) δ 173.7, 171.0, 170.9, 168.7, 156.4, 156.2, 136.0, 131.0, 128.6, 128.3, 128.1, 121.8, 114.0, 82.1, 81.2, 67.4, 55.5, 53.7, 51.8, 37.3, 31.8, 28.1, 28.0, 26.9. MS (ESI) m/z = 614.3 [M + H]$^+$, MS (ESI) m/z = 636.3 [M + Na]$^+$.

***tert*-Butyl (*S*)-4-((*S*)-2-(((benzyloxy)carbonyl)amino)-4-(*tert*-butoxy)-4-oxobutanamido)-5-((3-methoxyphenyl)amino)-5-oxopentanoate (63f).** Yield, 88%. ^{1}H NMR (500 MHz, Chloroform-*d*) δ 8.79 (s, 1H), 7.61 (d, *J* = 7.6 Hz, 1H), 7.33 – 7.13 (m, 6H), 7.08 – 6.92 (m, 2H), 6.53 (ddd, *J* = 8.1, 2.5, 1.0 Hz, 1H), 6.05 (d, *J* = 8.2 Hz, 1H), 5.18 – 4.94 (m, 2H), 4.61 – 4.41 (m, 2H), 3.65 (s, 3H), 2.77 (dd, *J* = 16.8, 5.3 Hz, 1H), 2.65 (dd, *J* = 16.8, 6.2 Hz, 1H), 2.39 – 2.30 (m, 1H), 2.26 (dt, *J* = 16.8, 6.8 Hz, 1H), 2.11 (dt, *J* = 13.4, 6.9 Hz, 1H), 1.94 (q, *J* = 5.7, 4.2 Hz, 1H), 1.33 (s, 9H), 1.30 (s, 9H). ^{13}C NMR (126 MHz, Chloroform-*d*) δ 173.2, 171.3, 170.7, 169.2, 160.0, 156.2, 139.1, 136.0, 129.4, 128.5, 128.2, 128.1, 112.4, 110.3, 105.7, 81.9, 81.0, 67.3, 55.2, 53.7, 51.8, 37.4, 31.7, 28.0, 27.9, 27.1. MS (ESI) m/z = 636.3 [M + Na]$^+$.

***tert*-Butyl (*S*)-4-((*S*)-2-(((benzyloxy)carbonyl)amino)-4-(*tert*-butoxy)-4-oxobutanamido)-5-oxo-5-((4-(trifluoromethoxy)phenyl)amino)pentanoate (63g).** Yield, 87%. ^{1}H NMR (500 MHz, Chloroform-*d*) δ 8.95 (s, 1H), 7.70 (d, *J* = 7.4 Hz, 1H), 7.54 (d, *J* = 8.6 Hz, 2H), 7.38 – 7.15 (m,

5H), 7.08 – 6.87 (m, 2H), 6.04 (d, *J* = 8.0 Hz, 1H), 5.36 – 4.93 (m, 2H), 4.49 (dp, *J* = 18.7, 6.4, 5.7 Hz, 2H), 2.77 (dd, *J* = 16.9, 5.2 Hz, 1H), 2.70 (d, *J* = 6.3 Hz, 1H), 2.51 – 2.31 (m, 1H), 2.27 (dt, *J* = 16.9, 6.6 Hz, 1H), 2.18 – 2.10 (m, 1H), 1.95 (q, *J* = 7.3, 6.9 Hz, 1H), 1.33 (s, 9H), 1.30 (s, 9H). ^{13}C NMR (126 MHz, Chloroform-*d*) δ 173.4, 171.4, 170.8, 169.3, 156.3, 145.2 (d, *J* = 2.0 Hz), 136.6, 136.0, 128.5, 128.2, 128.0, 121.4, 121.2, 119.4, 82.0, 81.2, 67.3, 53.9, 51.8, 37.3, 31.7, 28.0, 27.9, 26.8. MS (ESI) m/z = 690.3 $[M + Na]^+$.

***tert*-Butyl (*S*)-4-((*S*)-2-(((benzyloxy)carbonyl)amino)-4-(*tert*-butoxy)-4-oxobutanamido)-5-oxo-5-((3-(trifluoromethoxy)phenyl)amino)pentanoate (63h).** Yield, 84%. ^{1}H NMR (500 MHz, Chloroform-*d*) δ 8.87 (s, 1H), 7.60 (d, *J* = 19.4 Hz, 2H), 7.51 – 7.40 (m, 1H), 7.31 – 7.13 (m, 6H), 6.87 (ddt, *J* = 8.2, 2.3, 1.1 Hz, 1H), 5.83 (d, *J* = 7.7 Hz, 1H), 5.33 – 4.95 (m, 2H), 4.66 – 4.29 (m, 2H), 2.82 (dd, *J* = 16.8, 4.9 Hz, 1H), 2.70 (dd, *J* = 16.8, 6.2 Hz, 1H), 2.43 (ddd, *J* = 17.2, 8.4, 5.3 Hz, 1H), 2.32 – 2.24 (m, 1H), 2.13 (ddd, *J* = 13.8, 8.4, 4.3 Hz, 1H), 1.99 (dd, *J* = 14.0, 6.6 Hz, 1H), 1.37 (s, 9H), 1.34 (s, 9H). ^{13}C NMR (126 MHz, Chloroform-*d*) δ 174.0, 171.2, 170.9, 169.2, 156.3, 149.4, 139.3, 135.9, 129.8, 128.6, 128.3, 128.1, 120.4 (d, *J* = 257.3 Hz), 118.1, 116.3, 112.9, 82.3, 81.5, 67.4, 54.0, 51.9, 37.2, 31.8, 28.0, 27.9, 26.5. MS (ESI) m/z = 668.3 $[M + H]^+$, MS (ESI) m/z = 690.3 $[M + Na]^+$.

***tert*-Butyl (*S*)-4-((*S*)-2-(((benzyloxy)carbonyl)amino)-4-(*tert*-butoxy)-4-oxobutanamido)-5-((3,5-dimethoxyphenyl)amino)-5-oxopentanoate (63i).** Yield, 87%. ^{1}H NMR (500 MHz, Chloroform-*d*) δ 8.64 (s, 1H), 7.59 (d, *J* = 7.4 Hz, 1H), 7.40 – 7.27 (m, 5H), 6.86 (d, *J* = 2.3 Hz, 2H), 6.22 (t, *J* = 2.3 Hz, 1H), 5.91 (d, *J* = 8.1 Hz, 1H), 5.31 – 5.03 (m, 2H), 4.51 (td, *J* = 7.8, 4.7 Hz, 2H), 3.76 (s, 6H), 2.92 (dd, *J* = 16.9, 4.9 Hz, 1H), 2.72 (dd, *J* = 16.9, 6.0 Hz, 1H), 2.50 (ddd, *J* = 17.1, 8.2, 5.6 Hz, 1H), 2.35 (ddd, *J* = 17.1, 7.2, 5.5 Hz, 1H), 2.23 – 2.09 (m, 1H), 2.11 – 1.96 (m, 1H), 1.44 (s, 9H), 1.41 (s, 9H). ^{13}C NMR (126 MHz, Chloroform-*d*) δ 173.8, 171.2, 170.8,

169.0, 160.9, 156.2, 139.5, 135.9, 128.6, 128.3, 128.1, 98.3, 97.0, 82.1, 81.3, 67.4, 55.4, 53.9, 51.8, 37.2, 31.8, 28.1, 28.0, 26.9. MS (ESI) m/z = 644.3 $[M + H]^+$, MS (ESI) m/z = 666.3 $[M + Na]^+$.

***tert*-Butyl (*S*)-4-((*S*)-2-(((benzyloxy)carbonyl)amino)-4-(*tert*-butoxy)-4-oxobutanamido)-5-((3-methoxy-5-(trifluoromethyl)phenyl)amino)-5-oxopentanoate (63j).** Yield, 86%. ^{1}H NMR (500 MHz, Chloroform-*d*) δ 8.98 – 8.91 (m, 1H), 7.71 (d, *J* = 7.2 Hz, 1H), 7.63 (s, 1H), 7.43 – 7.27 (m, 6H), 6.94 – 6.80 (m, 1H), 6.00 – 5.76 (m, 1H), 5.30 – 5.06 (m, 2H), 4.66 – 4.35 (m, 2H), 3.82 (d, *J* = 0.9 Hz, 3H), 2.95 – 2.84 (m, 1H), 2.79 (dd, *J* = 16.8, 6.2 Hz, 1H), 2.50 (dtd, *J* = 17.3, 5.9, 5.3, 2.9 Hz, 1H), 2.37 (ddd, *J* = 17.2, 7.4, 5.2 Hz, 1H), 2.20 (ddd, *J* = 13.4, 9.1, 4.5 Hz, 1H), 2.08 (dt, *J* = 14.6, 7.4 Hz, 1H), 1.44 (s, 9H), 1.41 (s, 9H). ^{13}C NMR (126 MHz, Chloroform-*d*) δ 174.0 (d, *J* = 3.1 Hz), 171.2, 170.9, 169.4, 160.2, 156.3, 139.7, 135.9, 131.9 (d, *J* = 32.5 Hz), 128.6, 128.1, 123.8 (d, *J* = 272.5 Hz), 109.1, 108.6, 106.9 (d, *J* = 3.9 Hz), 82.3, 81.5, 67.4, 55.6, 54.1, 51.9, 37.2, 31.8, 28.0, 27.9, 26.4. MS (ESI) m/z = 682.3 $[M + H]^+$, MS (ESI) m/z = 704.3 $[M + Na]^+$.

***tert*-Butyl (*S*)-5-(benzo[*d*][1,3]dioxol-5-ylamino)-4-((*S*)-2-(((benzyloxy)carbonyl)amino)-4-(*tert*-butoxy)-4-oxobutanamido)-5-oxopentanoate (63k).** Yield, 88%. ^{1}H NMR (500 MHz, Chloroform-*d*) δ 8.61 (q, *J* = 5.9, 4.6 Hz, 1H), 7.54 (d, *J* = 7.4 Hz, 1H), 7.38 – 7.10 (m, 6H), 6.84 (d, *J* = 8.4 Hz, 1H), 6.61 (dq, *J* = 8.5, 1.7 Hz, 1H), 5.91 (d, *J* = 8.8 Hz, 1H), 5.83 (q, *J* = 1.6 Hz, 2H), 5.05 (q, *J* = 12.4 Hz, 2H), 4.45 (q, *J* = 6.8, 6.2 Hz, 2H), 2.79 (d, *J* = 3.7 Hz, 1H), 2.67 (dd, *J* = 16.9, 6.2 Hz, 1H), 2.48 – 2.31 (m, 1H), 2.27 (dt, *J* = 16.8, 6.6 Hz, 1H), 2.16 – 2.05 (m, 1H), 2.04 – 1.84 (m, 1H), 1.35 (d, *J* = 1.6 Hz, 9H), 1.33 (d, *J* = 1.5 Hz, 9H). ^{13}C NMR (126 MHz, Chloroform-*d*) δ 173.5, 171.1, 170.8, 168.8, 156.2, 147.6, 144.2, 136.0, 132.1, 128.5, 128.3, 128.1, 113.3, 107.9, 102.8, 101.1, 82.0, 81.2, 67.3, 53.7, 51.8, 37.3, 31.8, 28.1, 28.0, 27.0. MS (ESI) m/z = 628.3 $[M + H]^+$, MS (ESI) m/z = 650.3 $[M + Na]^+$.

***tert*-Butyl (5*S*,8*S*,11*S*)-8-(2-(*tert*-butoxy)-2-oxoethyl)-11-(isopentylcarbamoyl)-5-(naphthalen-2-ylmethyl)-3,6,9-trioxo-1-phenyl-2-oxa-4,7,10-triazatetradecan-14-oate (64a).** Yield, 81%. ^{1}H NMR (500 MHz, Chloroform-*d*) δ 7.75 – 7.59 (m, 3H), 7.58 – 7.52 (m, 2H), 7.44 (d, *J* = 8.1 Hz, 1H), 7.40 – 7.28 (m, 2H), 7.26 – 7.01 (m, 6H), 6.67 (t, *J* = 5.6 Hz, 1H), 5.54 (d, *J* = 5.7 Hz, 1H), 4.94 (s, 2H), 4.61 (ddd, *J* = 7.9, 6.4, 4.5 Hz, 1H), 4.54 – 4.41 (m, 1H), 4.33 (td, *J* = 8.6, 4.5 Hz, 1H), 3.27 (dd, *J* = 14.2, 5.0 Hz, 1H), 3.19 – 3.00 (m, 3H), 2.80 (dd, *J* = 16.9, 4.4 Hz, 1H), 2.53 (dd, *J* = 16.9, 6.5 Hz, 1H), 2.24 – 2.04 (m, 3H), 1.90 – 1.76 (m, 1H), 1.52 (dp, *J* = 13.3, 6.6 Hz, 1H), 1.30 (s, 9H), 1.28 (s, 11H), 0.81 (dd, *J* = 6.7, 3.0 Hz, 6H). ^{13}C NMR (126 MHz, Chloroform-*d*) δ 172.6, 171.6, 171.0, 170.5, 170.2, 156.7, 135.7, 133.4, 132.5, 128.6, 128.5, 128.3, 128.2, 128.0, 127.7, 127.6, 127.0, 126.3, 125.9, 82.0, 80.5, 67.5, 56.7, 53.1, 50.2, 38.2, 38.0, 36.5, 31.9, 28.1, 28.0, 27.1, 22.52, 22.50. MS (ESI) m/z = 775.2 $[M + H]^+$, MS (ESI) m/z = 797.2 $[M + Na]^+$.

***tert*-Butyl (5*S*,8*S*,11*S*)-8-(2-(*tert*-butoxy)-2-oxoethyl)-5-(naphthalen-2-ylmethyl)-3,6,9-trioxo-1-phenyl-11-(phenylcarbamoyl)-2-oxa-4,7,10-triazatetradecan-14-oate (64b).** Yield, 85%. ^{1}H NMR (500 MHz, DMSO-d_6) δ 9.92 (s, 1H), 8.55 (d, *J* = 7.9 Hz, 1H), 8.07 (d, *J* = 7.9 Hz, 1H), 7.88 (dd, *J* = 6.9, 2.2 Hz, 1H), 7.86 – 7.75 (m, 3H), 7.69 – 7.58 (m, 3H), 7.56 – 7.41 (m, 3H), 7.37 – 7.27 (m, 2H), 7.27 – 7.11 (m, 5H), 7.09 – 6.98 (m, 1H), 4.90 (d, *J* = 2.3 Hz, 2H), 4.66 (td, *J* = 7.8, 6.1 Hz, 1H), 4.43 (tdd, *J* = 10.9, 7.9, 4.3 Hz, 2H), 3.19 (dd, *J* = 13.9, 3.7 Hz, 1H), 2.94 (dd, *J* = 13.8, 10.9 Hz, 1H), 2.77 (dd, *J* = 16.2, 6.0 Hz, 1H), 2.56 (dd, *J* = 16.2, 7.8 Hz, 1H), 2.37 – 2.20 (m, 2H), 2.01 (ddd, *J* = 14.0, 6.8, 3.4 Hz, 1H), 1.90 – 1.73 (m, 1H), 1.38 (s, 9H), 1.32 (s, 9H). ^{13}C NMR (126 MHz, DMSO-d_6) δ 172.2, 172.0, 170.7, 170.1, 169.9, 156.3, 139.1, 137.4, 136.3, 133.4, 132.3, 129.2, 128.6, 128.3, 128.1, 127.99, 127.97, 127.91, 127.80, 127.7, 126.4, 125.9, 124.0,

119.8, 80.8, 80.2, 65.6, 56.6, 53.2, 50.1, 38.1, 37.6, 31.6, 28.13, 28.11, 27.8. MS (ESI) m/z = 781.1 $[M + H]^+$, MS (ESI) m/z = 803.1 $[M + Na]^+$.

***tert*-Butyl (5*S*,8*S*,11*S*)-8-(2-(*tert*-butoxy)-2-oxoethyl)-5-(naphthalen-2-ylmethyl)-3,6,9-trioxo-1-phenyl-11-((4-(trifluoromethyl)phenyl)carbamoyl)-2-oxa-4,7,10-triazatetradecan-14-oate (64c).** Yield, 74%. ^{1}H NMR (500 MHz, Chloroform-*d*) δ 8.81 (d, *J* = 7.1 Hz, 1H), 7.88 (d, *J* = 8.2 Hz, 2H), 7.85 – 7.62 (m, 6H), 7.59 – 7.51 (m, 2H), 7.51 – 7.43 (m, 2H), 7.35 – 7.12 (m, 6H), 5.33 (t, *J* = 9.6 Hz, 1H), 5.14 – 4.93 (m, 2H), 4.71 – 4.62 (m, 1H), 4.55 (d, *J* = 8.6 Hz, 1H), 4.48 (q, *J* = 5.1, 4.5 Hz, 1H), 3.43 (dd, *J* = 14.5, 4.9 Hz, 1H), 3.15 (dd, *J* = 14.2, 8.9 Hz, 1H), 3.00 (dd, *J* = 17.2, 4.4 Hz, 1H), 2.70 – 2.56 (m, 1H), 2.33 (p, *J* = 4.1 Hz, 3H), 2.01 – 1.91 (m, 1H), 1.41 (s, 9H), 1.36 (s, 9H). ^{13}C NMR (126 MHz, Chloroform-*d*) δ 172.4, 172.2, 171.2, 170.5, 169.6, 157.1, 141.3, 135.3, 133.4, 132.8, 132.6, 129.0, 128.6, 128.5, 128.3, 127.9, 127.8, 127.6, 126.6, 126.5, 126.2, 126.02, 125.96, 125.90, 125.6, 125.3, 123.2, 119.7, 82.5, 80.7, 68.0, 57.2, 53.9, 50.8, 37.7, 35.7, 32.1, 28.0, 27.9, 26.5. MS (ESI) m/z = 871.3 $[M + Na]^+$.

***tert*-Butyl (5*S*,8*S*,11*S*)-8-(2-(*tert*-butoxy)-2-oxoethyl)-5-(naphthalen-2-ylmethyl)-3,6,9-trioxo-1-phenyl-11-((3-(trifluoromethyl)phenyl)carbamoyl)-2-oxa-4,7,10-triazatetradecan-14-oate (64d).** Yield, 76%. ^{1}H NMR (500 MHz, Chloroform-*d*) δ 8.95 (s, 1H), 7.95 (s, 1H), 7.89 – 7.70 (m, 3H), 7.65 – 7.53 (m, 3H), 7.48 (d, *J* = 1.6 Hz, 1H), 7.28 (dd, *J* = 6.2, 3.3 Hz, 2H), 7.22 – 7.14 (m, 3H), 7.14 – 6.99 (m, 5H), 5.85 (d, *J* = 6.2 Hz, 1H), 4.89 (q, *J* = 12.3 Hz, 2H), 4.78 – 4.69 (m, 1H), 4.66 – 4.56 (m, 1H), 4.51 (q, *J* = 8.3, 5.8 Hz, 1H), 3.23 (dd, *J* = 14.3, 4.9 Hz, 1H), 3.04 (dd, *J* = 14.1, 8.8 Hz, 1H), 2.75 (dd, *J* = 17.1, 4.6 Hz, 1H), 2.61 (dd, *J* = 16.9, 7.0 Hz, 1H), 2.37 – 2.11 (m, 3H), 1.95 – 1.81 (m, 1H), 1.25 (s, 9H), 1.24 (s, 9H). ^{13}C NMR (126 MHz, Chloroform-*d*) δ 172.4, 172.2, 170.9 (d, *J* = 3.1 Hz), 169.7, 156.9, 138.8, 135.7, 133.5, 132.5, 131.0 (d, *J* = 32.2 Hz), 129.3, 128.55, 128.51, 128.4, 128.3, 128.1, 127.7, 127.6, 127.0, 126.3, 125.9, 125.1, 123.2,

123.0, 120.6, 116.9 (d, *J* = 4.0 Hz), 82.2, 80.8, 67.5, 56.8, 53.8, 50.4, 38.4, 36.7, 31.8, 28.0, 27.9, 26.9. MS (ESI) m/z = 871.3 $[M + Na]^+$.

***tert*-Butyl (5*S*,8*S*,11*S*)-8-(2-(*tert*-butoxy)-2-oxoethyl)-11-((4-methoxyphenyl)carbamoyl)-5-(naphthalen-2-ylmethyl)-3,6,9-trioxo-1-phenyl-2-oxa-4,7,10-triazatetradecan-14-oate (64e).** Yield, 83%. ^{1}H NMR (500 MHz, Chloroform-*d*) δ 8.46 (s, 1H), 7.77 – 7.62 (m, 3H), 7.58 – 7.48 (m, 5H), 7.38 – 7.34 (m, 2H), 7.26 – 7.11 (m, 6H), 6.74 (d, *J* = 9.0 Hz, 2H), 5.42 (d, *J* = 5.5 Hz, 1H), 4.95 (d, *J* = 2.7 Hz, 2H), 4.63 (ddd, *J* = 7.7, 6.2, 4.4 Hz, 1H), 4.46 (q, *J* = 5.5, 4.8 Hz, 2H), 3.68 (s, 3H), 3.40 – 3.20 (m, 1H), 3.07 (dd, *J* = 14.2, 8.6 Hz, 1H), 2.85 (dd, *J* = 17.2, 4.4 Hz, 1H), 2.54 (dd, *J* = 17.0, 6.3 Hz, 1H), 2.31 – 2.15 (m, 3H), 1.90 (dt, *J* = 11.9, 3.7 Hz, 1H), 1.29 (s, 9H), 1.28 (s, 9H). ^{13}C NMR (126 MHz, Chloroform-*d*) δ 172.6, 171.9, 171.1, 170.4, 168.8, 156.8, 156.3, 135.6, 133.4, 133.2, 132.6, 131.3, 128.7, 128.5, 128.3, 128.2, 128.0, 127.7, 127.6, 126.9, 126.4, 126.0, 121.7, 113.9, 82.2, 80.6, 67.6, 56.9, 55.4, 53.7, 50.4, 37.9, 36.2, 32.0, 28.0, 27.9, 26.9. MS (ESI) m/z = 833.3 $[M + Na]^+$.

***tert*-Butyl (5*S*,8*S*,11*S*)-8-(2-(*tert*-butoxy)-2-oxoethyl)-11-((3-methoxyphenyl)carbamoyl)-5-(naphthalen-2-ylmethyl)-3,6,9-trioxo-1-phenyl-2-oxa-4,7,10-triazatetradecan-14-oate (64f).** Yield, 80%. ^{1}H NMR (500 MHz, Chloroform-*d*) δ 8.65 (s, 1H), 7.81 – 7.55 (m, 5H), 7.54 – 7.47 (m, 1H), 7.37 (t, *J* = 2.2 Hz, 1H), 7.32 (dd, *J* = 6.2, 3.2 Hz, 2H), 7.23 – 6.99 (m, 8H), 6.58 – 6.45 (m, 1H), 5.64 (d, *J* = 5.8 Hz, 1H), 4.92 (s, 2H), 4.73 – 4.63 (m, 1H), 4.51 (ddd, *J* = 21.6, 10.8, 5.9 Hz, 2H), 3.63 (s, 3H), 3.26 (dd, *J* = 14.2, 5.0 Hz, 1H), 3.05 (dd, *J* = 14.1, 8.7 Hz, 1H), 2.80 (dd, *J* = 17.2, 4.4 Hz, 1H), 2.55 (dd, *J* = 17.0, 6.6 Hz, 1H), 2.30 – 2.11 (m, 3H), 1.91 – 1.77 (m, 1H), 1.27 (s, 9H), 1.27 (s, 9H). ^{13}C NMR (126 MHz, Chloroform-*d*) δ 172.5, 171.9, 171.0, 170.7, 169.3, 160.0, 156.8, 139.3, 135.7, 133.4 (d, *J* = 2.6 Hz), 132.5, 129.5, 128.6, 128.5, 128.3, 128.2, 128.0,

127.7, 127.6, 127.0, 126.3, 125.9, 112.4, 110.3, 105.6, 82.2, 80.6, 67.5, 56.8, 55.2, 53.8, 50.3, 38.2, 36.5, 31.9, 28.1, 28.0, 27.0. MS (ESI) m/z = 833.4 $[M + Na]^+$.

***tert*-Butyl (5*S*,8*S*,11*S*)-8-(2-(*tert*-butoxy)-2-oxoethyl)-5-(naphthalen-2-ylmethyl)-3,6,9-trioxo-1-phenyl-11-((4-(trifluoromethoxy)phenyl)carbamoyl)-2-oxa-4,7,10-triazatetradecan-14-oate (64g).** Yield, 79%. ^{1}H NMR (500 MHz, Chloroform-*d*) δ 8.64 (dd, *J* = 11.5, 4.6 Hz, 1H), 7.84 – 7.64 (m, 5H), 7.59 (d, *J* = 26.7 Hz, 3H), 7.44 – 7.32 (m, 2H), 7.25 – 7.13 (m, 6H), 7.07 (dd, *J* = 8.9, 3.3 Hz, 2H), 5.30 (d, *J* = 28.7 Hz, 1H), 5.11 – 4.84 (m, 2H), 4.68 – 4.54 (m, 1H), 4.50 – 4.25 (m, 2H), 3.44 – 3.26 (m, 1H), 3.07 (dd, *J* = 14.2, 8.8 Hz, 1H), 2.90 (d, *J* = 17.1 Hz, 1H), 2.54 (ddd, *J* = 17.0, 5.9, 2.3 Hz, 1H), 2.32 – 2.16 (m, 2H), 1.96 – 1.81 (m, 2H), 1.32 (s, 9H), 1.28 (s, 9H). ^{13}C NMR (126 MHz, Chloroform-*d*) δ 172.5, 172.2, 171.2, 170.4, 169.3, 157.0, 145.1, 136.9, 135.3, 133.4, 132.9, 132.6, 128.9, 128.6, 128.5, 128.3, 128.0, 127.7, 127.6, 126.7, 126.5, 126.1, 121.5, 121.2, 82.4, 80.7, 67.9, 57.2, 53.8, 50.7, 37.7, 35.7, 32.1, 28.0, 27.9, 26.6. MS (ESI) m/z = 887.4 $[M + Na]^+$.

***tert*-Butyl (5*S*,8*S*,11*S*)-8-(2-(*tert*-butoxy)-2-oxoethyl)-5-(naphthalen-2-ylmethyl)-3,6,9-trioxo-1-phenyl-11-((3-(trifluoromethoxy)phenyl)carbamoyl)-2-oxa-4,7,10-triazatetradecan-14-oate (64h).** Yield, 80%. ^{1}H NMR (500 MHz, Chloroform-*d*) δ 8.89 (s, 1H), 7.88 (d, *J* = 7.6 Hz, 1H), 7.80 (d, *J* = 8.1 Hz, 1H), 7.68 – 7.53 (m, 4H), 7.47 (dd, *J* = 15.1, 5.0 Hz, 2H), 7.28 (dd, *J* = 6.2, 3.2 Hz, 2H), 7.22 – 7.17 (m, 1H), 7.14 – 7.04 (m, 6H), 6.89 – 6.63 (m, 1H), 5.84 (d, *J* = 6.2 Hz, 1H), 4.89 (q, *J* = 12.3 Hz, 2H), 4.77 – 4.67 (m, 1H), 4.62 – 4.59 (m, 1H), 4.52 – 4.46 (m, 1H), 3.25 (dd, *J* = 14.2, 4.8 Hz, 1H), 3.05 (dd, *J* = 14.1, 8.8 Hz, 1H), 2.76 (dd, *J* = 17.1, 4.6 Hz, 1H), 2.60 (dd, *J* = 16.9, 6.9 Hz, 1H), 2.30 – 2.11 (m, 3H), 1.89 (s, 1H), 1.25 (s, 18H). ^{13}C NMR (126 MHz, Chloroform-*d*) δ 172.3, 172.1, 170.87, 170.86, 169.6, 156.9, 149.43, 149.41, 139.7, 135.7, 133.5, 133.4, 132.5, 129.8, 128.55, 128.50, 128.3, 128.1 (d, *J* = 2.2 Hz), 127.7, 127.6, 127.0, 126.3,

125.9, 120.5 (d, *J* = 257.1 Hz), 118.2, 116.1, 112.9, 82.2, 80.7, 67.5, 56.8, 53.8, 50.3, 38.4, 36.7, 31.8, 28.0, 27.9, 26.9. MS (ESI) m/z = 887.4 $[M + Na]^+$.

***tert*-Butyl (5*S*,8*S*,11*S*)-8-(2-(*tert*-butoxy)-2-oxoethyl)-11-((3,5-dimethoxyphenyl)carbamoyl)-5-(naphthalen-2-ylmethyl)-3,6,9-trioxo-1-phenyl-2-oxa-4,7,10-triazatetradecan-14-oate (64i).** Yield, 81%. ^{1}H NMR (500 MHz, Chloroform-*d*) δ 8.55 (s, 1H), 7.84 – 7.55 (m, 5H), 7.52 (d, *J* = 1.6 Hz, 1H), 7.38 – 7.29 (m, 2H), 7.21 – 7.11 (m, 6H), 6.92 (s, 2H), 6.13 (t, *J* = 2.3 Hz, 1H), 5.49 (d, *J* = 5.4 Hz, 1H), 4.94 (s, 2H), 4.63 (ddd, *J* = 7.6, 6.1, 4.4 Hz, 1H), 4.47 (h, *J* = 4.8 Hz, 2H), 3.64 (s, 6H), 3.27 (dd, *J* = 14.1, 5.1 Hz, 1H), 3.05 (dd, *J* = 14.2, 8.6 Hz, 1H), 2.84 (dd, *J* = 17.6, 4.2 Hz, 1H), 2.53 (dd, *J* = 17.3, 6.4 Hz, 1H), 2.29 – 2.13 (m, 3H), 1.91 (d, *J* = 24.4 Hz, 1H), 1.29 (s, 9H), 1.27 (s, 9H). ^{13}C NMR (126 MHz, Chloroform-*d*) δ 172.5, 171.9, 171.1, 170.6, 169.2, 160.9, 156.9, 139.9, 135.6, 133.4, 133.3, 132.6, 128.7, 128.5, 128.3, 128.2, 128.0, 127.7, 127.6, 126.9, 126.4, 126.0, 98.3, 97.0, 82.2, 80.6, 67.7, 56.9, 55.3, 53.8, 50.5, 38.0, 36.2, 32.0, 28.0, 27.9, 26.9. MS (ESI) m/z = 863.4 $[M + Na]^+$.

***tert*-Butyl (5*S*,8*S*,11*S*)-8-(2-(*tert*-butoxy)-2-oxoethyl)-11-((3-methoxy-5-(trifluoromethyl)phenyl)carbamoyl)-5-(naphthalen-2-ylmethyl)-3,6,9-trioxo-1-phenyl-2-oxa-4,7,10-triazatetradecan-14-oate (64j).** Yield, 82%. ^{1}H NMR (500 MHz, Chloroform-*d*) δ 8.82 (s, 1H), 7.75 – 7.54 (m, 6H), 7.50 (t, *J* = 2.5 Hz, 2H), 7.40 – 7.24 (m, 2H), 7.24 – 7.02 (m, 6H), 6.75 (t, *J* = 1.8 Hz, 1H), 5.58 (d, *J* = 5.6 Hz, 1H), 4.92 (s, 2H), 4.62 (td, *J* = 7.0, 4.8 Hz, 1H), 4.55 – 4.36 (m, 2H), 3.65 (s, 3H), 3.27 (dd, *J* = 14.2, 5.0 Hz, 1H), 3.04 (dd, *J* = 14.2, 8.7 Hz, 1H), 2.81 (dd, *J* = 17.1, 4.4 Hz, 1H), 2.58 (dd, *J* = 17.0, 6.5 Hz, 1H), 2.26 – 2.11 (m, 3H), 1.92 (s, 1H), 1.28 (s, 9H), 1.26 (s, 9H). ^{13}C NMR (126 MHz, Chloroform-*d*) δ 172.4, 172.2, 171.0, 170.7, 169.6, 160.2, 157.0, 140.0, 135.5, 133.4, 133.2, 132.6, 131.8 (q, *J* = 32.3 Hz), 128.7, 128.5, 128.4, 128.2, 128.0, 127.7, 127.6, 126.8, 126.4, 126.0, 125.0, 122.8, 109.1 (d, *J* = 4.3 Hz), 108.6, 106.9 (d, *J* =

4.1 Hz), 82.4, 80.7, 67.7, 57.0, 55.5, 53.8, 50.6, 38.0, 36.2, 31.9, 28.0, 27.9, 26.7. MS (ESI) m/z = 901.4 $[M + Na]^+$, MS (ESI) m/z = 877.2 $[M - H]^-$.

***tert*-Butyl (5*S*,8*S*,11*S*)-11-(benzo[*d*][1,3]dioxol-5-ylcarbamoyl)-8-(2-(*tert*-butoxy)-2-oxoethyl)-5-(naphthalen-2-ylmethyl)-3,6,9-trioxo-1-phenyl-2-oxa-4,7,10-triazatetradecan-14-oate (64k).** Yield, 80%. ^{1}H NMR (500 MHz, Chloroform-*d*) δ 8.54 (s, 1H), 7.65 (ddt, *J* = 17.6, 13.4, 5.0 Hz, 5H), 7.52 (d, *J* = 1.7 Hz, 1H), 7.43 – 7.31 (m, 2H), 7.30 – 7.26 (m, 1H), 7.22 – 7.09 (m, 6H), 6.93 – 6.85 (m, 1H), 6.59 (d, *J* = 8.4 Hz, 1H), 5.79 (s, 2H), 5.58 (d, *J* = 5.7 Hz, 1H), 4.93 (s, 2H), 4.76 – 4.58 (m, 1H), 4.48 (ddd, *J* = 19.7, 9.4, 5.0 Hz, 2H), 3.36 – 3.21 (m, 1H), 3.05 (dd, *J* = 14.2, 8.7 Hz, 1H), 2.81 (dd, *J* = 17.1, 4.5 Hz, 1H), 2.62 – 2.46 (m, 1H), 2.33 – 2.14 (m, 3H), 1.90 (dd, *J* = 14.9, 8.6 Hz, 1H), 1.28 (s, 9H), 1.27 (s, 9H). ^{13}C NMR (126 MHz, Chloroform-*d*) δ 172.5, 171.9, 171.0, 170.5, 168.9, 156.8, 147.5, 144.0, 135.7, 133.4, 133.3, 132.5, 132.4, 128.6, 128.5, 128.3, 128.2, 128.0, 127.7, 127.6, 127.0, 126.3, 125.9, 113.3, 107.9, 102.8, 101.1, 82.2, 80.6, 67.6, 56.8, 53.7, 53.5, 50.4, 38.1, 36.4, 32.0, 28.1, 28.0, 27.0. MS (ESI) m/z = 825.3 $[M + H]^+$, MS (ESI) m/z = 847.4 $[M + Na]^+$.

***tert*-Butyl (*S*)-4-((*S*)-4-(*tert*-butoxy)-2-((*S*)-2-(5-chloro-1*H*-indole-2-carboxamido)-3-(naphthalen-2-yl)propanamido)-4-oxobutanamido)-5-(isopentylamino)-5-oxopentanoate (65a).** Yield, 89%. ^{1}H NMR (500 MHz, Chloroform-*d*) δ 7.76 – 7.61 (m, 3H), 7.59 – 7.50 (m, 2H), 7.44 (d, *J* = 8.1 Hz, 1H), 7.39 – 7.31 (m, 2H), 7.26 – 7.08 (m, 6H), 6.67 (t, *J* = 5.6 Hz, 1H), 5.54 (d, *J* = 5.7 Hz, 1H), 4.94 (s, 2H), 4.61 (ddd, *J* = 7.9, 6.4, 4.5 Hz, 1H), 4.53 – 4.42 (m, 1H), 4.33 (td, *J* = 8.6, 4.5 Hz, 1H), 3.27 (dd, *J* = 14.2, 5.0 Hz, 1H), 3.20 – 2.92 (m, 3H), 2.80 (dd, *J* = 16.9, 4.4 Hz, 1H), 2.53 (dd, *J* = 16.9, 6.5 Hz, 1H), 2.28 – 2.00 (m, 3H), 1.84 (tt, *J* = 15.7, 7.0 Hz, 1H), 1.52 (dt, *J* = 13.4, 6.7 Hz, 1H), 1.30 (s, 9H), 1.28 (s, 9H), 0.81 (dd, *J* = 6.7, 3.0 Hz, 6H). ^{13}C NMR (126 MHz, Chloroform-*d*) δ 172.6, 171.6, 171.0, 170.5, 170.2, 156.7, 135.7, 133.4, 132.5, 128.6,

128.5, 128.3, 128.2, 128.0, 127.7, 127.6, 127.0, 126.3, 125.9, 82.0, 80.5, 67.5, 56.7, 53.1, 50.2, 38.2, 38.1, 38.0, 36.5, 31.9, 28.0, 27.9, 27.1, 25.8, 22.5. MS (ESI) m/z = 775.2 $[M + H]^+$, MS (ESI) m/z = 797.2 $[M + Na]^+$.

***tert*-Butyl (*S*)-4-((*S*)-4-(*tert*-butoxy)-2-((*S*)-2-(5-chloro-1*H*-indole-2-carboxamido)-3-(naphthalen-2-yl)propanamido)-4-oxobutanamido)-5-oxo-5-(phenylamino)pentanoate (65b).** Yield, 84%. ^{1}H NMR (500 MHz, DMSO-d_6) δ 9.92 (s, 1H), 8.55 (d, J = 7.9 Hz, 1H), 8.07 (d, J = 7.9 Hz, 1H), 7.88 (dd, J = 6.9, 2.2 Hz, 1H), 7.86 – 7.75 (m, 3H), 7.73 – 7.56 (m, 3H), 7.55 – 7.35 (m, 3H), 7.36 – 7.27 (m, 2H), 7.27 – 7.19 (m, 3H), 7.19 – 7.13 (m, 2H), 7.12 – 6.92 (m, 1H), 5.00 – 4.81 (m, 2H), 4.66 (td, J = 7.8, 6.1 Hz, 1H), 4.43 (tdd, J = 10.9, 7.9, 4.3 Hz, 2H), 3.23 – 3.09 (m, 1H), 2.94 (dd, J = 13.8, 10.9 Hz, 1H), 2.77 (dd, J = 16.2, 6.0 Hz, 1H), 2.56 (dd, J = 16.2, 7.8 Hz, 1H), 2.38 – 2.18 (m, 2H), 2.11 – 1.97 (m, 1H), 1.86 (ddt, J = 10.6, 5.2, 2.9 Hz, 1H), 1.38 (s, 9H), 1.32 (s, 9H). ^{13}C NMR (126 MHz, DMSO-d_6) δ 172.2, 172.0, 170.7, 170.1, 169.9, 156.3, 139.1, 137.4, 136.3, 133.4, 132.3, 129.2, 128.6, 128.3, 128.1, 127.99, 127.97, 127.91, 127.8, 126.4, 125.9, 119.8, 80.8, 80.2, 65.6, 56.6, 53.2, 50.1, 38.1, 37.6, 31.6, 28.13, 28.11, 27.8. MS (ESI) m/z = 781.1 $[M + H]^+$, MS (ESI) m/z = 803.1 $[M + Na]^+$.

***tert*-Butyl (*S*)-4-((*S*)-4-(*tert*-butoxy)-2-((*S*)-2-(5-chloro-1*H*-indole-2-carboxamido)-3-(naphthalen-2-yl)propanamido)-4-oxobutanamido)-5-oxo-5-((4-(trifluoromethyl)phenyl)amino)pentanoate (65c).** Yield, 72%. ^{1}H NMR (500 MHz, Chloroform-*d*) δ 11.05 – 10.69 (m, 1H), 8.90 (s, 1H), 8.10 (d, J = 7.5 Hz, 1H), 8.00 (d, J = 7.5 Hz, 1H), 7.89 (d, J = 8.5 Hz, 2H), 7.84 – 7.69 (m, 4H), 7.59 – 7.49 (m, 3H), 7.49 – 7.43 (m, 2H), 7.40 – 7.33 (m, 2H), 7.18 (dd, J = 8.8, 2.0 Hz, 1H), 6.87 (d, J = 4.5 Hz, 1H), 6.62 (d, J = 2.2 Hz, 1H), 4.87 (dd, J = 9.5, 4.9 Hz, 1H), 4.69 (ddd, J = 7.6, 6.0, 4.5 Hz, 1H), 4.44 (ddd, J = 11.0, 7.3, 3.5 Hz, 1H), 3.56 (dd, J = 14.2, 5.3 Hz, 1H), 3.28 (dd, J = 14.2, 9.1 Hz, 1H), 2.96 (dd, J = 16.9, 4.5

Hz, 1H), 2.82 – 2.58 (m, 1H), 2.53 – 2.32 (m, 3H), 2.30 – 2.21 (m, 1H), 1.49 (s, 9H), 1.20 (s, 9H). ^{13}C NMR (126 MHz, Chloroform-*d*) δ 174.3, 172.1, 170.9, 170.8, 169.8, 163.1, 141.1, 135.8, 133.5, 132.8, 132.7, 129.9, 129.2, 128.0, 127.78, 127.77, 127.5, 126.7, 126.5, 126.3, 126.2, 125.9 (d, *J* = 3.9 Hz), 125.8, 125.5, 125.3, 123.1, 121.0, 119.8, 113.7, 103.0, 82.5, 81.7, 56.4, 54.4, 51.0, 37.7, 35.7, 33.3, 28.1, 27.7, 27.5. MS (ESI) m/z = 914.3 $[M + Na]^+$, MS (ESI) m/z = 890.3 $[M – H]^–$.

***tert*-Butyl (*S*)-4-((*S*)-4-(*tert*-butoxy)-2-((*S*)-2-(5-chloro-1*H*-indole-2-carboxamido)-3-(naphthalen-2-yl)propanamido)-4-oxobutanamido)-5-oxo-5-((3-(trifluoromethyl)phenyl)amino)pentanoate (65d).** Yield, 70%. ^{1}H NMR (500 MHz, Acetone-d_6) δ 11.18 – 10.69 (m, 1H), 9.28 (s, 1H), 8.26 (dd, *J* = 7.2, 4.4 Hz, 2H), 8.10 (d, *J* = 2.0 Hz, 1H), 7.99 – 7.73 (m, 2H), 7.64 (d, *J* = 1.7 Hz, 1H), 7.61 – 7.49 (m, 3H), 7.47 (d, *J* = 2.0 Hz, 1H), 7.42 – 7.28 (m, 3H), 7.28 – 7.16 (m, 3H), 7.14 – 6.85 (m, 2H), 4.96 (ddd, *J* = 8.9, 6.9, 5.7 Hz, 1H), 4.66 (q, *J* = 6.8 Hz, 1H), 4.38 (ddd, *J* = 9.5, 7.7, 4.8 Hz, 1H), 3.33 (dd, *J* = 14.0, 5.7 Hz, 1H), 3.23 (dd, *J* = 14.0, 9.0 Hz, 1H), 2.75 (dd, *J* = 16.5, 6.5 Hz, 1H), 2.59 (dd, *J* = 16.5, 6.6 Hz, 1H), 2.27 (td, *J* = 9.3, 6.1 Hz, 2H), 2.21 – 2.08 (m, 1H), 1.98 – 1.87 (m, 1H), 1.25 (s, 9H), 1.17 (s, 9H). ^{13}C NMR (126 MHz, Acetone-d_6) δ 172.3, 172.1, 170.9, 170.14, 170.10, 162.0, 139.6, 135.3, 135.0, 133.6, 132.4, 132.0, 130.4 (q, *J* = 31.9 Hz), 129.6, 128.6, 127.9, 127.8, 127.5, 127.48, 127.47, 125.9, 125.5, 125.4, 125.3, 124.2, 123.2, 123.1, 120.0 (q, *J* = 3.8 Hz), 116.0 (q, *J* = 4.1 Hz), 113.8, 103.1, 80.9, 80.0, 55.9, 53.8, 50.8, 37.4, 36.8, 31.7, 27.4, 27.3, 27.0. MS (ESI) m/z = 914.3 $[M + Na]^+$, MS (ESI) m/z = 890.3 $[M – H]^–$.

***tert*-Butyl (*S*)-4-((*S*)-4-(*tert*-butoxy)-2-((*S*)-2-(5-chloro-1*H*-indole-2-carboxamido)-3-(naphthalen-2-yl)propanamido)-4-oxobutanamido)-5-((4-methoxyphenyl)amino)-5-oxopentanoate (65e).** Yield, 86%. ^{1}H NMR (500 MHz, Acetone-d_6) δ 11.13 – 10.78 (m, 1H), 9.00

(s, 1H), 8.29 (t, *J* = 7.0 Hz, 2H), 7.88 (d, *J* = 8.0 Hz, 1H), 7.68 (d, *J* = 1.6 Hz, 1H), 7.62 – 7.43 (m, 3H), 7.38 – 7.31 (m, 3H), 7.24 (dd, *J* = 6.3, 3.2 Hz, 2H), 7.16 – 6.97 (m, 2H), 6.92 – 6.56 (m, 2H), 5.17 – 4.93 (m, 1H), 4.76 (q, *J* = 6.9 Hz, 1H), 4.59 – 4.29 (m, 1H), 3.63 (s, 3H), 3.38 (dd, *J* = 14.0, 5.7 Hz, 1H), 3.27 (dd, *J* = 14.0, 9.0 Hz, 1H), 2.79 (dd, *J* = 16.4, 6.6 Hz, 1H), 2.62 (dd, *J* = 16.4, 6.6 Hz, 1H), 2.38 – 2.25 (m, 2H), 2.23 – 2.12 (m, 1H), 2.00 – 1.90 (m, 1H), 1.29 (s, 9H), 1.21 (s, 9H). ^{13}C NMR (126 MHz, Acetone-d_6) δ 172.3, 171.8, 170.8, 170.0, 169.1, 161.9, 156.2, 135.3, 135.1, 133.6, 132.4, 132.1, 131.9, 128.7, 127.9, 127.8, 127.6, 127.5, 127.4, 125.8, 125.4, 125.2, 124.2, 121.3, 120.9, 113.8, 113.7, 103.0, 80.8, 79.9, 55.7, 54.8, 53.6, 50.6, 37.6, 37.1, 31.7, 27.5, 27.4, 27.3. MS (ESI) m/z = 876.2 $[M + Na]^+$.

***tert*-Butyl (*S*)-4-((*S*)-4-(*tert*-butoxy)-2-((*S*)-2-(5-chloro-1*H*-indole-2-carboxamido)-3-(naphthalen-2-yl)propanamido)-4-oxobutanamido)-5-((3-methoxyphenyl)amino)-5-oxopentanoate (65f).** Yield, 81%. ^{1}H NMR (500 MHz, Chloroform-*d*) δ 10.75 (s, 1H), 8.76 (s, 1H), 8.61 (s, 1H), 8.31 (s, 1H), 7.62 (s, 1H), 7.49 – 7.35 (m, 5H), 7.33 – 7.26 (m, 1H), 7.24 – 7.08 (m, 4H), 7.08 – 6.93 (m, 3H), 6.87 (s, 1H), 6.50 (dt, *J* = 5.8, 2.7 Hz, 1H), 5.38 (s, 1H), 4.98 (s, 1H), 4.38 (s, 1H), 3.56 (s, 3H), 3.31 (t, *J* = 7.1 Hz, 1H), 3.23 (dd, *J* = 14.0, 7.8 Hz, 1H), 2.70 (qd, *J* = 17.1, 6.6 Hz, 2H), 2.42 – 2.07 (m, 3H), 1.94 (s, 1H), 1.33 (s, 9H), 1.05 (s, 9H). ^{13}C NMR (126 MHz, Chloroform-*d*) δ 173.4, 171.5, 171.2, 170.3, 169.6, 162.0, 160.0, 138.8, 135.5, 133.6, 133.3, 132.3, 130.9, 129.5, 128.3, 128.2, 127.9, 127.5, 127.4, 127.1, 126.0, 125.9, 125.6, 125.0, 121.1, 113.7, 112.9, 110.3, 106.5, 103.6, 81.9, 81.3, 55.2, 54.9, 54.2, 50.0, 38.9, 37.6, 32.2, 28.1, 27.7, 27.5. MS (ESI) m/z = 876.3 $[M + Na]^+$.

***tert*-Butyl (S)-4-((*S*)-4-(tert-butoxy)-2-((*S*)-2-(5-chloro-1H-indole-2-carboxamido)-3-(naphthalen-2-yl)propanamido)-4-oxobutanamido)-5-oxo-5-((4-(trifluoromethoxy)phenyl)amino)pentanoate (65g).** Yield, 86%. ^{1}H NMR (500 MHz,

Chloroform-*d*) δ 10.99 (s, 1H), 8.76 (s, 1H), 8.07 (d, *J* = 7.6 Hz, 1H), 7.90 – 7.69 (m, 7H), 7.52 (dt, *J* = 5.4, 2.9 Hz, 3H), 7.45 – 7.35 (m, 2H), 7.23 – 7.02 (m, 3H), 6.69 (d, *J* = 4.9 Hz, 1H), 6.55 (d, *J* = 2.6 Hz, 1H), 4.76 (s, 1H), 4.70 – 4.60 (m, 1H), 4.45 (ddd, *J* = 10.7, 7.6, 3.6 Hz, 1H), 3.61 (dd, *J* = 14.3, 4.9 Hz, 1H), 3.28 (dd, *J* = 14.3, 9.4 Hz, 1H), 3.00 (dd, *J* = 17.0, 4.4 Hz, 1H), 2.62 – 2.55 (m, 1H), 2.54 – 2.44 (m, 1H), 2.44 – 2.24 (m, 3H), 1.49 (s, 9H), 1.18 (s, 9H). ^{13}C NMR (126 MHz, Chloroform-*d*) δ 174.5, 172.2, 171.0, 170.6, 169.5, 163.3, 145.2, 136.9, 135.8, 133.5, 132.74, 132.70, 129.8, 129.4, 127.9, 127.8, 127.7, 127.5, 126.9, 126.4, 126.3, 125.6, 121.5, 121.2, 121.0, 119.5, 113.7, 102.9, 82.6, 81.7, 56.6, 54.3, 51.1, 37.5, 35.3, 33.5, 29.3, 28.1, 27.7. MS (ESI) m/z = 930.3 $[M + Na]^+$, MS (ESI) m/z = 906.2 $[M – H]^–$.

***tert*-Butyl (*S*)-4-((*S*)-4-(*tert*-butoxy)-2-((*S*)-2-(5-chloro-1*H*-indole-2-carboxamido)-3-(naphthalen-2-yl)propanamido)-4-oxobutanamido)-5-oxo-5-((3-(trifluoromethoxy)phenyl)amino)pentanoate (65h).** Yield, 76%. ^{1}H NMR (500 MHz, Chloroform-*d*) δ 10.93 (d, *J* = 8.7 Hz, 1H), 8.96 – 8.75 (m, 1H), 8.13 – 7.98 (m, 2H), 7.90 – 7.62 (m, 6H), 7.53 (q, *J* = 2.1 Hz, 1H), 7.48 – 7.31 (m, 4H), 7.31 – 7.24 (m, 1H), 7.17 (dt, *J* = 8.8, 2.3 Hz, 1H), 6.94 (d, *J* = 8.3 Hz, 2H), 6.68 (s, 1H), 4.99 (s, 1H), 4.77 – 4.61 (m, 1H), 4.43 (t, *J* = 8.0 Hz, 1H), 3.54 (d, *J* = 15.1 Hz, 1H), 3.34 – 3.20 (m, 1H), 2.92 (d, *J* = 17.6 Hz, 1H), 2.67 (dd, *J* = 20.8, 12.6 Hz, 1H), 2.49 – 2.31 (m, 3H), 2.23 (d, *J* = 9.1 Hz, 1H), 1.48 (d, *J* = 2.4 Hz, 9H), 1.20 (d, *J* = 3.3 Hz, 9H). ^{13}C NMR (126 MHz, Chloroform-*d*) δ 174.2, 171.9, 170.9, 170.8, 169.6, 162.8, 149.4, 139.5, 135.8, 133.5, 133.0, 132.6, 130.1, 129.7, 129.0, 128.0, 127.8, 127.4, 126.6, 126.2, 125.5, 121.5, 121.0, 119.5, 118.2, 116.2, 113.7, 112.9, 103.0, 82.5, 81.6, 56.2, 54.3, 50.9, 38.0, 36.1, 33.0, 28.1, 27.7, 27.4. MS (ESI) m/z = 930.3 $[M + Na]^+$, MS (ESI) m/z = 906.3 $[M – H]^–$.

***tert*-Butyl (*S*)-4-((*S*)-4-(*tert*-butoxy)-2-((*S*)-2-(5-chloro-1*H*-indole-2-carboxamido)-3-(naphthalen-2-yl)propanamido)-4-oxobutanamido)-5-((3,5-dimethoxyphenyl)amino)-5-**

oxopentanoate (65i). Yield, 83%. ^{1}H NMR (500 MHz, Chloroform-*d*) δ 10.86 (s, 1H), 8.73 (s, 1H), 8.40 (s, 1H), 8.22 (s, 1H), 7.61 (q, *J* = 11.7, 9.7 Hz, 4H), 7.51 (d, *J* = 2.0 Hz, 1H), 7.31 (t, *J* = 8.3 Hz, 5H), 7.15 (dd, *J* = 8.7, 2.0 Hz, 1H), 6.95 (d, *J* = 2.2 Hz, 2H), 6.85 (s, 1H), 6.19 (t, *J* = 2.2 Hz, 1H), 5.28 (s, 1H), 4.93 (s, 1H), 4.45 (s, 1H), 3.67 (s, 6H), 3.44 (dd, *J* = 14.0, 6.1 Hz, 1H), 3.31 (dd, *J* = 14.0, 8.1 Hz, 1H), 2.84 (dd, *J* = 16.7, 4.9 Hz, 1H), 2.74 (dd, *J* = 16.7, 7.4 Hz, 1H), 2.48 – 2.24 (m, 3H), 2.18 – 2.07 (m, 1H), 1.45 (s, 9H), 1.19 (s, 9H). ^{13}C NMR (126 MHz, Chloroform-*d*) δ 173.7, 171.5, 171.0, 170.5, 169.5, 162.3, 160.9, 139.5, 135.6, 133.38, 133.36, 132.4, 130.6, 128.5, 128.2, 127.9, 127.5, 127.4, 127.0, 126.2, 126.0, 125.8, 125.1, 121.0, 113.7, 103.3, 98.7, 96.9, 82.1, 81.4, 55.3, 55.3, 54.3, 50.3, 38.6, 37.0, 32.5, 28.1, 27.7, 27.5. MS (ESI) m/z = 906.4 $[M + Na]^{+}$.

***tert*-Butyl (*S*)-4-((*S*)-4-(*tert*-butoxy)-2-((*S*)-2-(5-chloro-1*H*-indole-2-carboxamido)-3-(naphthalen-2-yl)propanamido)-4-oxobutanamido)-5-((3-methoxy-5-(trifluoromethyl)phenyl)amino)-5-oxopentanoate (65j).** Yield, 80%. ^{1}H NMR (500 MHz, Chloroform-*d*) δ 10.86 (s, 1H), 8.92 (s, 1H), 8.31 (s, 1H), 8.14 (d, *J* = 7.3 Hz, 1H), 7.73 – 7.58 (m, 5H), 7.54 (d, *J* = 2.0 Hz, 1H), 7.50 (s, 1H), 7.42 – 7.27 (m, 4H), 7.16 (dd, *J* = 8.7, 2.0 Hz, 2H), 6.88 – 6.52 (m, 2H), 5.15 (d, *J* = 8.6 Hz, 1H), 4.80 (td, *J* = 7.5, 4.6 Hz, 1H), 4.49 – 4.30 (m, 1H), 3.74 (s, 3H), 3.46 (dd, *J* = 14.0, 6.1 Hz, 1H), 3.28 (dd, *J* = 14.0, 8.4 Hz, 1H), 2.92 – 2.78 (m, 1H), 2.81 – 2.69 (m, 1H), 2.48 – 2.28 (m, 3H), 2.17 (d, *J* = 6.1 Hz, 1H), 1.48 (s, 9H), 1.20 (s, 9H). ^{13}C NMR (126 MHz, Chloroform-*d*) δ 174.1, 171.8, 170.9, 170.8, 169.7, 162.5, 160.1, 139.7, 135.6, 133.4, 133.1, 132.5, 131.7 (d, *J* = 32.3 Hz), 130.3, 128.7, 128.1, 127.8, 127.6, 127.4, 126.7, 126.4, 126.1, 126.0, 125.3, 123.8 (q, *J* = 272.5 Hz), 121.0, 113.7, 109.2 (d, *J* = 4.1 Hz), 108.9, 106.8, 103.0, 82.4, 81.6, 55.6, 55.5, 54.4, 50.6, 38.4, 36.6, 32.7, 28.1, 27.7, 27.2. MS (ESI) m/z = 944.3 $[M + Na]^{+}$.

***tert*-Butyl (*S*)-5-(benzo[*d*][1,3]dioxol-5-ylamino)-4-((*S*)-4-(*tert*-butoxy)-2-((*S*)-2-(5-chloro-1*H*-indole-2-carboxamido)-3-(naphthalen-2-yl)propanamido)-4-oxobutanamido)-5-oxopentanoate (65k).** Yield, 88%. ^{1}H NMR (500 MHz, Chloroform-*d*) δ 10.75 (s, 1H), 8.73 (s, 1H), 8.63 (s, 1H), 8.36 (s, 1H), 7.65 (s, 1H), 7.49 – 7.33 (m, 5H), 7.27 – 7.09 (m, 5H), 7.05 (dd, *J* = 8.7, 2.0 Hz, 1H), 6.88 (s, 1H), 6.82 (dd, *J* = 8.4, 2.1 Hz, 1H), 6.51 (d, *J* = 8.3 Hz, 1H), 5.75 (d, *J* = 1.5 Hz, 1H), 5.70 (s, 1H), 5.39 (s, 1H), 5.01 (s, 1H), 4.40 (s, 1H), 3.33 (dd, *J* = 14.2, 6.3 Hz, 1H), 3.23 (d, *J* = 14.1 Hz, 1H), 2.76 (dd, *J* = 16.7, 8.0 Hz, 1H), 2.66 (d, *J* = 13.0 Hz, 1H), 2.42 – 2.10 (m, 3H), 1.94 (s, 1H), 1.33 (s, 9H), 1.05 (s, 9H). ^{13}C NMR (126 MHz, Chloroform-*d*) δ 173.3, 171.5, 171.1, 170.3, 169.5, 161.9, 147.6, 144.4, 135.5, 133.6, 133.3, 132.3, 131.8, 130.9, 128.3, 128.2, 127.9, 127.4, 127.3, 127.1, 126.0, 125.9, 125.6, 125.0, 121.0, 114.0, 113.7, 107.8, 103.8, 103.3, 101.2, 81.8, 81.2, 54.9, 53.9, 49.9, 38.9, 37.7, 32.1, 28.1, 27.7, 27.4. MS (ESI) m/z = 890.3 $[M + Na]^+$, MS (ESI) m/z = 866.3 $[M – H]^–$.

Ethyl (*S*)-4-(((benzyloxy)carbonyl)amino)-5-oxo-5-((4-(trifluoromethoxy)phenyl)amino)pentanoate (90). Yield, 76%. ^{1}H NMR (500 MHz, DMSO-d_6) δ 10.25 (s, 1H), 8.09 – 7.58 (m, 3H), 7.53 – 7.15 (m, 6H), 5.33 – 4.85 (m, 2H), 4.16 (td, *J* = 8.3, 5.6 Hz, 1H), 4.02 (qd, *J* = 7.1, 1.3 Hz, 2H), 2.38 (ddd, *J* = 8.5, 6.6, 3.8 Hz, 2H), 1.98 (pd, *J* = 6.1, 2.4 Hz, 1H), 1.94 – 1.78 (m, 1H), 1.14 (t, *J* = 7.1 Hz, 3H). ^{13}C NMR (126 MHz, DMSO-d_6) δ 172.5, 171.1, 156.5, 144.1, 138.5, 137.4, 128.8, 128.3, 128.2, 122.1, 121.6, 121.1, 119.6, 66.0, 60.4, 55.2, 30.6, 27.4, 14.5. MS (ESI) m/z = 469.2 $[M + H]^+$.

***tert*-Butyl (*S*)-4-((*S*)-2-((((9*H*-fluoren-9-yl)methoxy)carbonyl)amino)-3-(2*H*-tetrazol-5-yl)propanamido)-5-oxo-5-((4-(trifluoromethoxy)phenyl)amino)pentanoate (91a).** Yield, 60%. ^{1}H NMR (500 MHz, DMSO-d_6) δ 10.26 (s, 1H), 8.35 (d, *J* = 7.5 Hz, 1H), 7.88 (d, *J* = 7.5 Hz, 2H), 7.80 (d, *J* = 8.2 Hz, 1H), 7.75 – 7.69 (m, 2H), 7.66 (t, *J* = 8.4 Hz, 2H), 7.41 (tt, *J* = 7.5,

1.5 Hz, 2H), 7.31 (tt, *J* = 7.4, 1.3 Hz, 4H), 4.58 (td, *J* = 8.6, 5.3 Hz, 1H), 4.39 (td, *J* = 8.1, 5.1 Hz, 1H), 4.29 – 4.15 (m, 3H), 3.39 – 3.34 (m, 1H), 3.23 (dd, *J* = 15.3, 9.1 Hz, 1H), 2.37 – 2.18 (m, 2H), 1.99 (ddd, *J* = 9.9, 8.4, 5.2 Hz, 1H), 1.86 (dtd, *J* = 14.1, 9.2, 5.7 Hz, 1H), 1.33 (s, 9H). ^{13}C NMR (126 MHz, DMSO-d_6) δ 171.9, 170.8, 170.5, 156.2, 144.2, 141.1, 138.3, 128.1, 127.6, 127.5, 125.8, 125.7, 122.1, 121.6, 121.3, 120.6, 119.6, 80.2, 66.4, 55.4, 53.5, 53.3, 47.0, 31.6, 28.1, 27.5. MS (ESI) m/z = 724.3 $[M + H]^+$, 746.2 $[M + Na]^+$, 722.3 $[M – H]^–$.

Ethyl (*S*)-4-((*S*)-2-((((9*H*-fluoren-9-yl)methoxy)carbonyl)amino)-3-(2*H*-tetrazol-5-yl)propanamido)-5-oxo-5-((4-(trifluoromethoxy)phenyl)amino)pentanoate (91b). Yield, 69%. ^{1}H NMR (500 MHz, DMSO-d_6) δ 10.23 (s, 1H), 8.34 (d, *J* = 7.5 Hz, 1H), 7.88 (d, *J* = 7.5 Hz, 2H), 7.78 (d, *J* = 8.1 Hz, 1H), 7.74 – 7.69 (m, 2H), 7.66 (t, *J* = 8.4 Hz, 2H), 7.40 (tt, *J* = 7.6, 1.5 Hz, 2H), 7.31 (tt, *J* = 7.4, 1.4 Hz, 5H), 4.57 (td, *J* = 8.5, 5.4 Hz, 1H), 4.39 (td, *J* = 8.2, 5.4 Hz, 1H), 4.31 – 4.13 (m, 3H), 3.98 (qd, *J* = 7.1, 1.8 Hz, 2H), 3.22 (dd, *J* = 15.3, 9.0 Hz, 2H), 2.41 – 2.25 (m, 2H), 2.04 (ddt, *J* = 14.9, 9.8, 5.8 Hz, 1H), 1.95 – 1.82 (m, 1H), 1.10 (t, *J* = 7.1 Hz, 3H). MS (ESI) m/z = 696.2 $[M + H]^+$.

***tert*-Butyl 2-(((*S*)-1-(((*S*)-1-(((*S*)-5-(*tert*-butoxy)-1,5-dioxo-1-((4-(trifluoromethoxy)phenyl)amino)pentan-2-yl)amino)-1-oxo-3-(2*H*-tetrazol-5-yl)propan-2-yl)amino)-3-(naphthalen-2-yl)-1-oxopropan-2-yl)carbamoyl)-5-chloro-1*H*-indole-1-carboxylate (92a).** Yield, 56%. ^{1}H NMR (500 MHz, DMSO-d_6) δ 10.34 (s, 1H), 9.02 (d, *J* = 8.3 Hz, 1H), 8.65 (d, *J* = 7.7 Hz, 1H), 8.34 (d, *J* = 7.5 Hz, 1H), 7.84 (td, *J* = 41.5, 40.5, 8.7 Hz, 8H), 7.60 – 7.18 (m, 6H), 6.78 (s, 1H), 5.00 – 4.72 (m, 2H), 4.40 (q, *J* = 7.3 Hz, 1H), 3.31 – 2.87 (m, 4H), 2.28 (ddt, *J* = 20.7, 15.7, 7.7 Hz, 2H), 2.01 (p, *J* = 7.4, 6.9 Hz, 1H), 1.85 (h, *J* = 6.8, 6.2 Hz, 1H), 1.31 (s, 9H), 1.26 (s, 9H).

***tert*-Butyl 5-chloro-2-(((*S*)-1-(((*S*)-1-(((*S*)-5-ethoxy-1,5-dioxo-1-((4-(trifluoromethoxy)phenyl)amino)pentan-2-yl)amino)-1-oxo-3-(2*H*-tetrazol-5-yl)propan-2-yl)amino)-3-(naphthalen-2-yl)-1-oxopropan-2-yl)carbamoyl)-1*H*-indole-1-carboxylate (92b).** Yield, 58%. ^{1}H NMR (500 MHz, DMSO-d_6) δ 10.39 (d, J = 35.1 Hz, 1H), 9.00 (dd, J = 30.5, 8.3 Hz, 1H), 8.70 (dd, J = 48.7, 7.8 Hz, 1H), 8.39 (dd, J = 36.7, 7.4 Hz, 1H), 8.08 – 7.61 (m, 8H), 7.61 – 7.22 (m, 6H), 6.76 (d, J = 25.8 Hz, 1H), 4.99 – 4.70 (m, 2H), 4.40 (qd, J = 7.9, 4.9 Hz, 1H), 4.15 – 3.81 (m, 2H), 3.32 – 2.86 (m, 4H), 2.37 (qd, J = 9.5, 8.7, 4.3 Hz, 2H), 2.05 (d, J = 10.5 Hz, 1H), 1.98 – 1.77 (m, 1H), 1.26 (s, 9H), 1.17 – 0.91 (m, 3H). MS (ESI) m/z = 948.3 $[M + H]^+$, 970.3 $[M + H]^+$, 946.3 $[M – H]^–$.

***tert*-Butyl (*S*)-4-((*S*)-2-((*S*)-2-(4,6-dichloro-1*H*-indole-2-carboxamido)-3-(naphthalen-2-yl)propanamido)-3-(2*H*-tetrazol-5-yl)propanamido)-5-oxo-5-((4-(trifluoromethoxy)phenyl)amino)pentanoate (92c).** Yield, 53%. ^{1}H NMR (500 MHz, DMSO-d_6) δ 11.94 (d, J = 2.3 Hz, 1H), 10.29 (s, 1H), 8.97 (d, J = 8.4 Hz, 1H), 8.71 (d, J = 7.6 Hz, 1H), 8.31 (d, J = 7.5 Hz, 1H), 7.96 – 7.63 (m, 4H), 7.53 (dd, J = 8.5, 1.7 Hz, 1H), 7.48 – 7.25 (m, 4H), 7.21 (dd, J = 4.7, 1.7 Hz, 1H), 4.98 – 4.67 (m, 2H), 4.41 (td, J = 8.1, 5.1 Hz, 1H), 3.44 (dd, J = 15.3, 6.3 Hz, 1H), 3.30 - 3.28 (m, 2H), 3.14 (dd, J = 13.9, 11.0 Hz, 1H), 2.29 (qdd, J = 16.2, 11.8, 3.9 Hz, 2H), 2.02 (ddd, J = 15.2, 10.2, 5.4 Hz, 1H), 1.94 – 1.74 (m, 1H), 1.31 (d, J = 1.8 Hz, 9H).

(*S*)-2-Amino-*N*^{1}-(4-(trifluoromethoxy)phenyl)pentanediamide (95). Yield, 75%. ^{1}H NMR (500 MHz, DMSO-d_6) δ 7.91 – 7.62 (m, 2H), 7.43 – 7.12 (m, 3H), 6.71 (s, 1H), 3.45 – 3.15 (m, 3H), 2.26 – 2.05 (m, 2H), 1.86 (dddd, J = 13.4, 9.3, 6.6, 5.4 Hz, 1H), 1.75 – 1.58 (m, 1H). MS (ESI) m/z = 306.1 $[M + H]^+$, 304.2 $[M – H]^–$.

(9*H*-Fluoren-9-yl)methyl ((*S*)-1-(((*S*)-5-amino-1,5-dioxo-1-((4-(trifluoromethoxy)phenyl)amino)pentan-2-yl)amino)-1-oxo-3-(2*H*-tetrazol-5-yl)propan-2-

yl)carbamate (96). Yield, 71%. ^{1}H NMR (500 MHz, DMSO-d_6) δ 10.34 (s, 1H), 8.36 (d, J = 7.3 Hz, 1H), 7.88 (d, J = 7.6 Hz, 2H), 7.74 (dd, J = 8.5, 6.2 Hz, 3H), 7.67 (t, J = 8.2 Hz, 2H), 7.53 – 7.37 (m, 2H), 7.37 – 7.07 (m, 5H), 7.01 – 6.61 (m, 1H), 4.55 (td, J = 8.4, 5.4 Hz, 1H), 4.40 – 4.14 (m, 4H), 3.22 (dd, J = 15.3, 8.9 Hz, 2H), 2.15 (dt, J = 9.3, 6.3 Hz, 2H), 1.99 (s, 1H), 1.87 – 1.73 (m, 1H). ^{13}C NMR (126 MHz, DMSO-d_6) δ 173.9, 170.9, 170.8, 156.2, 144.2, 141.1, 138.4, 128.11, 127.6, 127.5, 125.8, 125.7, 122.0, 121.6, 121.4, 120.6, 119.6, 66.4, 60.2, 53.4, 47.0, 31.7, 28.0. MS (ESI) m/z = 667.3 $[M + H]^+$, 665.3 $[M – H]^–$.

***tert*-Butyl 2-(((*S*)-1-(((*S*)-1-(((*S*)-5-amino-1,5-dioxo-1-((4-(trifluoromethoxy)phenyl)amino)pentan-2-yl)amino)-1-oxo-3-(2*H*-tetrazol-5-yl)propan-2-yl)amino)-3-(naphthalen-2-yl)-1-oxopropan-2-yl)carbamoyl)-5-chloro-1*H*-indole-1-carboxylate (97).** Yield, 65%. ^{1}H NMR (500 MHz, DMSO-d_6) δ 10.33 (s, 1H), 9.01 (d, J = 8.4 Hz, 1H), 8.63 (d, J = 7.6 Hz, 1H), 8.39 (d, J = 7.3 Hz, 1H), 7.99 – 7.62 (m, 8H), 7.56 – 7.20 (m, 7H), 6.93 – 6.62 (m, 2H), 4.81 (dt, J = 7.6, 4.2 Hz, 2H), 4.37 (td, J = 7.8, 5.6 Hz, 1H), 3.43 – 3.03 (m, 4H), 2.30 – 2.12 (m, 2H), 2.03-1.99 (m,1H),1.88 (ddt, J = 11.8, 8.0, 3.6 Hz, 1H), 1.25 (s, 9H). MS (ESI) m/z = 919.3 $[M + H]^+$, 917.2 $[M – H]^–$.

Peptides, and Protein Expression and Purification.[35-36] Wild-type human β-catenin (residues 138−781) were cloned into a pET-28b vector carrying a C-terminal 6× histidine (Novagen) and transformed into *Escherichia coli* BL21 DE3 (Novagen). Cells were cultured in LB medium with 30 μg/mL kanamycin until the OD_{600} was approximately 0.8. The protein expression was then induced with 400 μM IPTG at 16 °C overnight. Cells were lysed by sonication. The proteins were purified by two steps of chromatography, including Ni-NTA affinity chromatography (30210, Qiagen) and size-exclusion chromatography with a HiLoad 26/600 Superdex 200 pg column (28–9893–36, GE Healthcare Life Science) using an AKTA Pure FPLC system (GE Healthcare Life

Science). Protein was eluted in the buffer containing 20 mM Tris (pH 8.5), 100 mM NaCl, and 2 mM DTT. The purity of β-catenin was greater than 95% as determined by SDS-PAGE gel analysis. Thermal-shift assay was performed on an CFX96 Real Time System (Bio-Rad) to monitor protein stability and detect protein aggregation. Protein unfolding was evaluated through measuring the fluorescence changes of fluorescent dye Sypro Orange when interacting with wild-type or mutant β-catenin proteins. A temperature increment of 1°/min was applied. All proteins were stable, and no aggregation was observed under storage or assay conditions. Proteins were aliquoted and stored at −80 °C. The SDS-PAGE result of the purified β-catenin is shown in Supplementary Figure S1.

C-terminally fluorescein-labeled human Tcf4 (residues 7−51), *C*-terminally fluorescein-labeled human E-cadherin (residues 819−873), and *C*-terminally fluorescein-labeled human APC-R3 (residues 1477−1519) were synthesized by InnoPep, Inc. (http://www.innopep.com/) and HPLC purified with purity >95%. The structures were validated by LC/MS (liquid chromatography/mass spectrometry). The sequences of these peptides were reported previously[29] and shown in Supplementary Table S1.

FP Competitive Inhibition Assays.[29, 45] Experiments were performed in 96-well Microfluor 2 black plates on a Synergy 2 plate reader (Biotek). The polarization was measured at room temperature with an excitation wavelength at 485 nm and an emission wavelength at 535 nm. The FP experiments were performed in an assay buffer of 25 mM Hepes (pH 7.4), 100 mM NaCl, 0.01% Triton X-100, and 100 μg/ml γ-globulin. The final reaction volume was set to 100 μL. For the β-catenin/Tcf assay, 10 nM human β-catenin (residues 138-781) was incubated with 2.5 nM *C*-terminally fluorescein-labeled human Tcf4 (residues 7−51) for 30 min at 4 °C, and then different concentrations of the compound in assay buffer were added. The negative control (equivalent to 0% inhibition) refers to 2.5 nM Tcf4 fluorescence tracer and 10 nM β-catenin in assay buffer

without the tested compound. The positive control (equivalent to 100% inhibition) refers to only 2.5 nM Tcf4 fluorescence tracer in assay buffer. For the *β*-catenin/cadherin assay, 150 nM human *β*-catenin (residues 138−781) was incubated with 5 nM C-terminally fluorescent-labeled human E-cadherin (residues 819−873) in assay buffer for 30 min at 4 °C. The negative control refers to 5 nM E-cadherin fluorescence tracer and 150 nM *β*-catenin in assay buffer with no inhibitor presenting. The positive control refers to 5 nM E-cadherin fluorescence tracer in assay buffer. For the *β*-catenin/APC-R3 assay, 2000 nM human *β*-catenin (residues 138−781) was incubated with 5 nM of *C*-terminally fluorescent-labeled human APC-R3 (residues 1477−1519) in assay buffer for 30 min at 4 °C. The negative control refers to 5 nM APC-R3 fluorescence tracer and 2,000 nM *β*-catenin in assay buffer without the tested compound. The positive control refers to 5 nM APC-R3 fluorescence tracer in assay buffer. Each assay plate was covered black and gently mixed on an orbital shaker at 4 °C for 2.5 h to reach equilibrium before the polarization values were read. The background of the tested inhibitors was corrected by subtracting the raw intensity values of the sample background well (all components except probe) from the raw intensity values of the corresponding test wells (all components). The IC_{50} values were determined by GraphPad Prism 5.0. The K_i values were derived from the IC_{50} values.[29] The equation used is $K_i = [I]_{50}/([L]_{50}/K_d + [P]_0/K_d + 1)$ (Where $[I]_{50}$ denotes the concentration of the free inhibitor at 50% inhibition, $[L]_{50}$ is the concentration of the free labeled ligand at 50% inhibition, $[P]_0$ is the concentration of the free protein at 0% inhibition, and K_d is the dissociation constant of the protein-ligand complex). All of the experiments were performed in triplicate and carried out in the presence of 1% DMSO for small-molecule inhibitors. Each compound was assayed at least by two independent experiments. The results were expressed as mean ± standard deviation. The Tcf/cahderin selectivity ratio was calculated on the basis of the respective K_i value of the *β*-catenin/E-cadherin interaction over that

of the β-catenin/Tcf4 interaction. The Tcf/APC selectivity ratio was calculated on the basis of the respective K_i value of the β-catenin/APC-R3 interaction over that of the β-catenin/Tcf4 interaction. The FP saturation binding assay curves and the K_ds of the β-catenin/Tcf, β-catenin/E-cadherin, and β-catenin/APC interactions are shown in Supplementary Figure S2.

MTS Cell Viability Assay. Colorectal cancer cells (SW480 and HCT116), TNBC cells (MDA-MB-231, MDA-MB-468, and BT-20), and lung cancer A549 cells were seeded in 96-well plates at 5×10^3 cells/well, maintained overnight at 37 °C, and incubated with the tested compounds at various concentrations. Cell viability was monitored after 72 h using a freshly prepared mixture of 1 part phenazine methosulfate (PMS, Sigma) solution (0.92 mg/mL) and 19 parts 3-(4,5-dimethylthiazol-2-yl)-5-(3-carboxymethoxyphenyl)-2-(4-sulfophenyl)-2H-tetrazolium (MTS, Promega) solution (2 mg/mL). Cells were incubated in 10 μL of this solution at 37 °C for 3 h, and A_{490} was measured. The effect of each compound is expressed as the concentration required to reduce A_{490} by 50% (IC_{50}) relative to DMSO-treated cells. Experiments were performed in triplicate.

Cell Transfection and Luciferase Assay. FuGENE 6 (E2962, Promega) in the 96-well plate format was used for the transfection of HEK293 cells according to the manufacturer's instructions. HEK293 cells were co-transfected with 45 ng of the TOPFlash or FOPFlash reporter gene, and 135 ng of pcDNA3.1–β-catenin. Cells were cultured in DMEM and 10% fatal bovine serum (FBS) at 37 °C for 24 h, and different concentrations of inhibitors were then added. After 24 h, the luciferase reporter activity was measured using the Dual-Glo system (E2940, Promega). Normalized luciferase activity in response to the treatment with the inhibitors was compared with that obtained from the cells treated with DMSO. Experiments were performed in triplicate.

Co-IP experiments. Two sets of co-IP experiments were conducted: one is the inhibitor was added onto the cell lysates, and the second is the inhibitor was added onto the live cells. For the cell lysate co-IP experiments, SW480 cells were lysed in buffer A containing 50 mM Tris, pH 7.4, 150 mM NaCl, 1% Nonidet P-40, 2 mM EDTA, and protease inhibitors. Different concentrations of the inhibitor were incubated with the SW480 cell lysates at 4 °C for 4 h. For the whole cell co-IP experiments, HCT116 cells at 1×10^6/mL were treated with different concentrations of the inhibitor for 24 h. Cells were then lysed in buffer containing 50 mM Tris, pH 7.4, 150 mM NaCl, 1% Nonidet P-40, 2 mM EDTA, and protease inhibitors. For both cell lysate and whole cell co-IP experiments, the lysates were preadsorbed to A/G plus agarose (sc-2003, Santa Cruz Biotechnology, Inc.) at 4 °C for 1 h. Preadsorbed lysates were incubated with a specific primary antibody overnight at 4 °C. A/G plus agarose was then added to the lysates mixture and incubated for 3 h. The beads were washed 5 times with the lysis buffer at 4 °C. The bound protein was eluted by boiling in the SDS sample buffer and loaded onto 8% SDS polyacrylamide gel for electrophoretic analysis. Separated proteins were transferred onto nitrocellulose membranes for immunoblot analysis. The primary antibodies were against β-catenin (610153, BD Biosciences) and Tcf4 (05−511, Millipore), E-cadherin (610404, BD Biosciences), and APC (MAB3785, Millipore). IRDye 680LT goat antimouse IgG (827-11080, LiCOR) was used as the secondary antibody. The images were detected by the Odyssey infrared imaging system (LiCOR). Experiments were performed in duplicate.

Scratch wound healing assay. To the confluent monolayer of MDA-MB-231 cells in 24-well plates, wounds will be made by scraping a sterile 200 μL pipette tip. Cells were maintained in DMEM containing 10% FBS with 10 μg/mL mitomycin to inhibit cell proliferation. Images of wounds were taken immediately and 14 h after wounding.

Matrigel invasion assay. MDA-MB-231 cells (5×10^4) suspended in 200 μL starvation medium were added to the upper chamber of a Matrigel coated insert (6.5 mm diameter, 8 mm pore size; Corning 353097), and the insert was placed in a 24-well plate containing 600 μL DMEM medium with 10% FBS. Inhibitors were added to both upper and the lower chambers. Invasion assays were performed for 24 h, and the cells were fixed with 3.7% formaldehyde. Cells were then stained with crystal violet staining solution. The cells on the upper side of the insert were removed with a cotton swab. Five randomly selected fields (×10 objectives) on the lower side of the insert were photographed, and the invaded cells were counted. Experiments were performed in triplicate.

ASSOCIATED CONTENT

Supporting Information

The Supporting Information is available free of charge on the ACS Publications website at DOI: Supplemental procedures, the chemical stability of **1** and **21**, the determination of the intracellular concentrations of **53** and **56**, FP and MTS cell viability assay curves of β-catenin/Tcf inhibitors, the sequences of the fluorescence tracers, the SDS-PAGE result of the purified β-catenin (residue 138–781), the full Western blot images of co-IP experiments, supplementary synthetic schemes 1–14, HPLC conditions and chromatograms, NMR spectra, and the supplementary references (PDF). Molecular formula strings (CSV)

AUTHOR INFORMATION

Corresponding Author

*H.J.: Phone, (813) 745-8070; Fax, (813) 745-4506; E-mail: Haitao.Ji@moffitt.org

[#]These two authors contribute equally to this work.

ORCID

Haitao Ji: 0000-0001-5526-4503

Notes

The authors declare the following competing financial interest: a provisional patent application has been filed based on these results.

ACKNOWLEDGMENTS

This work was supported by the Susan G. Komen Career Catalyst Research Grant CCR16380693. The H. Lee Moffitt Cancer Center & Research Institute is a NCI-designated Comprehensive Cancer Center, supported under NIH grant P30-CA76292.

ABBREVIATIONS USED

TCF, T-cell factor; Lef, lymphoid enhancer-binding factor; PPI, protein–protein interaction; SAR, structure-activity relationship; APC, adenomatous polyposis coli; Treg, regulator T cell; HTS, high-throughput screening; K_i, inhibition constant; BCL9, B-cell lymphoma 9; B9L, BCL9-like; CBP, CREB-binding protein; FP, fluorescence polarization; co-IP, co-immunoprecipitation.

REFERENCES

1. Clevers, H.; Nusse, R. Wnt/*β*-catenin signaling and disease. *Cell* **2012**, *149*, 1192-1205.
2. Nusse, R.; Clevers, H. Wnt/*β*-catenin signaling, disease, and emerging therapeutic modalities. *Cell* **2017**, *169*, 985-999.
3. Akhmetshina, A.; Palumbo, K.; Dees, C.; Bergmann, C.; Venalis, P.; Zerr, P.; Horn, A.; Kireva, T.; Beyer, C.; Zwerina, J.; Schneider, H.; Sadowski, A.; Riener, M. O.; MacDougald, O. A.; Distler, O.; Schett, G.; Distler, J. H. Activation of canonical Wnt signalling is required for TGF-beta-mediated fibrosis. *Nat. Commun.* **2012**, *3*, 735-746.
4. van de Wetering, M.; Sancho, E.; Verweij, C.; de Lau, W.; Oving, I.; Hurlstone, A.; van der Horn, K.; Batlle, E.; Coudreuse, D.; Haramis, A. P.; Tjon-Pon-Fong, M.; Moerer, P.; van den Born, M.; Soete, G.; Pals, S.; Eilers, M.; Medema, R.; Clevers, H. The *β*-catenin/TCF-4 complex imposes a crypt progenitor phenotype on colorectal cancer cells. *Cell* **2002**, *111*, 241-250.
5. Dow, L. E.; O'Rourke, K. P.; Simon, J.; Tschaharganeh, D. F.; van Es, J. H.; Clevers, H.; Lowe, S. W. Apc restoration promotes cellular differentiation and reestablishes crypt homeostasis in colorectal cancer. *Cell* **2015**, *161*, 1539-1552.
6. Lu, D.; Zhao, Y.; Tawatao, R.; Cottam, H. B.; Sen, M.; Leoni, L. M.; Kipps, T. J.; Corr, M.; Carson, D. A. Activation of the Wnt signaling pathway in chronic lymphocytic leukemia. *Proc. Natl. Acad. Sci. U.S.A.* **2004**, *101*, 3118-3123.
7. Sukhdeo, K.; Mani, M.; Zhang, Y.; Dutta, J.; Yasui, H.; Rooney, M. D.; Carrasco, D. E.; Zheng, M.; He, H.; Tai, Y. T.; Mitsiades, C.; Anderson, K. C.; Carrasco, D. R. Targeting the *β*-catenin/TCF transcriptional complex in the treatment of multiple myeloma. *Proc. Natl. Acad. Sci. U.S.A.* **2007**, *104*, 7516-7521.

8. Bafico, A.; Liu, G.; Goldin, L.; Harris, V.; Aaronson, S. A. An autocrine mechanism for constitutive Wnt pathway activation in human cancer cells. *Cancer cell* **2004**, *6*, 497-506.
9. Scheel, C.; Eaton, E. N.; Li, S. H.; Chaffer, C. L.; Reinhardt, F.; Kah, K. J.; Bell, G.; Guo, W.; Rubin, J.; Richardson, A. L.; Weinberg, R. A. Paracrine and autocrine signals induce and maintain mesenchymal and stem cell states in the breast. *Cell* **2011**, *145*, 926-940.
10. Brack, A. S.; Conboy, M. J.; Roy, S.; Lee, M.; Kuo, C. J.; Keller, C.; Rando, T. A. Increased Wnt signaling during aging alters muscle stem cell fate and increases fibrosis. *Science* **2007**, *317*, 807-810.
11. Lancaster, M. A.; Louie, C. M.; Silhavy, J. L.; Sintasath, L.; Decambre, M.; Nigam, S. K.; Willert, K.; Gleeson, J. G. Impaired Wnt-*β*-catenin signaling disrupts adult renal homeostasis and leads to cystic kidney ciliopathy. *Nat. Med.* **2009**, *15*, 1046-1054.
12. Malanchi, I.; Peinado, H.; Kassen, D.; Hussenet, T.; Metzger, D.; Chambon, P.; Huber, M.; Hohl, D.; Cano, A.; Birchmeier, W.; Huelsken, J. Cutaneous cancer stem cell maintenance is dependent on *β*-catenin signalling. *Nature* **2008**, *452*, 650-653.
13. Barker, N.; Ridgway, R. A.; van Es, J. H.; van de Wetering, M.; Begthel, H.; van den Born, M.; Danenberg, E.; Clarke, A. R.; Sansom, O. J.; Clevers, H. Crypt stem cells as the cells-of-origin of intestinal cancer. *Nature* **2009**, *457*, 608-611.
14. Yeung, J.; Esposito, M. T.; Gandillet, A.; Zeisig, B. B.; Griessinger, E.; Bonnet, D.; So, C. W. *β*-Catenin mediates the establishment and drug resistance of MLL leukemic stem cells. *Cancer cell* **2010**, *18*, 606-618.
15. Spranger, S.; Bao, R.; Gajewski, T. F. Melanoma-intrinsic *β*-catenin signalling prevents anti-tumour immunity. *Nature* **2015**, *523*, 231-235.

16. Spranger, S.; Dai, D.; Horton, B.; Gajewski, T. F. Tumor-residing Batf3 dendritic cells are required for effector T cell trafficking and adoptive T cell therapy. *Cancer cell* **2017**, *31*, 711-723.

17. Ding, Y.; Shen, S.; Lino, A. C.; Curotto de Lafaille, M. A.; Lafaille, J. J. *β*-Catenin stabilization extends regulatory T cell survival and induces anergy in nonregulatory T cells. *Nat. Med.* **2008**, *14*, 162-169.

18. Keerthivasan, S.; Aghajani, K.; Dose, M.; Molinero, L.; Khan, M. W.; Venkateswaran, V.; Weber, C.; Emmanuel, A. O.; Sun, T.; Bentrem, D. J.; Mulcahy, M.; Keshavarzian, A.; Ramos, E. M.; Blatner, N.; Khazaie, K.; Gounari, F. *β*-Catenin promotes colitis and colon cancer through imprinting of proinflammatory properties in T cells. *Sci. Transl. Med.* **2014**, *6*, 225ra28.

19. Kim, J. S.; Crooks, H.; Foxworth, A.; Waldman, T. Proof-of-principle: oncogenic *β*-catenin is a valid molecular target for the development of pharmacological inhibitors. *Mol. Cancer Ther.* **2002**, *1*, 1355-1359.

20. Ashihara, E.; Kawata, E.; Nakagawa, Y.; Shimazaski, C.; Kuroda, J.; Taniguchi, K.; Uchiyama, H.; Tanaka, R.; Yokota, A.; Takeuchi, M.; Kamitsuji, Y.; Inaba, T.; Taniwaki, M.; Kimura, S.; Maekawa, T. *β*-Catenin small interfering RNA successfully suppressed progression of multiple myeloma in a mouse model. *Clin. Cancer Res.* **2009**, *15*, 2731-2738.

21. Scholer-Dahirel, A.; Schlabach, M. R.; Loo, A.; Bagdasarian, L.; Meyer, R.; Guo, R.; Woolfenden, S.; Yu, K. K.; Markovits, J.; Killary, K.; Sonkin, D.; Yao, Y. M.; Warmuth, M.; Sellers, W. R.; Schlegel, R.; Stegmeier, F.; Mosher, R. E.; McLaughlin, M. E. Maintenance of adenomatous polyposis coli (APC)-mutant colorectal cancer is dependent on Wnt/*β*-catenin signaling. *Proc. Natl. Acad. Sci. U.S.A.* **2011**, *108*, 17135-17140.

22. Lepourcelet, M.; Chen, Y. N.; France, D. S.; Wang, H.; Crews, P.; Petersen, F.; Bruseo, C.; Wood, A. W.; Shivdasani, R. A. Small-molecule antagonists of the oncogenic Tcf/*β*-catenin protein complex. *Cancer cell* **2004**, *5*, 91-102.

23. Trosset, J. Y.; Dalvit, C.; Knapp, S.; Fasolini, M.; Veronesi, M.; Mantegani, S.; Gianellini, L. M.; Catana, C.; Sundstrom, M.; Stouten, P. F.; Moll, J. K. Inhibition of protein-protein interactions: the discovery of druglike *β*-catenin inhibitors by combining virtual and biophysical screening. *Proteins* **2006**, *64*, 60-67.

24. Gonsalves, F. C.; Klein, K.; Carson, B. B.; Katz, S.; Ekas, L. A.; Evans, S.; Nagourney, R.; Cardozo, T.; Brown, A. M.; DasGupta, R. An RNAi-based chemical genetic screen identifies three small-molecule inhibitors of the Wnt/wingless signaling pathway. *Proc. Natl. Acad. Sci. U.S.A.* **2011**, *108*, 5954-5963.

25. Tian, W.; Han, X.; Yan, M.; Xu, Y.; Duggineni, S.; Lin, N.; Luo, G.; Li, Y. M.; Han, X.; Huang, Z.; An, J. Structure-based discovery of a novel inhibitor targeting the *β*-catenin/Tcf4 interaction. *Biochemistry* **2012**, *51*, 724-731.

26. Wang, W.; Liu, H.; Wang, S.; Hao, X.; Li, L. A diterpenoid derivative 15-oxospiramilactone inhibits Wnt/*β*-catenin signaling and colon cancer cell tumorigenesis. *Cell Res.* **2011**, *21*, 730-740.

27. Fang, L.; Zhu, Q.; Neuenschwander, M.; Specker, E.; Wulf-Goldenberg, A.; Weis, W. I.; von Kries, J. P.; Birchmeier, W. A small-molecule antagonist of the *β*-catenin/TCF4 interaction blocks the self-renewal of cancer stem cells and suppresses tumorigenesis. *Cancer Res.* **2016**, *76*, 891-901.

28. Shin, S. H.; Lim, D. Y.; Reddy, K.; Malakhova, M.; Liu, F.; Wang, T.; Song, M.; Chen, H.; Bae, K. B.; Ryu, J.; Liu, K.; Lee, M. H.; Bode, A. M.; Dong, Z. A small molecule inhibitor of

the *β*-catenin-TCF4 interaction suppresses colorectal cancer growth in vitro and in vivo. *EBioMedicine* **2017**, *25*, 22-31.

29. Zhang, M.; Catrow, J. L.; Ji, H. High-throughput selectivity assays for small-molecule inhibitors of *β*-catenin/T-cell factor protein-protein interactions. *ACS Med. Chem. Lett.* **2013**, *4*, 306-311.
30. Halbedl, S.; Kratzer, M. C.; Rahm, K.; Crosta, N.; Masters, K. S.; Zippert, J.; Brase, S.; Gradl, D. Synthesis of novel inhibitors blocking Wnt signaling downstream of *β*-catenin. *FEBS Lett.* **2013**, *587*, 522-527.
31. Grossmann, T. N.; Yeh, J. T.; Bowman, B. R.; Chu, Q.; Moellering, R. E.; Verdine, G. L. Inhibition of oncogenic Wnt signaling through direct targeting of *β*-catenin. *Proc. Natl. Acad. Sci. U.S.A.* **2012**, *109*, 17942-17947.
32. Hsieh, T. H.; Hsu, C. Y.; Tsai, C. F.; Chiu, C. C.; Liang, S. S.; Wang, T. N.; Kuo, P. L.; Long, C. Y.; Tsai, E. M. A novel cell-penetrating peptide suppresses breast tumorigenesis by inhibiting *β*-catenin/LEF-1 signaling. *Sci. Rep.* **2016**, *6*, 19156-19167.
33. Dietrich, L.; Rathmer, B.; Ewan, K.; Bange, T.; Heinrichs, S.; Dale, T. C.; Schade, D.; Grossmann, T. N. Cell permeable stapled peptide inhibitor of Wnt signaling that targets *β*-catenin protein-protein interactions. *Cell Chem. Biol.* **2017**, *24*, 958-968.
34. Schneider, J. A.; Craven, T. W.; Kasper, A. C.; Yun, C.; Haugbro, M.; Briggs, E. M.; Svetlov, V.; Nudler, E.; Knaut, H.; Bonneau, R.; Garabedian, M. J.; Kirshenbaum, K.; Logan, S. K. Design of peptoid-peptide macrocycles to inhibit the *β*-catenin TCF interaction in prostate cancer. *Nat. Commun.* **2018**, *9*, 4396-4405.

35. Yu, B.; Huang, Z.; Zhang, M.; Dillard, D. R.; Ji, H. Rational design of small-molecule inhibitors for *β*-catenin/T-cell factor protein-protein interactions by bioisostere replacement. *ACS Chem. Biol.* **2013**, *8*, 524-529.

36. Huang, Z.; Zhang, M.; Burton, S. D.; Katsakhyan, L. N.; Ji, H. Targeting the Tcf4 $G^{13}ANDE^{17}$ binding site to selectively disrupt *β*-catenin/T-cell factor protein-protein interactions. *ACS Chem. Biol.* **2014**, *9*, 193-201.

37. Catrow, J. L.; Zhang, Y.; Zhang, M.; Ji, H. Discovery of selective small-molecule inhibitors for the *β*-catenin/T-cell factor protein-protein interaction through the optimization of the acyl hydrazone moiety. *J. Med. Chem.* **2015**, *58*, 4678-4692.

38. de Sa Alves, F. R.; Barreiro, E. J.; Fraga, C. A. From nature to drug discovery: the indole scaffold as a 'privileged structure'. *Mini Rev. Med. Chem.* **2009**, *9*, 782-793.

39. Sravanthi, T. V.; Manju, S. L. Indoles - a promising scaffold for drug development. *Eur. J. Pharm. Sci.* **2016**, *91*, 1-10.

40. Banoglu, E.; Jha, G. G.; King, R. S. Hepatic microsomal metabolism of indole to indoxyl, a precursor of indoxyl sulfate. *Eur. J. Drug Metab. Pharmacokinet.* **2001**, *26*, 235-240.

41. Kondreddi, R. R.; Jiricek, J.; Rao, S. P.; Lakshminarayana, S. B.; Camacho, L. R.; Rao, R.; Herve, M.; Bifani, P.; Ma, N. L.; Kuhen, K.; Goh, A.; Chatterjee, A. K.; Dick, T.; Diagana, T. T.; Manjunatha, U. H.; Smith, P. W. Design, synthesis, and biological evaluation of indole-2-carboxamides: a promising class of antituberculosis agents. *J. Med. Chem.* **2013**, *56*, 8849-8859.

42. Piscitelli, F.; Ligresti, A.; La Regina, G.; Coluccia, A.; Morera, L.; Allara, M.; Novellino, E.; Di Marzo, V.; Silvestri, R. Indole-2-carboxamides as allosteric modulators of the cannabinoid CB(1) receptor. *J. Med. Chem.* **2012**, *55*, 5627-5631.

43. Ban, F.; Leblanc, E.; Li, H.; Munuganti, R. S.; Frewin, K.; Rennie, P. S.; Cherkasov, A., Discovery of 1H-indole-2-carboxamides as novel inhibitors of the androgen receptor binding function 3 (BF3). *J. Med. Chem.* **2014**, *57*, 6867-6872.

44. Stec, J.; Onajole, O. K.; Lun, S.; Guo, H.; Merenbloom, B.; Vistoli, G.; Bishai, W. R.; Kozikowski, A. P. Indole-2-carboxamide-based MmpL3 inhibitors show exceptional antitubercular activity in an animal model of tuberculosis infection. *J. Med. Chem.* **2016**, *59*, 6232-6247.

45. Zhang, M.; Huang, Z.; Yu, B.; Ji, H. New homogeneous high-throughput assays for inhibitors of *β*-catenin/Tcf protein-protein interactions. *Anal. Biochem.* **2012**, *424*, 57-63.

46. Liljebris, C.; Larsen, S. D.; Ogg, D.; Palazuk, B. J.; Bleasdale, J. E. Investigation of potential bioisosteric replacements for the carboxyl groups of peptidomimetic inhibitors of protein tyrosine phosphatase 1B: identification of a tetrazole-containing inhibitor with cellular activity. *J. Med. Chem.* **2002**, *45*, 1785-1798.

47. Poy, F.; Lepourcelet, M.; Shivdasani, R. A.; Eck, M. J. Structure of a human Tcf4-*β*-catenin complex. *Nat. Struct. Biol.* **2001**, *8*, 1053-1057.

48. Graham, T. A.; Ferkey, D. M.; Mao, F.; Kimelman, D.; Xu, W. Tcf4 can specifically recognize *β*-catenin using alternative conformations. *Nat. Struct. Biol.* **2001**, *8*, 1048-1052.

49. Sampietro, J.; Dahlberg, C. L.; Cho, U. S.; Hinds, T. R.; Kimelman, D.; Xu, W. Crystal structure of a *β*-catenin/BCL9/Tcf4 complex. *Mol. Cell* **2006**, *24*, 293-300.

50. Sun, J.; Weis, W. I. Biochemical and structural characterization of *β*-catenin interactions with nonphosphorylated and CK2-phosphorylated Lef-1. *J. Mol. Biol.* **2011**, *405*, 519-530.

51. Huber, A. H.; Weis, W. I. The structure of the *β*-catenin/E-cadherin complex and the molecular basis of diverse ligand recognition by beta-catenin. *Cell* **2001**, *105*, 391-402.

52. Eklof Spink, K.; Fridman, S. G.; Weis, W. I. Molecular mechanisms of β-catenin recognition by adenomatous polyposis coli revealed by the structure of an APC-β-catenin complex. *EMBO J.* **2001**, *20*, 6203-6212.

53. Ha, N. C.; Tonozuka, T.; Stamos, J. L.; Choi, H. J.; Weis, W. I. Mechanism of phosphorylation-dependent binding of APC to β-catenin and its role in β-catenin degradation. *Mol. Cell* **2004**, *15*, 511-521.

54. Xing, Y.; Clements, W. K.; Le Trong, I.; Hinds, T. R.; Stenkamp, R.; Kimelman, D.; Xu, W. Crystal structure of a β-catenin/APC complex reveals a critical role for APC phosphorylation in APC function. *Mol. Cell* **2004**, *15*, 523-533.

55. Hulsken, J.; Birchmeier, W.; Behrens, J. E-cadherin and APC compete for the interaction with β-catenin and the cytoskeleton. *J. Cell Biol.* **1994**, *127*, 2061-2069.

56. Omer, C. A.; Miller, P. J.; Diehl, R. E.; Kral, A. M. Identification of Tcf4 residues involved in high-affinity β-catenin binding. *Biochem. Biophys. Res. Commun.* **1999**, *256*, 584-590.

57. Orsulic, S.; Huber, O.; Aberle, H.; Arnold, S.; Kemler, R. E-cadherin binding prevents β-catenin nuclear localization and β-catenin/LEF-1-mediated transactivation. *J. Cell Sci.* **1999**, *112*, 1237-1245.

58. Choi, H. J.; Huber, A. H.; Weis, W. I. Thermodynamics of β-catenin-ligand interactions: the roles of the N- and C-terminal tails in modulating binding affinity. *J. Biol. Chem.* **2006**, *281*, 1027-1038.

59. Beiter, K.; Hiendlmeyer, E.; Brabletz, T.; Hlubek, F.; Haynl, A.; Knoll, C.; Kirchner, T.; Jung, A. β-Catenin regulates the expression of tenascin-C in human colorectal tumors. *Oncogene* **2005**, *24*, 8200-8204.

60. Oskarsson, T.; Acharyya, S.; Zhang, X. H.-F.; Vanharanta, S.; Tavazoie, S. F.; Morris, P. G.; Downey, R. J.; Manova-Todorova, K.; Brogi, E.; Massagué, J. Breast cancer cells produce tenascin C as a metastatic niche component to colonize the lungs. *Nat. Med.* **2011**, *17*, 867-874.

61. Stein, U.; Arlt, F.; Walther, W.; Smith, J.; Waldman, T.; Harris, E. D.; Mertins, S. D.; Heizmann, C. W.; Allard, D.; Birchmeier, W.; Schlag, P. M.; Shoemaker, R. H. The metastasis-associated gene S100A4 is a novel target of beta-catenin/T-cell factor signaling in colon cancer. *Gastroenterology* **2006**, *131*, 1486-1500.

62. Jenkinson, S. R.; Barraclough, R.; West, C. R.; Rudland, P. S. S100A4 regulates cell motility and invasion in an in vitro model for breast cancer metastasis. *Br. J. Cancer.* **2004**, *90*, 253-262.

63. Ambartsumian, N. S.; Grigorian, M. S.; Larsen, I. F.; Karlstrøm, O.; Sidenius, N.; Rygaard, J.; Georgiev, G.; Lukanidin, E. Metastasis of mammary carcinomas in GRS/A hybrid mice transgenic for the mts1 gene. *Oncogene* **1996**, *13*, 1621-1630.

64. Davies, M. P.; Rudland, P. S.; Robertson, L.; Parry, E. W.; Jolicoeur, P.; Barraclough, R. Expression of the calcium-binding protein S100A4 (p9Ka) in MMTV-neu transgenic mice induces metastasis of mammary tumours. *Oncogene* **1996**, *13*, 1631-1637.

65. Lloyd, B. H.; Platt-Higgins, A.; Rudland, P. S.; Barraclough, R. Human S100A4 (p9Ka) induces the metastatic phenotype upon benign tumour cells. *Oncogene* **1998**, *17*, 465-473.

66. Ravindranath, A.; Yuen, H. F.; Chan, K. K.; Grills, C.; Fennell, D. A.; Lappin, T. R.; El-Tanani, M. Wnt-*β*-catenin-Tcf-4 signalling-modulated invasiveness is dependent on osteopontin expression in breast cancer. *Br. J. Cancer* **2011**, *105*, 542-551.

67. Howe, L. R.; Watanabe, O.; Leonard, J.; Brown, A. M. Twist is up-regulated in response to Wnt1 and inhibits mouse mammary cell differentiation. *Cancer Res.* **2003**, *63*, 1906-1913.

68. Yook, J. I.; Li, X. Y.; Ota, I.; Fearon, E. R.; Weiss, S. J. Wnt-dependent regulation of the E-cadherin repressor snail. *J. Biol. Chem.* **2005**, *280*, 11740-11748.

69. Yook, J. I.; Li, X. Y.; Ota, I.; Hu, C.; Kim, H. S.; Kim, N. H.; Cha, S. Y.; Ryu, J. K.; Choi, Y. J.; Kim, J.; Fearon, E. R.; Weiss, S. J. A Wnt-Axin2-GSK3β cascade regulates Snail1 activity in breast cancer cells. *Nat. Cell Biol.* **2006**, *8*, 1398-1406.

70. Wu, Z. Q.; Li, X. Y.; Hu, C. Y.; Ford, M.; Kleer, C. G.; Weiss, S. J. Canonical Wnt signaling regulates Slug activity and links epithelial-mesenchymal transition with epigenetic Breast Cancer 1, Early Onset (BRCA1) repression. *Proc. Natl. Acad. Sci. U. S. A.* **2012**, *109*, 16654-16659.

71. Emami, K. H.; Nguyen, C.; Ma, H.; Kim, D. H.; Jeong, K. W.; Eguchi, M.; Moon, R. T.; Teo, J. L.; Kim, H. Y.; Moon, S. H.; Ha, J. R.; Kahn, M. A small molecule inhibitor of β-catenin/CREB-binding protein transcription. *Proc. Natl. Acad. Sci. U. S. A.* **2004**, *101*, 12682-12687.

72. Rautio, J.; Meanwell, N. A.; Di, L.; Hageman, M. J. The expanding role of prodrugs in contemporary drug design and development. *Nat. Rev. Drug Discov.* **2018**, *17*, 559-587.

73. Teuscher, K. B.; Zhang, M.; Ji, H. A versatile method to determine the cellular bioavailability of small-molecule inhibitors. *J. Med. Chem.* **2017**, *60*, 157-169.

Table of Contents Graphic

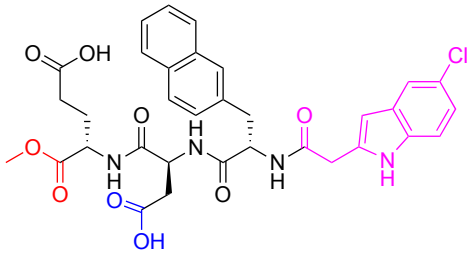

1 (UU-T02)

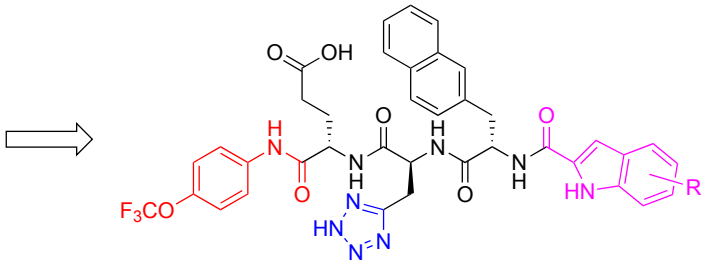

Inhibitors with submicromolar K_i for the β-catenin/Tcf PPI

53, R = 5-Cl, K_i = 0.64 ± 0.12 μM

57, R = 4, 6-diCl, K_i = 0.44 ± 0.098 μM